

Università degli Studi dell'Insubria
Dipartimento di Scienza ed Alta Tecnologia
Dottorato in Scienze Chimiche



***Developing active packaging solutions through
incorporation of organic/inorganic active
components in renewable materials***

PhD dissertation of
Joana Andreia Saraiva Mendes

Tutor: Professor Massimo Mella
External Tutor: Dr. Graziano Elegir

XXVIII ciclo – 2012-2015

NewGenPak

New Generation of Functional Cellulose Fibre Based Packaging Materials for Sustainability

Marie Curie Actions - Interdisciplinary research training network

People Programme

7th Research Framework Programme

Developing active packaging solutions through incorporation of organic/inorganic active components in renewable materials

Joana Andreia Saraiva Mendes

Host organization: Innovhub SSI – Paper Division, Milan, Italy

The research leading to these results has received funding from the People Programme (Marie Curie Actions) of the European Union's Seventh Framework Programme FP7/2007-2013/ under REA grant agreement n°: 290098.



“In life, nothing is to be feared, everything is to be understood.”

Marie Curie

To my parents and Giacomo.

Abstract

The development of new antimicrobial active packaging systems have been gaining a raising interest due to its potential to increase product shelf-life and provide food quality and safety benefits allied to society demands on food-related health risks, multi-drug resistance and environmental problems. A great variety of organic substances such as phenolic compounds and essential oils as well as inorganic metal oxide nanoparticles such as Ag⁺, ZnO and TiO₂ have been intensively studied for having antimicrobial properties, although their efficiency is highly dependent on the target microorganisms, the material or media where they act as well as the surrounding environment are relevant (Burt, 2004; Suppakul *et al.*, 2003; Visai *et al.*, 2011). Recent research in active packaging is mostly focused on the use of natural renewable material resources including preservatives to develop biodegradable and recyclable packaging products. Accordingly, the NEWGENPAK project was funded within ITN-Marie Skłodowska-Curie EU program with the aim “to take wood cellulose based material a significant step forward by replacing petroleum-based additives used in paper and board packaging materials in order to achieve the barrier and other crucial properties needed for competitive, low carbon footprint, packaging materials”.

NEWGENPAK, the acronym for New Generation of Cellulose Fibre Based Packaging Materials for Sustainability, just finished in December 2015, was an interdisciplinary research training network (ITN) constituted by 8 European universities, 3 research institutes and 6 enterprises from all over Europe, with 13 researchers working full time developing their own individual researcher projects, making collaborations and receiving training on the field. This PhD thesis was carried out within this project and developed mainly at Innovhub SSI – Paper Division, Milan, Italy.

The main target of this work was to attain antibacterial cellulose-based materials for food packaging applications, following two approaches based in the incorporation of active organic components or active nanoparticles as active agents. Besides, it was studied the possibility to develop an antibacterial packaging for medical applications, in order to prevent medical cross

contamination. The fate of the nanoparticles in the recycling process and their effect on the biodegradability of the packaging was initially assessed as an important part of environmental aspects related to the end of life of packaging products.

The first approach, described in the chapter 2, aimed to explore the possibilities to extract polyphenols from black tea brewing residues and use them as active compounds for the development of active cellulosic-based surfaces. Therefore, the chemical characterization of black tea residues as well as the antioxidant and antimicrobial properties of their extracts were addressed. The best infusion conditions, considering the yield of extraction, the antioxidant activity and the total phenolic content, were found to be at 80°C for 7.5 minutes for an infusion of 2.5 g of tea residue in 100 mL of water, and just 1.1 mg of these extract were enough to provide a bactericidal effect. The resulting paper coated with 3.8 g/m² of polyphenols-based coating formulation attained a complete killing effect against *S. aureus*.

In the second approach, several papers were functionalized with formulations based on photo-active TiO₂ NPs by dip-coating and compared regarding their antibacterial activity. The results presented in the chapter 3 have shown that both handsheets of bleached Kraft pulp (BK) and chemithermomechanical pulp (CTMP) displayed a bactericidal effect against gram-positive *Staphylococcus aureus* and gram-negative *Pseudomonas aeruginosa*, even after three weeks of storage either in light and dark conditions, while pre-coated recycled paper (PCR) and bleached pre-coated Kraft (BPK) paper samples did not show any antibacterial activity. The effect of TiO₂ NPs against *S. aureus* was inhibited in: i) PCR samples due to the presence of considerable amounts of inorganic compounds, such as calcium carbonate, that shielded the effect of active nanoparticles; and ii) BPK samples, most likely due to their high hydrophobicity that did not permit a good retention of the NPs and homogenous coating distribution. Accordingly, different preparation methods and deposition techniques were considered for hydrophobic surfaces and compared regarding the amount of TiO₂ incorporated in nanofibrillated cellulose (NFC) loaded and finally retained on the BPK paper surfaces. Under the best conditions with the polyelectrolyte-assisted deposition 90% of nanoparticles retention was attained against only 25% for the direct-mixture formulations. The antibacterial activity of the paper samples reached approximately 2 log bacterial reduction of *S. aureus* showing the possibility to achieve a contact active surface based on layer-by layer assembly NFC-TiO₂ formulation. Moreover a scale-up pilot demonstration of an over-print varnish based on ZnO nanoparticles was performed to be loaded by flexographic printing at industrial scale for medical packaging applications. The

SAFEBOX packaging demonstrator produced was loaded with only 5.6 mg/m² of ZnO NPs based varnish, due to some technical production constraints and restrictions, therefore it presented a slightly bacteriostatic effect with less than one log reduction. However, with the possibility to increase the amount of NPs loaded on the paper surface, promising results can be achieved. Preliminary results obtained at lab scale showed a bactericidal effect, up to 4 log reduction, for papers with about 1,5g/m² of ZnO NPs on the surface. Regarding the preliminary studies on environmental impact of NPs, towards packaging end-of-life options presented also in the chapter 3, laboratory tests have shown only marginal effect of active ingredients on biodegradability performance whereas recyclability tests have shown a reasonable good retention of TiO₂ nanoparticles (approximately 90%) in the recycled fibres after one recycling loop.

Abbreviations

AIR - acid-insoluble residue

ASL - Acid soluble substances

aW - water activity

BC - bacterial cellulose

BK - bleached Kraft pulp

BPK - bleached pre-coated Kraft pulp

C - catechins

CAF - caffeine

CG - catechin gallate

CFU - Colony Forming Units

CMC - carboxymethyl cellulose

CTMP - chemithermomechanical pulp

DLS - dynamic light scattering

DM - direct-mixture coating formulations

DP - degree of polymerization

DPPH - 2,2-diphenyl-1-picrylhydrazyl

EC - Epicatechin

ECDC - European Centre for Disease Prevention and Control

ECG - epicatechin-3-gallate

EGC - epigallocatechin

EGCG - epigallocatechin-3-gallate

ESR - early-stage-researcher

GA - gallic acid

GAE - gallic acid equivalents

GC - gallocatechin

GCG - gallocatechin gallate

HAIs - healthcare-associated infections

ICP-MS - inductively coupled plasma mass spectrometry

LbL - layer-by-layer

MAP - modified atmosphere packaging

MFC - microfibrillated cellulose

MIC - minimum inhibitory concentration

MPS - Multipackaging Solutions

NB - nutrient broth

NF - nitrogen-to-protein conversion multiplier (N factor)

NFC - nanofibrillated cellulose

NGP - NewGenPak project

NPs - nanoparticles

NREL - National Renewable Energy Laboratory

OS - oxygen scavengers

OTMS - octyltrimethoxysilane

OWD - oven-dry weight

PCA - plate count agar

PCR - pre-coated recycled paper

PE - layer-by-layer/polyelectrolyte-assisted coating formulations

PEs - polyelectrolytes solutions

PITC - phenyl isothiocyanate

POD - peroxidase

PPCMC - tea residue extracts based coating formulation

PPO - polyphenol oxidase (PPO)

PTMS - phenyltrimethoxysilane

R - antibacterial efficiency

RDA - retro Diels-Alder reaction

ROS - reactive oxygen species

SAFEBOX - ZnO NPs-based packaging demonstrator

SEM-EDX - Scanning electron microscopy with energy dispersive X-ray spectroscopy

TEOS - tetraethoxysilane

TF - theaflavin

TFDG - theaflavin-3,3'-digallate

TF3G - theaflavin-3-gallate

TF3'G - theaflavin-3'-gallate

TG - theogallin

TPC - total phenolic content

UHPLC-MS - ultra-high-performance liquid chromatography - mass spectrometry

WP - workpackage

Table of Contents

CHAPTER 1. LITERATURE REVIEW	1
1. PACKAGING.....	1
1.1 <i>Paper and paper-based products as sustainable fibre-based packaging materials</i>	3
2. OVERVIEW ON ACTIVE PACKAGING.....	5
2.1 <i>Oxygen scavenging technology</i>	6
2.2 <i>Carbon dioxide scavengers and emitters</i>	7
2.3 <i>Ethylene scavengers</i>	7
2.4 <i>Ethanol emitters</i>	8
2.5 <i>Moisture regulators</i>	8
2.6 <i>Antimicrobial packaging concepts</i>	8
CHAPTER 2. BLACK TEA RESIDUES: A POTENTIAL SOURCE OF ACTIVE COMPOUNDS FOR CELLULOSE-BASED PACKAGING PRODUCTS	11
1. INTRODUCTION.....	11
1.1 <i>Tea: types and processing</i>	12
1.2 <i>Chemistry of major active compounds in tea</i>	13
1.3 <i>Antioxidant and Antibacterial activity of tea polyphenols</i>	16
2. MATERIALS AND METHODS.....	17
2.1 <i>Black tea residues</i>	17
2.2 <i>Chemical characterization of tea residues</i>	17
2.3 <i>Preparation and characterization of black tea residue extracts</i>	20
2.4 <i>Preparation of coated papers based on tea residue extracts coating formulations</i>	23
2.5 <i>Antibacterial activity assays</i>	23
3. RESULTS AND DISCUSSION.....	25
3.1 <i>Chemical Composition of the black tea residue</i>	25
3.2 <i>Studies on the tea residues potential</i>	26
3.3 <i>Development of active paper surfaces based on tea residues</i>	40
4. CONCLUSIONS.....	41
CHAPTER 3. USE OF ACTIVE NANOPARTICLES TO DEVELOP ANTIBACTERIAL PAPER PRODUCTS AND THEIR INFLUENCE ON PACKAGING END OF LIFE OPTIONS	43
1. INTRODUCTION.....	43
1.1 <i>TiO₂ history and properties</i>	44
1.2 <i>ZnO nanoparticles: mechanism, structure and paper applications</i>	49
2. MATERIALS AND METHODS.....	50
2.1 <i>Nanoparticles suspensions</i>	50
2.2 <i>Paper sheets</i>	50

2.3	<i>Functionalization of paper surfaces with active nanoparticles</i>	51
2.4	<i>Photo-activation of the TiO₂ NPs</i>	52
2.5	<i>Characterization of coated papers</i>	52
2.6	<i>Antibacterial assessment</i>	54
2.7	<i>Recycling test</i>	55
2.8	<i>Biodegradability assays</i>	55
3.	RESULTS AND DISCUSSION	56
3.1	<i>Studies on TiO₂ photo-active NPs coated papers</i>	56
3.2	<i>Advances on ZnO NPs cellulose-based packaging to reduce medical cross contamination</i>	66
3.3	<i>Sustainability – Packaging End of life</i>	72
4.	CONCLUSIONS	75
	CHAPTER 4. CONCLUDING REMARKS	77
	CHAPTER 5. BIBLIOGRAPHY	79
	APPENDIX	I

List of Figures

FIGURE 1. PARTIAL STRUCTURE OF CELLULOSE.....	3
FIGURE 2. ALCOHOLS PRECURSOR OF LIGNIN: (A) <i>P</i> -COUMARYL, (B) CONIFERYL AND (C) SINAPYL.....	4
FIGURE 3. IRON OXIDATION REACTION SCHEME.....	7
FIGURE 4. OVERVIEW ON TEA PROCESSING.....	12
FIGURE 5. GALLIC ACID, R=H; THEOGALLIN, R= QUINIC ACID.....	14
FIGURE 6. L-THEANINE.....	16
FIGURE 7. GALLIC ACID STANDARD CURVE – REFERENCE FOR TOTAL PHENOLIC CONTENT.....	28
FIGURE 8. TOTAL PHENOLIC CONTENT OF EXTRACTS EXPRESSED AS GALLIC ACID EQUIVALENTS (GAE, MG/G OF TEA RESIDUE EXTRACT).....	28
FIGURE 9: % INHIBITION OF DPPH BY EXTRACTS OBTAINED FROM THE AQUEOUS INFUSION OF 2.5% (W/V) TEA RESIDUES.....	29
FIGURE 10: % INHIBITION OF DPPH BY EXTRACTS OBTAINED FROM THE AQUEOUS INFUSION OF 5% (W/V) TEA RESIDUES.....	30
FIGURE 11: % INHIBITION OF DPPH FOR A7.5 AND B7.5 TEA RESIDUE EXTRACTS.....	30
FIGURE 12: % INHIBITION OF DPPH BY WATER (W) AND ETHANOL (E) EXTRACTS AND RELATIVE IC ₅₀	31
FIGURE 13. UHPLC-UV CHROMATOGRAMS OF EXTRACTS OBTAINED BY INFUSION PROCEDURES (A7.5) AND SOXHLET EXTRACTION WITH WATER (W) AND ETHANOL (E), RECORDED AT 280 NM.....	32
FIGURE 14. DISTRIBUTION PROFILE OF IDENTIFIED COMPOUNDS IN A7.5, W AND E EXTRACTS.....	34
FIGURE 15. RETRO DIELS-ALDER FRAGMENTATION OF CATECHINS.....	35
FIGURE 16: TEST OF INHIBITORY ACTIVITY AGAINST <i>S. AUREUS</i> FOR (A) REFERENCE, (B) 2.0 MG AND (C) 4.0 MG OF EXTRACT.....	37
FIGURE 17: ANTIBACTERIAL ACTIVITY OF THE EXTRACTS AGAINST (A) <i>S. AUREUS</i> AND (B) <i>E. COLL</i>	38
FIGURE 18: ANTIBACTERIAL ACTIVITY OF TEA EXTRACTS AGAINST <i>S. AUREUS</i> , USING MIC DETERMINATION.....	39
FIGURE 19: ANTIBACTERIAL ACTIVITY OF PPCMC COATED PAPERS AGAINST <i>S. AUREUS</i>	40
FIGURE 20. CRYSTALLINE FORMS OF TiO ₂ : RUTILE (A), ANATASE (B) AND BROOKITE (C).....	45
FIGURE 21. SCHEME OF THE FORMATION OF HOLES AND ELECTRONS AFTER UV EXCITATION.....	46
FIGURE 22. PHOTO-INDUCED HYDROPHILIC MECHANISM AND HYDROPHOBIC CONVERSION ON TiO ₂ SURFACES....	47
FIGURE 23. TETRAHEDRAL COORDINATION OF WURTZITE STRUCTURE OF ZNO.....	49
FIGURE 24: WATER ABSORPTION APPARATUS.....	53
FIGURE 25. ZETA POTENTIAL IN FUNCTION OF pH FOR THE TiO ₂ NANOPARTICLES SUSPENSION.....	56
FIGURE 26: ANTIBACTERIAL ACTIVITY AGAINST <i>S. AUREUS</i> AND <i>P. AERUGINOSA</i> AS A FUNCTION OF THE NPS RETAINED ON THE BK COATED PAPER.....	57
FIGURE 27: ANTIBACTERIAL ACTIVITY OF BK COATED PAPER AGAINST <i>S. AUREUS</i> AT DIFFERENT STORAGE CONDITIONS.....	58
FIGURE 28: ANTIBACTERIAL ACTIVITY OF BK COATED PAPER AGAINST <i>P. AERUGINOSA</i> AT DIFFERENT STORAGE CONDITIONS.....	58
FIGURE 29: CELLULOSE DEGREE OF POLYMERIZATION REDUCTION BEHAVIOUR OVER TIME.....	59

FIGURE 30: BRIGHTNESS BEHAVIOUR OF BK PAPER AS A FUNCTION OF TIME.	60
FIGURE 31: ANTIBACTERIAL ACTIVITY TOWARD (A) <i>S. AUREUS</i> AND (B) <i>P. AERUGINOSA</i> OF THE CTMP COATED PAPER.	60
FIGURE 32: BRIGHTNESS BEHAVIOUR OF CTMP COATED PAPER AS A FUNCTION OF TIME.	61
FIGURE 33. ANTIBACTERIAL ACTIVITY OF TiO ₂ PCR COATED PAPER AGAINST <i>S. AUREUS</i>	62
FIGURE 34. SEM-EDX ANALYSIS OF THE PCR PAPER SURFACE.	63
FIGURE 35: RELATION BETWEEN THE AMOUNTS OF TiO ₂ NPs INITIALLY ADDED AND FINALLY RETAINED ON THE NFC.	65
FIGURE 36: RHEOLOGY MEASUREMENTS OF ZNO OVERPRINT VARNISH AND COMMERCIAL REFERENCE VARNISHES.	67
FIGURE 37: CROSS-SECTION OF THE CARDBOARD USED FOR THE PACKAGING DEMONSTRATOR.	68
FIGURE 38: LAYOUT DESIGN OF SAFEBOX.	69
FIGURE 39: DESIGN AND DIFFERENT STEPS IN THE DEVELOPMENT OF SAFEBOX.	69
FIGURE 40: BRIGHTNESS BEHAVIOUR OF THE SAFEBOX AND REFERENCE BOARDS.	70
FIGURE 41: SEM IMAGE OF SAFEBOX SURFACE.	71
FIGURE 42: ANTIBACTERIAL ACTIVITY AGAINST <i>S. AUREUS</i> AS FUNCTION OF ZNO NPs LOAD IN THE COATING FORMULATION.	71
FIGURE 43: PREPARATION OF RECYCLED PAPER SAMPLES.	72
FIGURE 44. DEGREE OF BIODEGRADATION OVER TIME FOR KRAFT PAPER COATED WITH NANOPARTICLES.	73
FIGURE 45. DEGREE OF BIODEGRADATION OVER TIME FOR SAFEBOX AND REFERENCE SAMPLES.	75

List of Tables

TABLE 1. FUNCTIONS OF PACKAGING AND RESPECTIVE MAIN FEATURES.	1
TABLE 2. MAIN ACTIVE PACKAGING SYSTEMS, MECHANISMS, APPLICATIONS AND COMMERCIAL EXAMPLES.	6
TABLE 3. CLASSES OF PHENOLIC COMPOUNDS.	14
TABLE 4. GLYCOSYLATED FORMS OF FLAVONOLS.	14
TABLE 5. MAJOR THEAFLAVINS.	15
TABLE 6. PRINCIPAL ALKALOIDS AND L-THEANINE.	16
TABLE 7. CHEMICAL COMPOSITION OF TEA INFUSION RESIDUE.	25
TABLE 8. EXTRACTION YIELDS OF TEA RESIDUES IN WATER AT 80 °C UNDER DIFFERENT CONDITIONS OF INFUSION.	27
TABLE 9. PHENOLIC COMPOUNDS, AMINOACIDS AND ALKALOIDS IDENTIFIED IN THE TEA EXTRACTS.	33
TABLE 10. LOG REDUCTION OF THE NUMBER OF COLONIES OF <i>S. AUREUS</i> AND <i>E. COLI</i> AFTER 8H OF CONTACT TIME.	38
TABLE 11: SIZE VALUES OF INHIBITION ZONE FOR THE CMC COATING FORMULATIONS.	40
TABLE 12. OVERVIEW ON TiO ₂ STRUCTURES, PROPERTIES, SYNTHESIS AND GENERAL APPLICATIONS.	44
TABLE 13. CHARACTERISTICS OF THE PAPERS USED FOR THE DIP-COATING TREATMENT.	57
TABLE 14. ANTIBACTERIAL RESULTS FOR BPK COATED SAMPLES.	63
TABLE 15. RETENTION EFFICIENCY OF THE NFC/TiO ₂ NPs BASED COATING FORMULATIONS.	64
TABLE 16. ANTIBACTERIAL ACTIVITY OF ROD-COATED NFC/TiO ₂ BASED BPK PAPER BOARD AGAINST <i>S. AUREUS</i>	65
TABLE 17. SPECIFICATIONS OF THE CARDBOARD USED FOR THE PACKAGING DEMONSTRATOR.	68
TABLE 18. ANTIBACTERIAL RESULTS FOR ZNO NPs BASED SAMPLES.	70
TABLE 19. TiO ₂ CONCENTRATION OF THE PAPER SAMPLES.	73

Chapter 1. Literature Review

1. Packaging

Packaging refers to “all products made of any materials of any nature to be used for the containment, protection, handling, delivery and presentation of goods, from raw materials to processed goods, from the producer to the user or the consumer” as defined in the European Parliament and Council Directive 94/62/EC of 20 December 1994 on packaging and packaging waste and following amendments, likewise it is used all over the world in numerous fields including food and beverages, healthcare and cosmetics. In Table 1 are listed the main features of the most considered functions of packaging: containment, protection, convenience and information (ECR, 2009).

Table 1. Functions of packaging and respective main features.

Function	Features
Containment and Protection	Contain the product Mechanical protection Barrier to moisture, gases, light, flavours and aromas Prevent contamination Increase shelf life Prevent adulteration and theft
Convenience	Product preparation and serving Product storage Portioning
Information	Identification and Description of product List of ingredients Product features & benefits (storage, preparation, usage and nutritional data) Opening instructions Promotional messages (sales) and branding Safety warnings Contact information End of life management

There are three different levels of packaging (EU, 1994; Robertson, 2012):

- i. Primary packaging: provides the initial protection barrier, being in direct contact with the packed product and defined also as sales packaging units, as it is normally the package that the final user/consumer purchases in the point of sale;

- ii. Secondary packaging or grouped packaging: contains several primary packages, is normally the unit used by the retailer and it serves to group the sales units and/or to fill the shelves;
- iii. Tertiary packaging: defined as transport packaging, serves to facilitate the handling and the transport of the secondary packages or a number of primary packages, preventing their damage (not include road, rail, ship and air containers).

Since ancient times, social and market demands step-up the packaging development. More recently, in a global economy, the increasing awareness for a sustainable society allowed the progression on: high-performance packaging, for instance, high-barrier materials and active and intelligent packaging; inclusion of nanotechnology; use of sustainable fibre-based packaging materials (like cellulose in paper-based packaging) reducing the fossil-based products; and impositions on waste reducing and recycling targets. Accordingly, the amount of package should be only the necessary to perform their role, so a proper balance should be found in order to avoid excess of package (over-packaging), the damage and spoilage of the product contents (under-packaging), not to waste valuable resources (EU, 1994). In the global packaging market, Smithers Pira in the report “The Future of Global Packaging to 2018” forecasts that the sales value will reach over one trillion US dollars, where the food and beverages industry sectors account for around 40% of total sales of packaging. Moreover, the food packaging industry has a vital role, to contribute for increasing shelf-life and reduction of food loss, even more taking into consideration that worldwide, a billion of people is starving when up to one third of the food produced (human consumption) is lost or wasted (FAO, 2014). Currently, smart packaging, which includes active packaging, intelligent packaging and modified atmosphere packaging (MAP), represent around 4.5% of the market (Statistics, 2015).

In packaging, many different types of materials can be used depending on the packed product requirements: paper and board, rigid and flexible plastics, glass and metals. Paper and paper board materials are the largest segment of the global packaging market accounting to almost 35% of the total packaging products. The second segment is rigid plastics with 27%, whereas flexible plastics totalize only 10% and glass and beverage cans represent around 11% and 6%, respectively, of the worldwide packaging market (EY, 2013).

1.1 Paper and paper-based products as sustainable fibre-based packaging materials

Paper and paper-based products are made of cellulose fibres originated mainly from wood (97%) and some other sources of biomass, as hemp, flax, bamboo (non-wood fibres). Secondary/recycled fibres obtained from recovered used paper represent a large share of cellulose fibres utilized in packaging products especially secondary packaging. Typical paper based packaging products include: envelopes, paper bags or sacks, boxes, containerboard, so they could constitute a primary and/or a secondary packaging and normally are used together with coatings, plastic materials and/or other components that guarantee additional specific properties as barrier and sealability (ECR, 2009; Robertson, 2012).

Several steps are involved in the paper production (Bajpai, 2015):

- Raw material preparation and handling: debarking, chipping, conveying, etc.;
- Chemical, semi-chemical and mechanical pulping;
- Chemical recovery: evaporation, recovery boiler, recausticizing, calcining;
- Mechanical or chemical pulp bleaching;
- Stock preparation;
- Papermaking: dewatering, pressing and drying, finishing.

The main chemical composition of wood fibres and the most common pulping methods are further explained.

1.1.1 Wood cell wall compounds

Wood fibres constitute a renewable raw material and their cell wall is mainly composed by cellulose (40-45%), hemicelluloses (15-25%) and lignin (20-30%) (Roger *et al.*, 2012). Cellulose is the most abundant organic compound found in nature, built up with units of β -D-glucopyranose ($C_6H_{11}O_5$) linked by β -(1 \rightarrow 4) glucosidic bonds. The repetition unit of cellulose is constituted by two-glucose units, named cellobiose (Figure 1), and the degree of polymerization (DP), correspondent to the number of glucose units, is around 10000 in native wood (Roger *et al.*, 2012).

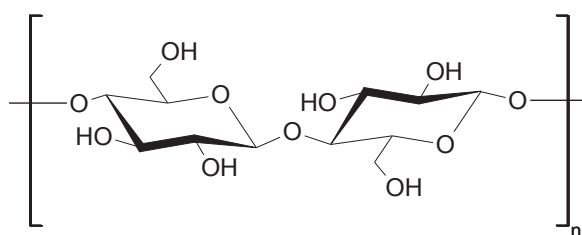


Figure 1. Partial structure of cellulose.

The linear cellulose polymer chains, through their hydroxyl groups, have the ability to form intra- and inter-molecular hydrogen bonds. The chains align in parallel, where amorphous regions (low order) alternate with crystalline regions (high order), creating an assembly of microfibrils and subsequent fibre structures, that will influence the physical properties of cellulose. The hydroxyl groups from the low-order regions are accessible to chemical reactions, while the high order regions are of difficult access. Cellulose can be easily converted into water-soluble sugars by acidic hydrolysis, being relatively resistant to oxidants. So, cellulose through bleaching could be purified without losing its strength (Robertson, 2012; Roger *et al.*, 2012; Vuoti *et al.*, 2013).

Hemicelluloses are highly branched hetero-polysaccharides, with lower DP, relatively to cellulose. They can be constituted by: pentoses, as D-xylose and L-arabinofuranose; hexoses, as D-galactose, D-mannose and L-rhamnose; and also by uronic acids like D-glucuronic acid. They are normally soluble in weak alkalis (Robertson, 2012; Roger *et al.*, 2012).

The compounds of the cell wall are naturally bond by lignin, the aim of which is to reinforce the structure of wood. Lignin is a highly branched copolymer with a very complex alkylaromatic structure, constituted by units of phenylpropane. The alcohols: *p*-coumaryl, coniferyl and sinapyl (Figure 2) are their main precursors (Robertson, 2012; Roger *et al.*, 2012).

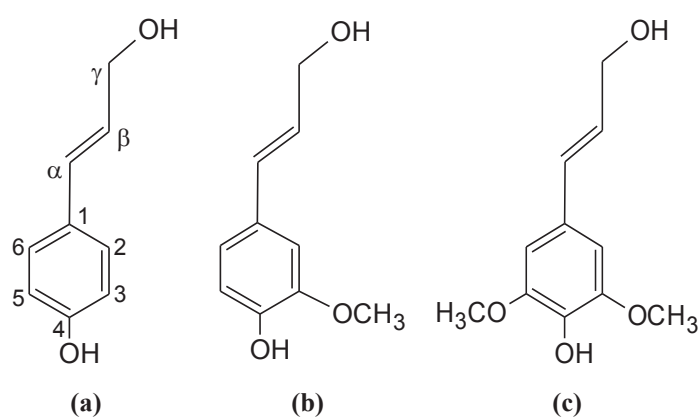


Figure 2. Alcohols precursor of lignin: (a) *p*-coumaryl, (b) coniferyl and (c) sinapyl.

1.1.2 Pulp production technologies

Cellulose pulp is a fibrous mass constituted mainly by cellulose, obtained from defibration of wood or other lignocellulosic material by mechanical, chemical or a combination of both processes, i.e. pulping. Different pulping processes provide pulps with different properties, the most common are chemical pulps that account for 90% of the total production and show the best mechanical properties although they present a low fibre yield (45-55%) in comparison to

the yield (89-95%) of the mechanical pulping processes (Bajpai, 2015; Robertson, 2012; Sixta *et al.*, 2008).

The preparation of chemical pulps is based on sulfate (Kraft) and sulfite cooking processes and involves the remotion of lignin with preservation of the carbohydrates and of pulp properties, to a certain extent. In the Kraft process are used sodium sulphide and sodium hydroxide, as cooking liquor (white liquor); the resulting pulp of this alkaline pulping is stronger than with sulfite pulping. For the sulfite pulping is used an acidic liquor constituted by sulfurous acid and bisulfite ion (HSO_3^-), the resulting pulps are more suitable for speciality papers like fine paper, can be better bleached (normally with hydrogen peroxide) and relatively to Kraft pulp, present higher brightness, higher yields of delignification and lower investment costs. Mechanical pulping can be divided into groundwood or refining pulping, depending if the mechanical wood defibration is performed by a grindstone or a disc refiner, respectively. Contrarily to chemical pulps, almost all the wood fibres are used to produce groundwood pulp, so with a very high level of lignin (high kappa number); the resulting fibres are consequently very stiff, bulky and with the lowest strength, being mainly used for low quality paper, newsprint and magazine papers and board for several applications. The chemithermomechanical pulp (CTMP) is a sub-type of refining pulp, resulting from the combination of chemical and mechanical pulping processes, where wood chips are previous treated with sodium sulfite and sodium carbonate solutions at temperatures up to 150 °C, and only after submitted to mechanical refining under pressure. CTMP pulping provides fibres with the highest strength, strong color and brightness (Bajpai, 2015; Blechschmidt *et al.*, 2008; Sixta *et al.*, 2008; Robertson, 2012).

2. Overview on Active packaging

Active packaging, unlike traditional packaging that are inert, actively interact with the packaged product and/or the packaging headspace, enhancing the performance of the system. Active food contact materials and articles, including active food packaging, as stated in the Regulation (EC) n° 1935/2004, “are designed to deliberately incorporate active components intended to absorb substances from the food or to be released into the food”, in order to extend the shelf-life or to improve or maintain the quality of the food (EU, 2004, 2009). Moreover, regulation (EC) n° 450/2009 and general requirements from Regulation (EC) No 1935/2004 regulate the use and the safety of active packaging destined to be in contact with food.

Active packaging systems can be used for many different purposes, and include: oxygen and ethylene scavengers, carbon dioxide scavengers and emitters, moisture regulators, flavour/odour absorbers, and antioxidant and antimicrobial packaging. Some of the mechanisms associated to active packaging systems, their food applications and few commercial examples are presented in Table 2 (Kerry *et al.*, 2008; Pereira *et al.*, 2015; Robertson, 2012) and described further.

Table 2. Main active packaging systems, mechanisms, applications and commercial examples.

Systems	Mechanisms	Food applications	Commercial examples
O ₂ scavengers	Iron based, metal/acid, Nylon MXD6, metal (e.g. platinum) catalyst, ascorbate/metallic salts, enzyme based	Bread, cakes, cooked rice, biscuits, pizza, pasta, cheese, cured meats and fish, coffee, snack foods, dried foods and beverages	Ageless® (Mitsubishi Gas Chemical Co., Japan), in sachet, pressure-sensitive label or card formats; FreshPax® packets and strips (Multisorb Technologies, Inc., USA); OXY-GUARD® (Clariant International Ltd, Switzerland)
CO ₂ scavengers/emitters	Iron oxide/calcium hydroxide, ferrous carbonate/metal halide, calcium oxide/activated charcoal, ascorbate/sodium bicarbonate	Coffee, fresh meats and fish, nuts and other snack food products and sponge cakes	Verifrais® (S.A.R.L. Codimer, France); Dual action CO ₂ scavenger and O ₂ emitter: Ageless®G in sachet, pressure-sensitive label or card formats (Mitsubishi Gas Chemical Co., Japan), sachet (EMCO Packaging Systems Ltd, UK).
Ethylene scavengers	Potassium permanganate, activated carbon, activated clays/zeolites	Fruit, vegetables and other horticultural products	Power Pellet sachets (Ethylene Control, Inc., USA); Air Repair (DeltaTrak, Inc., USA); Green bags™ for food storage (Evert-Fresh, USA)
Ethanol emitters	Encapsulated ethanol	Pizza crusts, cakes, bread, biscuits, fish and bakery products	Antimold-Mild® (Freund Co., Japan)
Moisture regulators	Polyvinyl acetate blanket, Activated clays and minerals, Silica gel	Fish, meats, poultry, snack foods, cereals, dried foods, sandwiches, fruit and vegetables	DesiPak® sachets (Multisorb Technologies Inc., U.S.A.); Dri-Fresh™ (Sirane Ltd., UK)
Preservative releasers	Organic acids, silver zeolite, spice and herb extracts, BHA/BHT antioxidants, vitamin E antioxidant, chlorine dioxide/sulphur dioxide	Cereals, meats, fish, bread, cheese, snack foods, fruit and vegetables	Agion® antimicrobial technology (Sciessent, USA); Food Touch® paper (Microbeguard Co., USA); Food grade compounds (BASF Group, Germany)

2.1 Oxygen scavenging technology

The presence of oxygen in the headspace of a package could: reduce the nutritional value of food products; cause changes of colour, flavour and texture; and contribute to microbial proliferation; leading to an increase of the food metabolism and consequent fast degradation. Therefore, the use of oxygen scavengers (OS) to remove O₂ will: inhibit the oxidation reactions, preventing the loss of oxygen-sensitive nutrients, discoloration of food and changes in flavour and texture; prevent the growth of microorganisms; reduce or even avoid the incorporation of

preservatives/anti-oxidants compounds in food, leading to an increment of the shelf-life of the food. At a commercial level, oxygen scavengers are the most important type of active packaging, being normally provided as small, oxygen permeable sachets and then incorporated in the package. Besides, the substances that constitute the scavenger can also be delivered in a bag, strip or label, as an independent system or even combined in the package structure itself, being used alone or combined with modified atmosphere packaging (MAP). Among several O₂ scavenging technologies, the widest is based on the iron oxidation. The iron powder within the sachet oxidizes (undergoes rusting) and consumes the oxygen of the headspace of the food packaging in the presence of some moisture, until saturation. The iron oxidation reaction can be seen in the scheme of Figure 3 (Kerry *et al.*, 2008; Lim, 2011; Pereira de Abreu *et al.*, 2012; Vermeiren *et al.*, 1999).

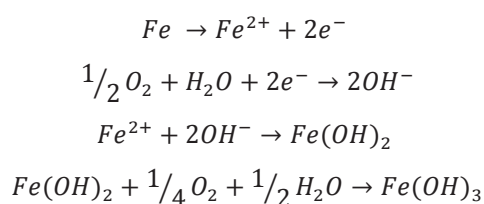


Figure 3. Iron oxidation reaction scheme.

Nonetheless, the type and size of scavenger required depends on the: nature of the food; water activity (a_w) and moisture content; initial oxygen content in the package headspace; permeability of the packaging to O₂; and the maximum acceptable O₂ intake for the requested food shelf-life (Lim, 2011; Robertson, 2012).

2.2 Carbon dioxide scavengers and emitters

CO₂ is liberated as a product of the aerobic respiration of fresh produce but also toasted and roasted food products can liberate CO₂. Carbon dioxide can inhibit the growth of microorganisms on the packed food but an excessive amount in the packaging headspace can cause food degradation and/or packaging swelling/bursting. Many types of CO₂ absorbers and emitters can be found in the market, mainly with a dual system action: absorption of O₂ together with emission or retention of CO₂. The most common carbon dioxide scavenger is constituted by calcium hydroxide that is converted in calcium carbonate and water by reaction with CO₂ (Brody *et al.*, 2001; Kerry *et al.*, 2008; Piergiovanni *et al.*, 2010; Robertson, 2012).

2.3 Ethylene scavengers

Ethylene is a plant hormone that could have beneficial or undesirable effects in fresh produce, being responsible of accelerating the respiration rate and consequent ripening. In packaged food

it is very important to slow down the effects of ethylene in order to increase the shelf-life and this could be achieved through ethylene scavengers. The most common types are delivered in sachets for inclusion in the packaging, like potassium permanganate, or incorporated directly in the packaging material, like zeolites or clays (Kerry *et al.*, 2008; Pereira de Abreu *et al.*, 2012; Vermeiren *et al.*, 1999).

2.4 Ethanol emitters

Ethanol with its anti-septic characteristics can prevent microbial growth especially on high water activity baked products. The release of ethanol vapour, absorbed or encapsulated in a carrier material inside sachets or in strips, into the packaging headspace, could therefore extend the shelf-life of the packaged food (Kerry *et al.*, 2008; Suppakul *et al.*, 2003).

2.5 Moisture regulators

Excess of moisture is one of the major causes of food spoilage. In moisture-sensitive packed foods if the condensate is not removed it will cause proliferation of molds and microbials, leading to food spoilage and/or fogging of the package. The use of moisture absorbers in the form of sachets, strips or blankets inside of a packaging is very important to prevent the side-effects of the moisture in the food (Pereira de Abreu *et al.*, 2012; Suppakul *et al.*, 2003).

2.6 Antimicrobial packaging concepts

Antimicrobial packaging aim to extend shelf-life by retarding, reducing or inhibiting microbial growth on perishable food, maintaining product quality and safety. There are several antimicrobial packaging concepts, involving the use of migratory or non-migratory active agents, such as (Appendini *et al.*, 2002; Dainelli *et al.*, 2008):

- i. Volatile antimicrobial compounds incorporated in sachets or pads;
- ii. Volatile and non-volatile antimicrobial compounds included into polymers;
- iii. Antimicrobials coated or adsorbed onto polymer surfaces;
- iv. Antimicrobials immobilization by ionic or covalent linkages to polymers;
- v. Antimicrobial polymers.

Several compounds incorporated or immobilized into packaging systems have been tested regarding their antimicrobial activity for food and medical packaging applications (Lim, 2011; Pereira de Abreu *et al.*, 2012; Suppakul *et al.*, 2003). Active packaging based on migratory agents implies a controlled release to the packaged product, one example is allyl isothiocyanate (AITC), a natural compound found in food, as horseradish and mustard. AITC is used as food

preservative, impregnated in a label inside of the packaging, for instance, acting by vapor release protecting the food from spoilage, therefore promoting a longer preservation. CO₂, ethanol, SO₂, essential oils and plant extracts act in the same way. The main advantage of volatile antimicrobial agents is that they do not need to be in direct contact with the food, an amount above the minimum inhibitory concentration (MIC) just needs to be released in the headspace of the packaging, in order to be effective. In contrast, non-migratory active agents implies the direct contact between the package and the product. Examples of non-volatile antimicrobial agents are organic acids (sorbic, benzoic and propionic acids), potassium and calcium sorbate, bacteriocins such as nisin and imazalil, non-volatile fractions of natural spice and herbs and metals (Appendini *et al.*, 2002; Lim, 2011; Pereira de Abreu *et al.*, 2012; Robertson, 2012). The use of chitosan as a carrier for antimicrobials agents or film matrix for food packaging applications is well known. This inherent antimicrobial polymer consists of a linear polysaccharide (β -(1 \rightarrow 4)-*N*-acetyl-D-glucosamine) that can be extracted from crustaceans, fungi and yeast and is the main natural polymer after cellulose (Lim, 2011). Peng *et al.*, 2013, improved the active efficacy of chitosan film by incorporating tea extracts, that also have contributed to enhance the water vapour barrier properties of the films, despite the decrease of the mechanical properties. Bacterial (BC), microfibrillated (MFC) and nanofibrillated (NFC) cellulose have recently raised a great deal of interest as a matrix for active compounds. For instance, Fernandes *et al.*, 2013 developed antimicrobial bacterial cellulose membranes by chemical grafting the nanofibrillated network structure with aminoalkyl groups, with improved mechanical and thermal properties. More recently, within the NEWGENPAK project, antimicrobial surfaces were developed by grafting MFC with active molecules, such as phenyl isothiocyanate (PITC) and the β -lactam antibiotic benzyl penicillin (Saini *et al.*, 2015a; Saini *et al.*, 2015b).

Chapter 2. Black Tea Residues: A Potential Source of Active Compounds for cellulose-based packaging products

1. Introduction

Tea is one of the most common and consumed beverage around the world, just surpassed by water, resulting from the brewing of the dried leaves and buds of the plant *Camellia sinensis*, first cultivated in China and brought to Europe in the 15th-17th centuries (Wang *et al.*, 2009). Black tea represents more than 75% of the worldwide tea production and is the tea infusion with the higher consumption on the Western part, of almost 80% of the 40 L world per capita tea consumption (Almajano *et al.*, 2008; Wang *et al.*, 2009). The polyphenols extracted in water during tea infusion are a very well-known source of beneficial antioxidant and antiradical compounds. Their properties are widely studied and their positive effects on human health are well recognized; accordingly, they are already used as additives in food industry, for pharmaceutical applications, in cosmetics and agriculture (Almajano *et al.*, 2008; Anesini *et al.*, 2008; Atoui *et al.*, 2005; Daglia, 2012; Schieber *et al.*, 2001; Stratil *et al.*, 2006). Nonetheless, although a significant part of these compounds are not fully extracted during tea infusion, much less information is available concerning the chemical characterization of the tea residues as well as their potential application in different industrial fields (Yang *et al.*, 2015; Yuda *et al.*, 2012).

A large amount of tea waste is potentially available not only from household collection but also from industries producing tea-based beverages. These waste materials are an interesting bio-based chemical feedstock which can be exploited for many potential applications. This part of the work aimed to explore the possibilities to extract polyphenols from tea residues and use them to develop antioxidant and antimicrobial paper based surfaces. Initially, we have addressed the chemical characterization of black tea residues as well as the antioxidant and antimicrobial properties of their extracts. After investigating the best extraction conditions, including parameters such as temperature and time of extraction, the potential applications of the most feasible extract to develop paper-based packaging materials was finally studied.

1.1 Tea: types and processing

Fresh leaves of *Camellia sinensis* are mainly constituted by polyphenols, but also by alkaloids, enzymes, proteins and aminoacids, carotenoids, chlorophylls, carbohydrates, lipids, minerals, volatile/flavour compounds, organic acids, vitamins and other minor compounds (Cabrera *et al.*, 2003; Engelhardt, 2010; Namal Senanayake, 2013).

There are several tea varieties with different characteristics mainly depending on the level of oxidation (generally designated by fermentation level) that tea leaves are subjected during processing. The three more common types of tea are: green tea (non-fermented tea), oolong tea (partially fermented tea), and black tea (fully fermented tea) representing respectively around 20%, 2% and 78% of the tea consumption worldwide (Li *et al.*, 2013; Pękal *et al.*, 2011; Wang *et al.*, 2009).

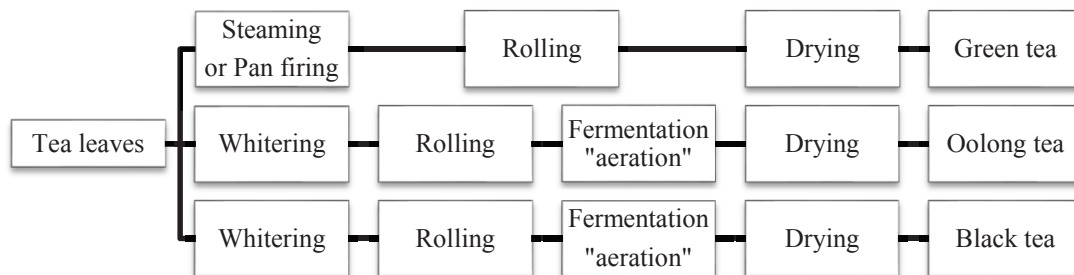


Figure 4. Overview on tea processing.
(adapted from Engelhardt, 2010)

1.1.1 Green tea

The manufacturing of green tea implies an inactivation of the oxidizing enzymes, like polyphenol oxidase (PPO) and peroxidase (POD), by steaming (Japanese green tea) or pan firing (Chinese green tea) tea leaves, just before plucking and followed by rolling and drying processes. Likewise, the original polyphenol content of the leaves, mainly catechins, and their green colour are mostly maintained by stopping the fermentation (Bansal *et al.*, 2013; Wang *et al.*, 2009).

1.1.2 Oolong tea

For the processing of Oolong tea, after plucking, tea leaves are withered, this bringing about moisture loss and enzymatic reactions. After rolling, a partial oxidation occurs that terminates with the drying process (firing). The resulting semi-fermented tea presents characteristics between green and black tea, with a significant amount of the original polyphenols (Wang *et al.*, 2009).

1.1.3 Black tea

The black tea production is characterized by a complete fermentation, where catechins (the main polyphenols from tea leaves) are partially oxidized and polymerized into theaflavins and thearubigins. Those compounds are associated to the dark colour and characteristic bitter taste of black tea (Peřkal *et al.*, 2011).

1.2 Chemistry of major active compounds in tea

In fresh green tea leaves there are several active compounds: alkaloids, flavonoids, steroids, phenols and terpenoids (Anand *et al.*, 2015). The manufacturing process of tea, specially harvesting and fermentation, and also brewing are associated to the differences in the antioxidant and antiradical activity of tea and their infusions, as they influence the chemical composition and content of the active compounds. In green tea, polyphenols, mainly catechins, are the main active compounds, representing 25-35% of the dry weight of the leaves. Black tea contains larger amounts of gallic acid and also theaflavins and thearubigins, resulting from the partial oxidation and condensation of around 85% of the total phenolic compounds, occurring during tea fermentation. In the Oolong tea catechins are mainly present, but also some theaflavins and thearubigins, due to a partial fermentation of the leaves in the tea process. All types of tea contain caffeine, in the range of 1-5% (Almajano *et al.*, 2008; Li *et al.*, 2013; Perva-Uzunalić *et al.*, 2006).

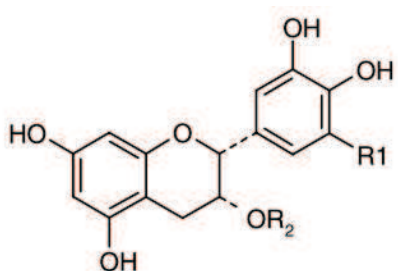
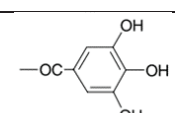
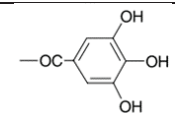
1.2.1 Phenolic compounds

Phenolic compounds are the most common antioxidants found in nature and range from simple phenolic molecules to highly polymerised structures. The most representative classes of these compounds are flavonoids and phenolic acids (Anand *et al.*, 2015; Tan *et al.*, 2015).

1.2.1.1 Flavonoids

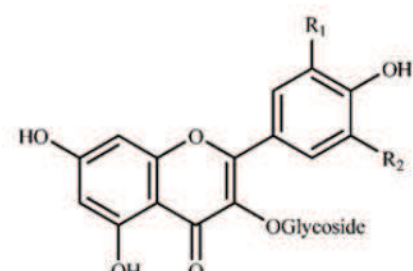
Flavonoids are sub-divided in to catechins (mainly) and flavonols, flavones, flavanones, isoflavones and anthocyanidins, representing around 1/3 of the water-extractable solid content of a typical tea beverage. The catechins: (-) epicatechin (EC), (-) epigallocatechin (EGC), (-) epicatechin-3-gallate (ECG) and (-) epigallocatechin-3-gallate (EGCG) are the principal tea flavonoids (Table 3). Although in minor content, (+) Catechin (C), (-) catechin gallate (CG), (+) gallic acid (GA) and (-) gallic acid gallate (GCG) are also present. In green tea, EGCG alone represents half of the total content of polyphenols (Anand *et al.*, 2015; Cabrera *et al.*, 2003; Perva-Uzunalić *et al.*, 2006; Sang *et al.*, 2011).

Table 3. Classes of phenolic compounds.

Compound	Main structure	R1	R2
(-) Epicatechin (EC)		H	H
(-) Epigallocatechin (EGC)		H	
(-) Epicatechin-3-gallate (ECG)		OH	H
(-) Epigallocatechin-3-gallate (EGCG)		OH	

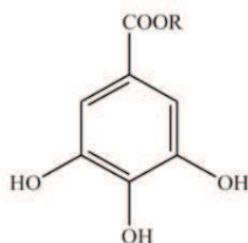
Flavonols, including quercetin, kaempferol, myricetin, and their glycosylated forms, represented in Table 4, and flavones (apigenin and luteolin) are also present in tea, in smaller amounts (Perva-Uzunalić *et al.*, 2006; Sang *et al.*, 2011).

Table 4. Glycosylated forms of flavonols.

Compound	Main structure	R1	R2
Kaempferol glycoside		H	H
Quercetin glycoside		OH	H
Myricetin glycoside		OH	OH

1.2.1.2 Phenolic acids

In fresh tea leaves, gallic acid (GA) and theogallin (TG; 5-galloylquinic acid) are the main simple phenolic compounds (Figure 5). GA is present in higher amounts in black tea, due to the oxidation of phenolic compounds during fermentation, whereas the amount of TG decreases by the condensation of this compound together with (-) epicatechin (EC) into theogallin (Li *et al.*, 2013; Sang *et al.*, 2011).

**Figure 5.** Gallic acid, R=H; Theogallin, R= quinic acid.

1.2.1.3 Theaflavins and thearubigins

Theaflavins and thearubigins are formed during the fermentation process, mainly by oxidation of catechins through polyphenol oxidase (PPO) and peroxidase (POD) enzymes (Harbowy *et al.*, 1997; Wang *et al.*, 2009). Likewise, they are mostly found in black tea and are the main contributors to the yellow to brown colours of the tea. Theaflavins are very well characterized regarding their molecular structure and health promotion and represent around 2-6% of the solids on the water-soluble fraction of black tea. Theaflavin (TF), theaflavin-3-gallate (TF3G), theaflavin-3'-gallate (TF3'G) and theaflavin-3,3'-digallate (TFDG) are the four major theaflavins (Table 5) found in black tea (Haslam, 2003; Sang *et al.*, 2004).

Table 5. Major theaflavins.

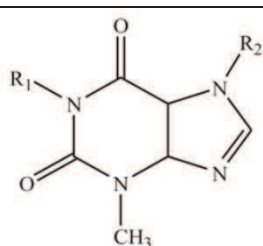
Compound	Main structure	R1	R2
Theaflavin (TF)		H	H
Theaflavin-3-gallate (TF3G)			H
Theaflavin-3'-gallate (TF3'G)		H	
Theaflavin-3,3'-digallate (TFDG)			

Thearubigins are present in much higher quantity than theaflavins in black tea leaves, accounting for up than 20% of dry weight and due to their high water solubility could reach 60% of the solids in the black tea beverage. Several authors have been suggesting the further oxidation of catechins and even theaflavins for the formation of these compounds, however much more information about their molecular structures and mechanisms are still missing (Haslam, 2003; Sang *et al.*, 2011; Stodt *et al.*, 2015; Wang *et al.*, 2009).

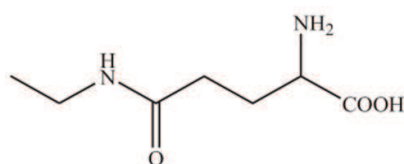
1.2.2 Alkaloids and Aminoacids

Caffeine is the richest alkaloid present in tea leaves, while theobromine and theophylline are relatively much less abundant (Table 6). Moreover, contrarily to what happens for the last two classes of compounds, caffeine was found to be a very stable xanthine during fermentation, as its content (2-5% dry weight of water soluble extracts) did not present significative differences after either black or green tea processing (Carloni *et al.*, 2013; Chow *et al.*, 2011; Harbowy *et al.*, 1997; Li *et al.*, 2013; Sang *et al.*, 2011; Yi *et al.*, 2015).

Table 6. Principal Alkaloids and L-theanine.

Compound	Main structure	R1	R2
Caffeine (CAF)		CH3	CH3
Theobromine		H	CH3
Theophylline		CH3	H

L-Theanine (Figure 6) is only found in tea and represents more than half of the total aminoacids. It accounts up to 3% of water-extractable solid content but is highly dependent on tea processing (Engelhardt, 2010; Sang *et al.*, 2011).

**Figure 6.** L-Theanine.

1.3 Antioxidant and Antibacterial activity of tea polyphenols

Phenolic compounds are the most common antioxidants found in nature and the antioxidant/antimicrobial activity correlates with their capacity for scavenging and/or reducing free radicals, like reactive oxygen species (ROS). Thus inhibiting the enzymes involved in the oxidative stress and the chelation of transition metal ions have been widely studied (Akrami *et al.*, 2015; Almajano *et al.*, 2008; Anesini *et al.*, 2008; Atoui *et al.*, 2005; Bansal *et al.*, 2013; Cabrera *et al.*, 2003; Carloni *et al.*, 2013; Chan *et al.*, 2011; Cheynier, 2012; Chow *et al.*, 2011; Cushnie *et al.*, 2011; Daglia, 2012; Farhoosh *et al.*, 2007; Friedman *et al.*, 2006; Ignat *et al.*, 2013; Jeszka-Skowron *et al.*, 2015; Kikuzaki *et al.*, 2002; Namal Senanayake, 2013; Pękal *et al.*, 2011; Perva-Uzunalić *et al.*, 2006; Radji *et al.*, 2013; Sang *et al.*, 2011; Sang *et al.*, 2004; Schieber *et al.*, 2001; Siripatrawan *et al.*, 2010; van der Pijl *et al.*, 2015; Yang *et al.*, 2015; Yi *et al.*, 2014; Yuda *et al.*, 2012; Zandi *et al.*, 1999). Tea benefits associate mostly to the content and mechanism of action of flavonoids, which are dependent on the fermentation process. The exploitation of tea residues for the development of functional ingredients for commercial applications might have a great potential. Among the few studies reported on this matter, Zandi *et al.*, 1999, already demonstrated the maintenance of the antioxidant activity by old leaves compared to the initial raw material, showing that this “waste” is still rich of high-value compounds. Multifunctional coatings based on polyphenols were performed by Sileika *et al.*,

2013, using tannic acid (TA) or pyrogallol (PG), their building blocks and trihydroxyphenyl-containing molecules as coating precursors instead of monolayer adsorbates or ingredients in multicomponent coatings, like other authors have reported (Huang *et al.*, 2007; Payra *et al.*, 2016; Sileika *et al.*, 2013; Silva *et al.*, 2007; Zhao *et al.*, 2008). The main advantages of these polyphenol-inspired coatings are the simple substrate application, wide materials deposition, absence of absence of colour and low cost, together with their proved antibacterial properties against both *P. aeruginosa* and *S. aureus* strains when deposited as a film in polycarbonate disks (Barrett *et al.*, 2014; Sileika *et al.*, 2013). Furthermore, Payra *et al.*, 2016, reported the contact-based bacteria killing and good barrier ability against corrosive media of modified polyphenols based thin-films on solid surfaces and Yang *et al.*, 2015, described the high potential of tea waste as a substrate for oyster mushroom cultivation, revealing a high yield, biological efficiency and a relatively shorter cropping time.

2. Materials and Methods

2.1 Black tea residues

Black tea leaves were purchased from commercial stores and then subjected to a typical household infusion for 5 minutes, in order to obtain the residue. The solid residue was then collected on a filter, dried at room temperature, stored in sealed plastic bags and kept at -20 °C before analysis.

2.2 Chemical characterization of tea residues

The black tea residue was grounded according to the National Renewable Energy Laboratory (NREL) sample preparation method (Technical Report NREL/TP-510-42620, 2008), then the collected material was sieved to obtain a sample with particle size in the range of 200-1000 microns, before proceeding to chemical analysis. The chemical characterization was carried out at least in duplicate (for each procedure), following mainly the methods proposed by NREL for the biomass analysis.

2.2.1 Total solids content

The total solids content was determined by drying around 1 g of sample at 105 °C in an oven, until constant weight (Technical Report NREL/TP-510-42621, 2008) and calculated using Equation 1.

$$\% \text{ Total solids} = \frac{\text{Weight}_{\text{dry sample}}}{\text{Weight}_{\text{sample as received}}} \times 100 \quad \text{Equation 1}$$

Consequently, for further analysis, the oven-dry weight (ODW) of a sample could be calculated by Equation 2.

$$ODW = \frac{Weight_{sample} \times \%Total\ solids}{100} \quad \text{Equation 2}$$

2.2.2 Ashes

For the determination of the ashes content (i.e., inorganic material), about 1 g of oven-dried sample was placed overnight in a muffle furnace at 575 °C. The methodology described in the Technical Report NREL/TP-510-42622, 2008 was followed and the ashes percentage was calculated using Equation 3.

$$\% Ashes = \frac{Weight_{ashes}}{Weight_{oven-dry\ tea\ sample}} \times 100 \quad \text{Equation 3}$$

2.2.3 Acetone extracts

In order to determine the acetone extracts (TAPPI T280 PM-99), approximately 10 g of sample were weighted in tared extraction thimbles and transferred to the Soxhlet extractor. Subsequently, 150 mL of acetone was added to a round-bottom flask, which was then connected to the Soxhlet extraction apparatus. After 4 h extraction period, the solvent was evaporated to dryness using a rotary evaporator and the acetone extracts content was determined (Equation 4).

$$\%Acetone\ extractives = \frac{ODW_{extract}}{ODW_{sample}} \times 100 \quad \text{Equation 4}$$

2.2.4 Hexane extracts

The hexane extracts were determined using an internal method, similar to the methodology used for acetone extraction. Approximately 5 g of sample were weighted in tared extraction thimbles and transferred to a Soxhlet extractor. Subsequently, 150 mL of hexane was added to a round-bottom flask, which was then connected to the Soxhlet extraction apparatus. After 4 h extraction period, the solvent was evaporated to dryness using a rotary evaporator and the hexane extracts content was determined (Equation 5).

$$\%Hexane\ extractives = \frac{ODW_{extract}}{ODW_{sample}} \times 100 \quad \text{Equation 5}$$

2.2.5 Extracts in water and ethanol

Water and ethanol extracts were quantified following a two-steps procedure (Technical Report NREL/TP-510-42619). First, 10 g of tea residues were placed in an extraction thimble and a

Soxhlet extraction was carried out with 200 mL of water for 8 hours. The water extracts were then removed, but the thimble was kept in the Soxhlet extractor. Subsequently, 200 mL of ethanol were added to a new round-bottom flask, which was then connected to the Soxhlet apparatus, in order to submit the water-extracted sample to 16 h of ethanol extraction. The extracted solids were removed from the thimble, washed with ethanol and filtered through a filter paper using a Buchner funnel. Water and ethanol in both round-bottom flasks were removed by evaporation using a rotary evaporator. Finally, the round-bottom flasks containing the dry extracts were weighed, and the water and ethanol extracts were calculated using Equation 6.

$$\% \text{ Extractives} = \frac{\text{Weight}_{\text{flask plus extractives}} - \text{Weight}_{\text{flask}}}{\text{ODW}_{\text{sample}}} \times 100 \quad \text{Equation 6}$$

2.2.6 Proteins

Protein content (Technical Report NREL/TP-510-42625) was determined indirectly by the measurement of nitrogen content according to the Kjeldahl method. The Kjeldahl method consists of three basic steps: 1) digestion of the sample in sulfuric acid with a catalyst, which results in conversion of nitrogen to ammonia; 2) distillation of ammonia into a trapping solution; and 3) quantification of ammonia by titration with a standard solution. Approximately 1g of sample was weighted onto a digestion flask and then were added 16.7 g K₂SO₄, 0.01 g anhydrous copper sulfate, 0.6 g TiO₂, 3 g pumice and also 20 mL of H₂SO₄ at 95-98%. The flask was placed on the preheated burner (adjusted to bring 250 mL water at 25°C to rolling boil in 5 min) and heated for 40 minutes. 250 mL of distilled water were added and the system was cooled to room temperature (less than 25 °C). For the distillation, the titration flask was prepared by adding accurately 15 mL of HCl (37%) into 70 mL of water. For the reagent blank, it was used 1 mL of acid to 85 mL of water. Then, were added 3 to 4 drops of methyl red indicator solution and also 2 to 3 drops of tributyl citrate for reducing foaming. 45% sodium hydroxide solution was added in excess to make the mixture strongly alkaline. The flask was immediately connected to the distillation apparatus and the mixture was distilled at about 7.5 boil rate (temperature set to bring 250 mL water at 25 °C to boil in 7.5 min) until a minimum of 150 mL distillate collected in titrating flask. The excess acid was then titrated with a standard NaOH solution and the volume was recorded to nearest 0.01 mL (V_{NaOH}). The reagent blank (B) was titrated similarly. The nitrogen content was determined using Equation 7.

$$\% N = \frac{(V_{\text{HCl}} \times N_{\text{HCl}}) - (V_{\text{BK}} \times N_{\text{NaOH}}) - (V_{\text{NaOH}} \times N_{\text{NaOH}})}{1.4007 \times W} \quad \text{Equation 7}$$

The protein content was then calculated, using a nitrogen-to-protein conversion multiplier (N factor) of 6.25, following Equation 8.

$$\% \text{ Protein} = \% \text{ Nitrogen} \times NF \quad \text{Equation 8}$$

Where: NF (N factor) = 6.25.

2.2.7 Structural Carbohydrates and Lignin

Acetone extracted free samples were incubated with 72% (w/w) H₂SO₄ for 1 h, in a water bath (30°C) with manual shaking every 15 min. Then the samples were diluted with water to a final concentration of 4% (w/w) H₂SO₄, transferred into screwed cup bottles of 250 mL (Schott, Germany), and placed in the autoclave for 1 h at 121 °C. After completion of the autoclave cycle and subsequent cooling, the resultant liquid hydrolysed suspension was filtered through pre-weighed oven-dried filters (glass microfiber filter 300 microns). The liquid phase was treated with calcium carbonate until pH 5-6 to avoid sugars degradation; the supernatant collected after removal of precipitated salt was characterized using HPLC with a SHODEX SP0810 column, for glucose, xylose, arabinose, galactose and mannose quantification (external standards were used for each analysed compound). The solid acid insoluble residue deposited in the filtering crucibles was washed with distilled water to neutralise acidity thus avoiding weight loss during drying. The filters were dried for 18 h at 105 °C, cooled down in the desiccator, weighed and then incinerated in the muffle for 5 h at 550 °C. The dry mass corrected for the ash content and proteins was quantified as acid-insoluble residue (AIR) (Equation 9). Each sample was processed, at least, in duplicate.

$$\% \text{ AIR} = \frac{\text{Weight}_{\text{filter plus AIR}} - \text{Weight}_{\text{filter}}}{\text{ODW}_{\text{sample}}} \times 100 \quad \text{Equation 9}$$

Acid soluble substances (ASL) were analysed by spectrophotometry at 240 nm after proper dilution and calculated based on the molar absorptivity indicated in the Technical Report NREL/TP-510-42618 (Equation 10).

$$\% \text{ ASL} = \frac{\text{UV}_{\text{abs}} \times \text{Volume}_{\text{filtrate}} \times \text{Dilution}}{\text{Absorptivity of biomass} \times \text{ODW}_{\text{sample}} \times \text{Pathlength}} \times 100 \quad \text{Equation 10}$$

2.3 Preparation and characterization of black tea residue extracts

Infusion extracts were prepared by submitting black tea residues to a single extraction step by infusion at controlled temperature, 70, 80 or 90 °C. For this, 100 mL of distilled water were poured over the samples (2.5 or 5.0 g dry weight) in an Erlenmeyer flask and placed in a water bath at constant temperature, under stirring at 200 rpm for 5, 7.5 or 10 min. The infusions

(extract mixture) were filtered, first through a filter paper and then through a 0.45 µm porosity membrane. The infusion samples were then treated in different ways, depending on the further analysis:

- a. fresh infusion - kept in the fridge at 4 °C and analysed in few days or kept in the freeze at -20 °C and analysed after several weeks;
- b. concentrated infusion - the 15 fold concentrated extract obtained on a rotary evaporator (50 °C) was kept in the fridge at 4 °C and analysed within few days or kept in the freeze at -20 °C and analysed after several weeks;
- c. drying extracts - freeze-dried and kept the solid extracts in a desiccator, until further analysis.

Black tea residues were also fully extracted with water and ethanol by Soxhlet extraction, to examine the total extractable amount, using the methodology reported in section 2.2.5 (Technical Report NREL/TP-510-42619) with some modifications: each extraction was carried out in one single step for 8 h, using 2.5 g of tea residue per 200 mL of solvent, instead of 10 g per 150 mL. Extract mixtures were kept in the fridge at 04 °C and analysed within days or kept in the freeze at -20 °C and analysed after several weeks.

The extraction yield of the infusions and water/ethanol extract mixtures was calculated by determining the solid weight fraction of each extract mixture.

2.3.1 Determination of the total phenolic content

The Folin-Ciocalteu method was used to assess the total phenolic content (TPC) of infusion samples and Soxhlet water and ethanol extracts (Anesini *et al.*, 2008; Peşkal *et al.*, 2012). Aliquots (1.0 mL) of fresh tea residue extracts were transferred into different test tubes containing 5.0 mL of 10-fold diluted Folin-Ciocalteu's reagent in water. The tubes were placed in the dark at room temperature for 5 minutes. Subsequently, 4.0 mL of a Na₂CO₃ aqueous solution (7.5% w/v) were added to the mixture and kept at the same conditions for 60 minutes more, to allow the stabilization of the resulting blue coloration. The absorbance of the samples was then measured at 765 nm, using an UV-VIS Scanning Spectrophotometer – Shimadzu, against a reagent-free blank. Gallic acid was used as a standard, and a calibration curve was acquired using solutions in the range 5-100 µg/mL. All the measurements were carried out in triplicate, and the TPC was expressed as gallic acid equivalents (GAE).

2.3.2 Polyphenols characterization – UHPLC-MS

The phenolic compounds of infusion samples, ethanol and water extracts obtained from black tea residues, were characterized by ultra-high-performance liquid chromatography - mass spectrometry (UHPLC-MS). The UHPLC system consisted of a variable loop Accela auto sampler (set at room temperature), an Accela 1200 LC pump, and an Accela 80Hz PDA and a LTQ ion trap mass spectrometry detectors (Thermo Fisher Scientific, San Jose, CA, USA). Analyses were carried out using an Alltima C₁₈column (150 mm × 2.1 mm, 5 μm). The separation of the compounds was carried out at room temperature with a mobile phase gradient containing a mixture of water with 0.2% (V/V) acetic acid, methanol and acetonitrile (96:2:2 v/v/v), at a flow rate of 0.4 mL/min. The injection volume in the HPLC system was 20 μL. Single online detection was carried out with the PDA detector, at 280 nm and 340 nm, and UV spectra in the range of 200-600 nm were also recorded for relevant chromatographic peaks. The LTQ ion trap mass spectrometer was equipped with an H-ESI II source operating in positive and negative modes. The flow rate of nitrogen sheath and auxiliary gas was 50 and 15 (arbitrary units), respectively. The spray voltage was 4 kV, heater temperature 400 °C, and capillary temperature was 360 °C both in positive and negative mode. The capillary voltages were set at -9 V (positive) and -35 V (negative), and tune lens voltages were +100 V in positive and -100 V in negative mode, respectively. The spectra analysis was performed in the range of *m/z* 100-1000. The scan time was equal to 3x250 ms. The data acquisition was performed using a Xcalibur[®] data system (ThermoFinnigan, San Jose, CA, USA). Quantification was done against catechin concentration, utilized as external standard. Concentrations were expressed in g/kg.

2.3.3 Antioxidant activity assessment – DPPH method

The assessment of the antioxidant activity of the tea residue infusion extracts was based on the DPPH[•] free radical (2,2-diphenyl-1-picrylhydrazyl) method, and calculated (Equation 11) as percentage of inhibition in order to obtain the values in the adequate linear range and evaluate the IC₅₀ index – the amount of sample necessary to reduce the initial radical concentration by 50%.

$$\% \text{ Inhibition} = \frac{A_{t_0} - A_{t_f}}{A_{t_0}} \times 100 \quad \text{Equation 11}$$

Where *A*₀ and *A*_f correspond to the absorbance at 515 nm of the radical at *t*₀ and of the sample at steady state, respectively, measured using an UV-VIS Scanning Spectrophotometer from Shimadzu. All the extract samples were analysed.

2.4 Preparation of coated papers based on tea residue extracts coating formulations

A coating formulation based on tea residue extracts and carboxymethyl cellulose (CMC), as a thickening agent, was prepared and named PPCMC. Freeze-dried extracts (3.00 g) obtained from black tea residue infusion were gently added to an aqueous dispersion of CMC of 9.2% solid content, under mechanical stirring until complete dissolution of the CMC. Likewise, a reference coating was prepared without the addition of extracts. Handsheets of bleached Kraft pulp (BK) were rod-coated (60 mm/s) with the coating formulations (± 125 mL/m²). The coated paper was dried at 105 °C for 2 minutes and then kept in a conditioned room until further analysis. Different samples were prepared with one, two or three layers of coating formulation.

2.5 Antibacterial activity assays

The antibacterial activity was evaluated following one or more methodologies: a) inhibition zone method, b) minimum inhibitory concentration (MIC) method, c) Shake flask method (under dynamic contact conditions) or d) AATCC test method 100-2004 (under static conditions).

2.5.1 Zone of Inhibition test

The ability of tea residue infusion extracts to inhibit microbial growth was evaluated using the method BISFA 2002 (quantitative method A), inoculating around 10⁴ Colony Former Units (CFU) per mL of *S. aureus* or *P. aeruginosa* suspension in Plate Count Agar (PCA). The PCA inoculated was dropped in the plates and let to solidify. Then, dilutions of the concentrated infusion were deposited in a hole with a known diameter previous made in the centre of the plate. Finally, the plates were incubated at 37°C and the size of inhibition zone were measured over time.

2.5.2 MIC determination

The Minimum Inhibitory Concentration (MIC) to inhibit *S. aureus* was assessed for tea residue extracts. Previously, tea residues infusion samples were sterilized with a sterile filter of 0.45 µm (Sartorius) and an inoculum of 10⁴ CFU/mL of *S. aureus* was prepared. To prepare the test samples 1 mL of sterilized sample (2-fold concentrated) was placed into an Eppendorf and 1 mL of inoculum was added. The inoculum reference was prepared by adding 1 mL of inoculum to 1 mL of sterilized water and the control was prepared by adding 1 mL of nutrient broth (NB) at 40% (V/V) to 1 mL of sterilized water. All the samples were incubated at 37 °C, at two different contact times: 7 and 24 hours, in triplicate. After each contact time, the samples were

diluted with 10 mL of neutralizing solution to extract the surviving bacteria. Aliquots of each sample were taken, diluted (10^0 - 10^{-5}) with physiologic solution and plated with PCA. Using the plate count agar method, the number of living cells were determined and the antibacterial efficiency (R) of the samples was calculated, after 24 h of incubation at 37 °C, using the Equation 12.

$$R \text{ (average log Reduction CFU)} = \text{Log (B/C)} \quad \text{Equation 12}$$

where: B is the average CFU of control corresponding to the living bacteria cells and C is the average CFU of examined sample, both after incubation time. In general two antibacterial effects can be distinguished:

- i. Bacteriostatic: inhibition of bacteria growth under testing conditions favourable to bacteria proliferation, evaluated in respect to the growth of the blank sample (CFU at time 24h);
- ii. Bactericidal: reduction (killing) of the number of bacteria initially inoculated (CFU at time 0);

2.5.3 Shake flask assay

The shake flask test based on the methods ASTM E2149-10 and BISFA 2002 (quantitative method B) was performed to evaluate the antibacterial activity against *S. aureus* and *P. aeruginosa*, under dynamic contact conditions. For the bacterial analysis the pre-inoculum was prepared using 20 mL of nutrient broth (NB) and placed at 37 °C for 18 h under stirring. The pre-inoculum was then diluted with a sterile buffer solution in order to obtain an inoculum with a concentration of 1.0×10^4 CFU/mL determined by a calibration curve at 540 nm. Tests were performed by adding 20 mL of inoculum to several dilutions of concentrated infusion and then maintained at 37°C under stirring. Aliquots were taken at different intervals of contact time, diluted (10^0 - 10^{-6}) with physiologic solution and plated with PCA for the bacterial counting as determined by count plate agar method, described before in section 2.5.2.

2.5.4 AATCC Test Method 100-2004

The AATCC Test Method 100-2004, was performed to assess the activity of the paper samples based on tea residue extracts against the gram-positive bacteria *S. aureus*. The antibacterial tests were conducted by spreading on the surface of the paper samples a known number of living cells (approximately 10^5 CFU - Colony Forming Units). The inoculated samples were then incubated 24 hours under optimal bacterial growing conditions (20% (V/V) NB, temperature

37 °C). Using 50 mL of neutralizing solution (L- α -Lecithin 3 g/L, sodium thiosulphate 5 g/L, L-Hystidine 1 g/L, Polysorbate80 30 g/L, KH₂PO₄ 10 mL/L (pH 7.2 \pm 0.2)) the surviving bacteria were extracted from the samples and the number of living cells and the antibacterial efficiency (R) were determined also by the count plate agar method.

3. Results and Discussion

3.1 Chemical Composition of the black tea residue

Previous to the studies regarding the antioxidant and antibacterial activity potential of the tea residue extracts towards the development of active paper-based packaging solutions, black tea residues were initially characterized concerning their chemical composition as can be observed in Table 7.

Table 7. Chemical composition of tea infusion residue.

Components		rel. abundance, % dry sample
Ashes		3.2
Extracts	Water	20.5
	Ethanol	27.5
Organic extracts	Hexane	2.4
	Acetone	9.1
Acid-insoluble residue (mainly polyphenolic substances)		25.4
Acid soluble substances		5.2
Proteins (nitrogen factor - 6.25)		12.9
Total glucose		11.9
Cellulose		8.6
Starch		3.3
Hemicelluloses	Xylose	2.3
	Galactose	4.5
	Arabinose	2.1
	Mannose	1.8
Total structural polysaccharides		22.7

This residue still contains high amounts of extractable substances, 20.5% in water and 27.5% in ethanol, respectively. On the contrary, the amount of acetone extracts is much lower and is almost negligible in a non-polar solvent such as hexane. The material after extraction is mainly constituted by acid-insoluble residues (25.4%), mainly polyphenolic compounds, as well as structural polysaccharides (cellulose, hemicelluloses and starch) as can be seen in Table 7. The protein content is also significant, being over 10% of the residue. The proportion of polyphenol and polysaccharide components with respect to the initial material is fairly similar. It shall be noted that the amount of cellulose is calculated by the amount of glucose obtained by HPLC after acid hydrolysis subtracting the amount of glucose measured by enzymatic hydrolysis with highly specific amylases. The amount of enzymatically hydrolysed glucose corresponds to starch. The other neutral sugars (xylose, galactose, arabinose and mannose) are associated to hemicelluloses (hetero-polysaccharides constituted principally by units of neutral sugars). In general, the chemical composition of the tea residues shows a fairly high amount (20-27%) of extractable substances in polar non-toxic solvents.

In view of increasing the value of this by-product, the composition and the active properties of the extracts were further investigated as well as their application for paper-based packaging materials. The remaining part of the tea residue, which accounts for approximately 70-80% of the initial material, was not considered in this study; however, it is envisaged that it might represent an interesting source of polysaccharides and proteins that deserves to be investigated.

3.2 Studies on the tea residues potential

The total phenolic content and the antioxidant activity of aqueous extracts obtained by infusion of black tea residues were evaluated and related to the yield of extraction, in order to understand the best infusion conditions. Then, the most suitable extracts were fully characterized concerning their phenolic composition by HPLC-MS and their antibacterial activity. An active coating formulation based on tea residue extracts was finally prepared and the antioxidant and antibacterial activities of coated paper surfaces were assessed. Ethanol and water extracts obtained by Soxhlet extraction were also characterized regarding the extraction yield, total phenolic content, antioxidant activity and phenolic composition.

3.2.1 Optimization of infusion procedures

Different infusion procedures in water were performed to extract compounds from black tea residues, tuning parameters such as: temperature, time and also concentration of residue.

Initially, the appropriate temperature for the infusion was selected at 80 °C according to the studies carried out by Perva-Uzunalić *et al.*, 2006, considering the maintenance of the activity of the compounds despite their degradation.

The concentration of extracts in the water infusion and the extraction yield, considering the initial amount of residues, are shown in Table 8.

Table 8. Extraction yields of tea residues in water at 80 °C under different conditions of infusion.

Tea Residue (% w/v)	Infusion time (min.)	[Extracts] (mg/mL)	Extraction Yield (%w/w)	Extracts identification
2.5	5	3.32±0.04	13.3	A-5
	7.5	3.63±0.06	14.5	A-7.5
	10	3.90±0.04	15.6	A-10
5	5	5.39±0.04	10.8	B-5
	7.5	6.51±0.28	13.0	B-7.5
	10	6.47±0.24	12.9	B-10

The highest absolute amount of aqueous extracts were obtained at 5% tea residue concentration, in all different conditions tested. However, higher extraction yields were achieved with 2.5% tea residue concentration obtaining values of 13.3, 14.5 and 15.6% (w/w), respectively. A clear saturation behaviour was observed increasing the extraction time, at both concentrations the saturation point was reached after only 7.5 minutes of infusion. Considering the total amount of aqueous extracts in the sample, equal to 20.5% (w/w) as obtained by Soxhlet extraction of 1.25% of tea residues, it can be verified that at the best infusion conditions, i.e. 10 minutes extraction of 2.5% tea residue, around 76% of the extracts was successfully extracted.

Regarding the Soxhlet extraction of 1.25% of tea residues using ethanol (E) as a solvent, it was possible to extract 3.5 mg/mL of compounds, correspondent to 27.5% (w/w) of the initial material.

3.2.1.1 Total phenolic content

The total phenolic content (TPC) of tea residue extracts were assessed by the Folin-Ciocalteu method. A standard curve of gallic acid (Figure 7) was obtained for the assay and the results (Figure 8) are expressed as grams of gallic acid equivalents (GAE).

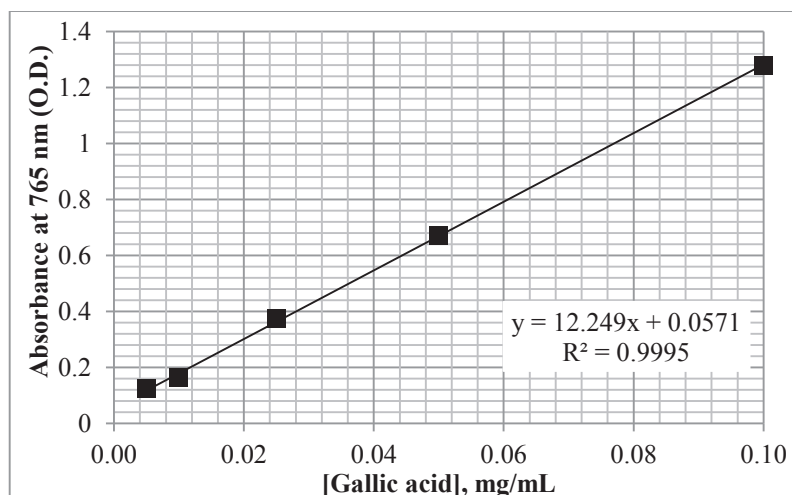


Figure 7. Gallic acid standard curve – reference for total phenolic content.

The TPC (Figure 8) of the extracts obtained by infusion of 2.5% (A-5, A-7.5, A-10) and 5% (B-5, B-7.5, B-10) of tea residue, for 5, 7.5 and 10 minutes at 80 °C under stirring, were compared. Additionally, the extracts obtained by Soxhlet extraction in water (sample W) and ethanol (sample E) were also evaluated regarding their phenolic content.

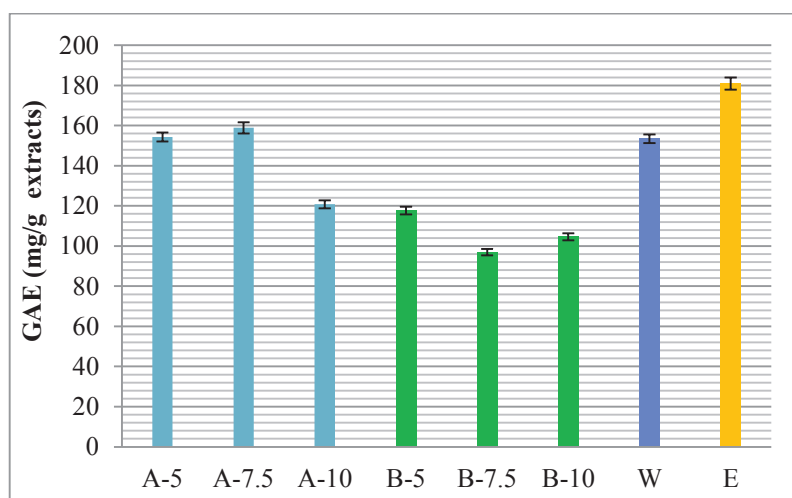


Figure 8. Total phenolic content of extracts expressed as gallic acid equivalents (GAE, mg/g of tea residue extract).

As can be seen in Figure 8, the TPC of the extracts obtained by infusion procedures (samples A and B) were found to vary from 96.9 to 158.9 mg GAE/g. Regarding the Soxhlet extractions, the extracts obtained by water extraction (W) present a TPC in GAE of 153.4 mg/g and the extracts obtained in ethanol (E) present the highest value on the total phenolic content of all extracts, corresponding to 181.0 mg/g of extract. Almajano *et al.*, 2008 for a 5 minutes infusion of black tea leaves at 1.5% (w/v) concentration, reported a TPC in gallic acid equivalents of 122.9 g/kg of initial sample, and Pełkal *et al.*, 2011 with a very similar procedure ($\approx 1\%$

concentration) using a black commercial tea (Yellow Label, Lipton brand) obtained 420 g GAE/kg. Our values for the same 5 minutes of infusion time, although at 2.5% (sample A-5) and at 5% (sample B-5) concentrations, exhibits a TPC of 20.52 g/kg and 12.68 g/kg of initial sample, respectively (i.e., 154.27 and 117.65 mg GAE/g extract - Figure 8). Despite the lower contents, that was even expected as we used pre-brewed tea leaves, our tea residues samples are still a promising source of phenolic compounds. Especially the sample A-7.5, that is the infusion extract with the highest total phenolic content, corresponding to a total phenolic content of 23.07 g GAE/kg of tea residue.

3.2.1.2 Antioxidant activity assessment

The antioxidant activity, normally associated with the phenolic content, can be assessed by determining the percentage of inhibition of the stable DPPH radical (Jeszka-Skowron *et al.*, 2015, Ignat *et al.*, 2013). The scavenging activity of DPPH by the extracts at different concentrations was measured in order to calculate the IC_{50} (i.e. to determine the necessary amount of antioxidant required to inhibit 50% of the radical DPPH presented in the sample solutions). The antioxidant activity of extracts obtained through the infusion of 2.5% (w/V) of tea residue was evaluated, as can be seen in Figure 9 with their correspondent IC_{50} values.

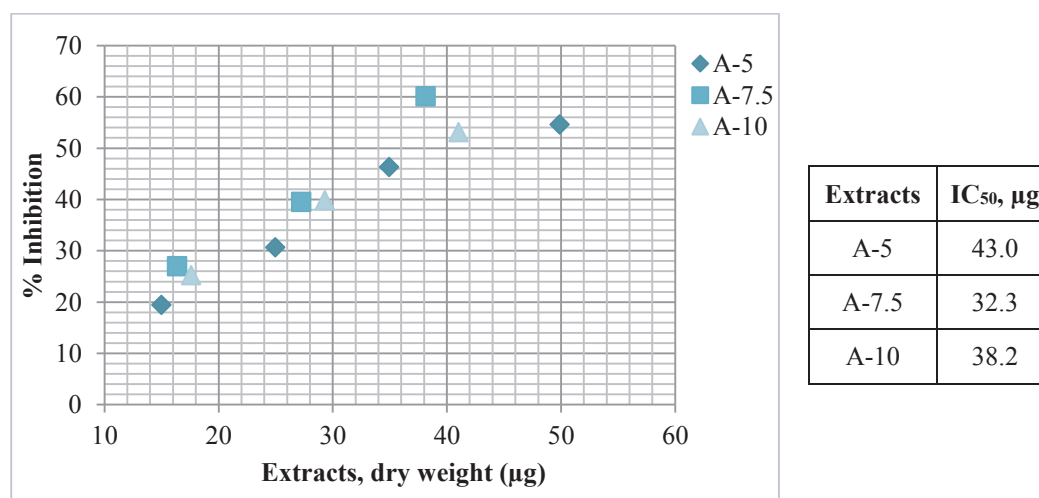


Figure 9: % Inhibition of DPPH by extracts obtained from the aqueous infusion of 2.5% (w/V) tea residues.

In Figure 10, it is shown the evaluation of the antioxidant activity and IC_{50} values of the extracts obtained through the aqueous infusion of 5.0% (w/V) of tea residue. Therefore, the capacity to scavenge the radical DPPH and the relative IC_{50} values for each type of extract were compared.

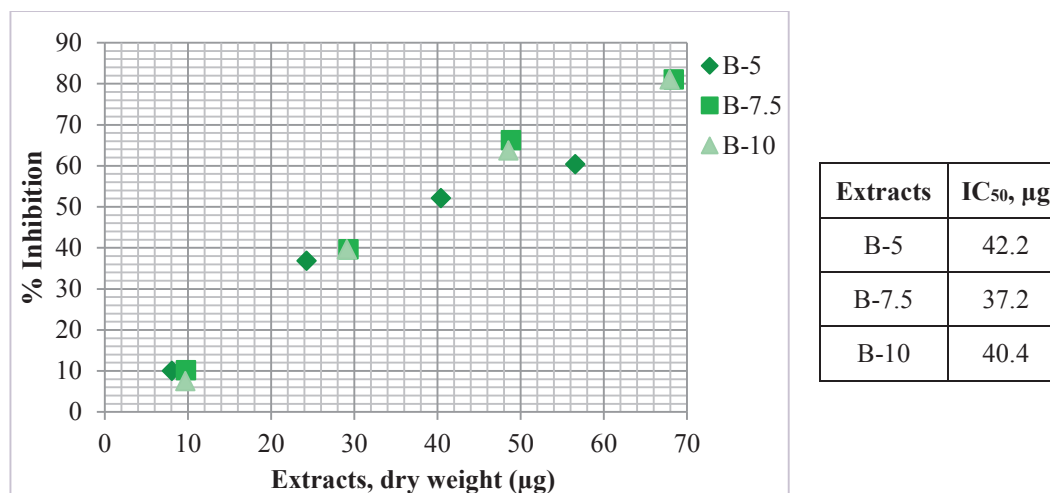


Figure 10: % Inhibition of DPPH by extracts obtained from the aqueous infusion of 5% (w/V) tea residues.

The lower IC₅₀ values were obtained for the extracts A7.5 and B7.5, with only 32.3 and 37.2 µg of extract, respectively, necessary to inhibit 50% of the radical DPPH present in the solution. The extracts showing the lower IC₅₀ (A7.5 and B7.5) are compared in Figure 11 to verify the effect of increasing residues concentration on antioxidant activity.

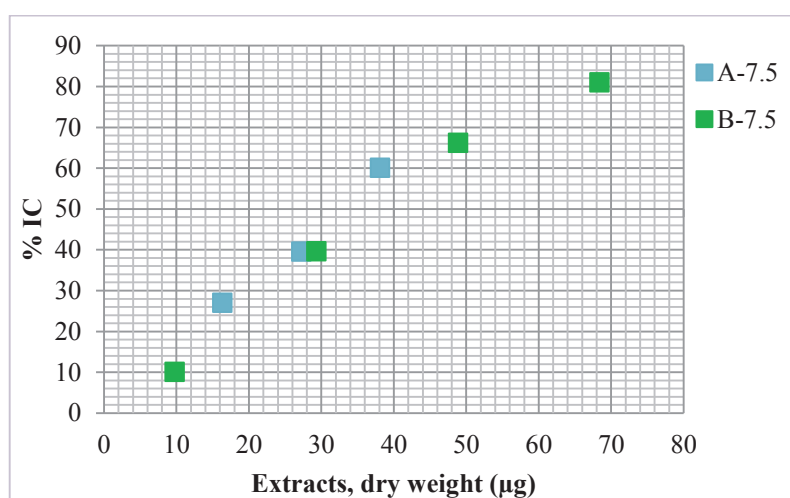


Figure 11: % Inhibition of DPPH for A7.5 and B7.5 tea residue extracts.

The behaviour of the extracts A7.5 and B7.5 on the inhibition of the radical DPPH in function of their quantity are very similar for both types of infusion (2.5% and 5% of tea residues, respectively), as shown in Figure 11. It can be therefore concluded that when the residue concentration is increased during the extraction, the share of antioxidant components is not affected, in other words the extract does not lose its efficacy even with a higher quantity of material submitted to the infusion process.

Additionally, the capacity to scavenge the radical DPPH was also studied for different concentrations of water (W) and ethanol (E) extracts obtained from Soxhlet extraction (Figure 12).

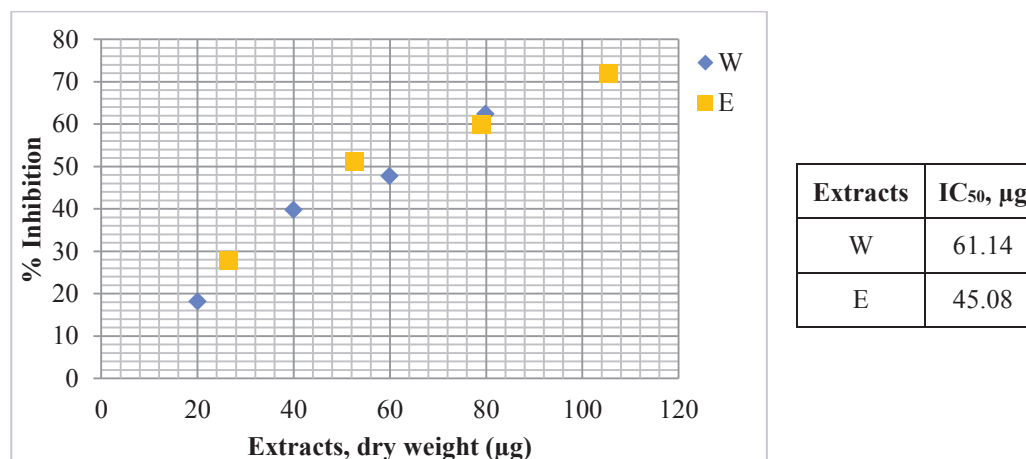


Figure 12: % Inhibition of DPPH by water (W) and ethanol (E) extracts and relative IC₅₀.

The W and E Soxhlet extracts, as can be noted from the results of Figure 12, present a lower scavenging capacity in comparison to short-time water extracts. Therefore, it can be concluded that among all types of extraction, the infusion at lower temperature and time of extraction seems to be a better and sustainable option to extract active compounds. Accordingly, the sample A-7.5 obtained at short time of infusion was considered to be the most suitable extract due to its high yield of extraction, highest value of total phenolic compounds in the infusion extracts (158.9 mg GAE/g extract) and correspondently higher antioxidant activity (IC₅₀=32.3 µg of extract). Therefore it was further investigated regarding its polyphenols characterization, antibacterial assessment and development of based coating formulations.

3.2.2 Identification and quantification of phenolic compounds

Black tea residues extracts were characterized by UHPLC-MS analysis in order to identify and quantify their phenolic compounds. To verify the influence of the type of extraction, the freeze-dried samples obtained by infusion procedures (A7.5) and Soxhlet extraction with water (W) and ethanol (E), were compared. In the Figure 13 is possible to observe the UV-chromatograms recorded at 280 nm.

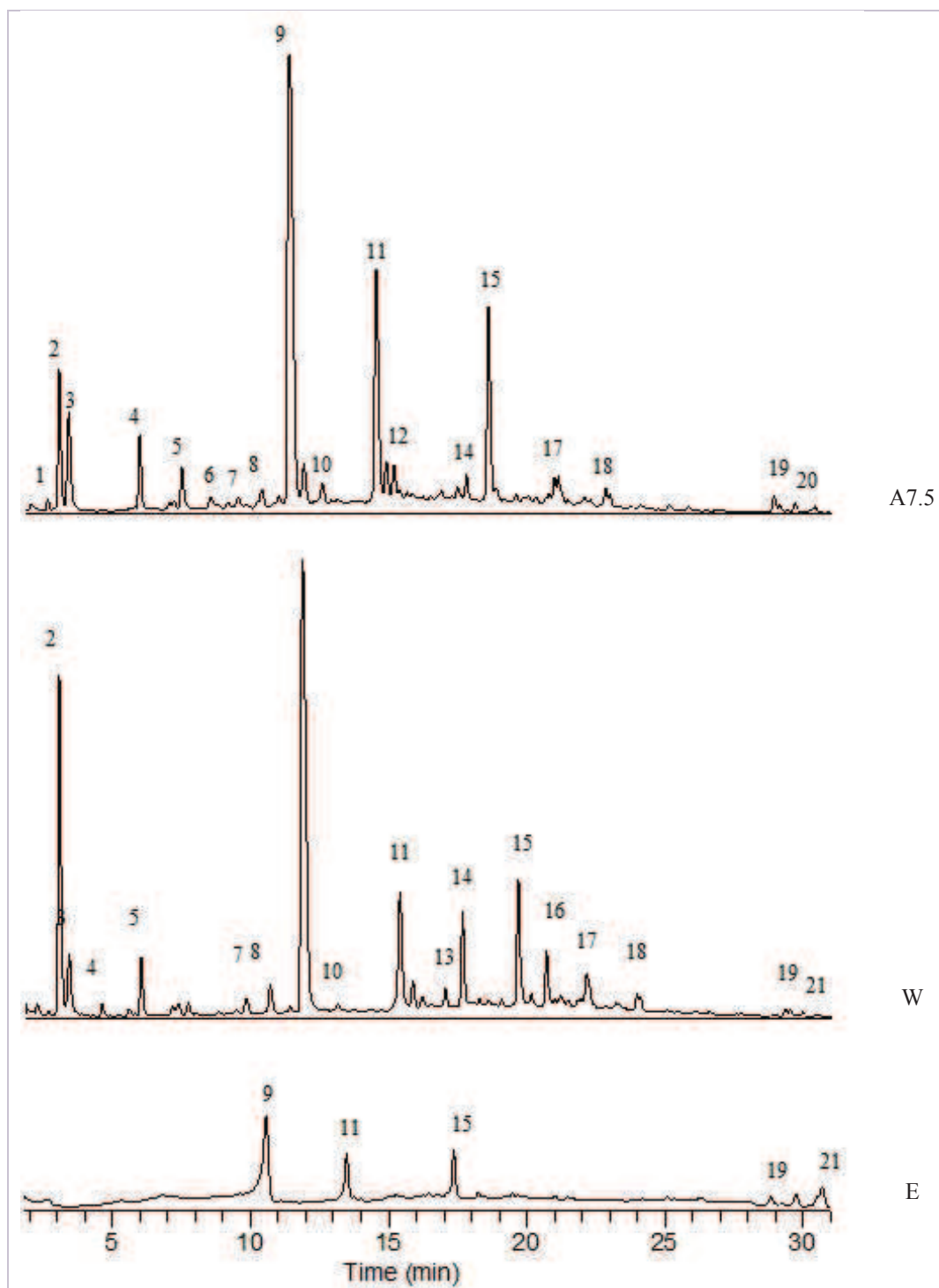


Figure 13. UHPLC-UV chromatograms of extracts obtained by infusion procedures (A7.5) and Soxhlet extraction with water (W) and ethanol (E), recorded at 280 nm.

The compounds listed in Table 9 were identified by comparing their UV-Vis data and MS fragmentation patterns with standards or published data, as discussed further on. The quantification in each extract was obtained from the response of the diode array detector.

Table 9. Phenolic compounds, aminoacids and alkaloids identified in the tea extracts.

	Compound	λ max (nm)	Phenolic content (mg/g extract)		
			A-7.5	W	E
1	L-Theanine	-	0.99	0.40	-
2	Gallic acid isomer	270	19.57	57.11	0.32
3	Gallic acid isomer	270	16.02	10.31	-
4	Theobromine	270	9.95	9.77	0.96
5	Kaempferol derivative	262-350	6.14	1.99	0.54
7	Coumarin isomer	280-300	1.65	3.47	-
8	(-)-Epigallocatechin	-	2.09	5.68	-
9	Caffeine	258-270	124.82	137.80	40.70
10	Caffeic acid	220-235-320	3.19	0.77	-
11	(-)-Galocatechin-3-gallate	238sh-274	43.81	27.91	12.43
12	(+)-Catechin or (-)-Epicatechin	275	4.88	5.01	0.50
13	Coumarin	280-300	4.20	2.30	-
14	(-)-Epigallocatechin-3-gallate	238sh-274	2.98	16.21	0.48
15	Theaflavin	-	31.22	24.20	12.53
16	(-)-Epicatechin-3-gallate	238sh-274	0.97	8.79	-
17	Quercetin-3-glucoside	254-350	6.79	7.47	-
18	Kaempferol-3-glucoside	262-346	4.44	4.76	-
19	Quercetyn-3-glucoside derivative	266-314	1.97	1.95	2.64
20	Theaflavin-3-monogallate	274-374-545	1.51	0.68	3.71
21	Theaflavin-3,3'-digallate	-	1.28	0.68	9.55
Total identified compounds			288.46	327.26	84.36
Phenolic compounds			152.69	179.29	42.70
Alkaloids			134.78	147.57	41.66
Aminoacids			0.99	0.40	-
Others/Non identified			20.51	20.11	7.45
Total			308.97	347.37	91.81

The total phenolic content normally correlates well with antioxidant activity; nevertheless, the extracts present a high complexity and sub-classes might present different efficiency. Table 9 shows that while water extracts are similar in terms of phenolic content, the ethanol extract is much lower (4.3% against 15.3% and 17.9% (w/w) for the A7.5 and W extracts respectively).

These data are in contradiction with the measure of TPC (181.0 mg/g of extract); however they could explain the lower antioxidant activity (higher IC₅₀) of ethanol extract. Comparing the water extracts it is worth noticing that some components such as Kaempferol derivative, (-)-Gallocatechin-3-gallate and Theaflavin are present in higher percentage in the short time water infusion extract and therefore the greater antioxidant activity might be attributed to the higher share of these compounds. Nonetheless, it shall not be forgotten that by HPLC-MS was possible to identify only a part (15.3%) of all components.

The quantitative distribution by type of compounds are represented in Figure 14 and for better understanding, the phenolic compounds were divided in sub-classes: catechins, flavonols, theaflavins and phenolic acids together with coumarins.

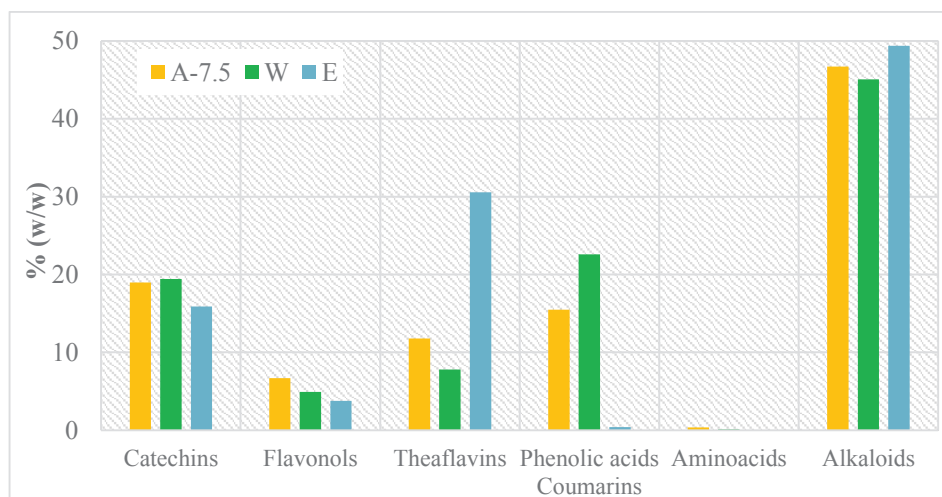


Figure 14. Distribution profile of identified compounds in A7.5, W and E extracts.

The relative amount of catechins in all three extracts reaches almost 20% (w/w) of the identified compounds, as can be seen in Figure 14. Flavonols correspond to 6.7%, 4.9% and 3.8% in A7.5, W and E extracts. The E extracts present the highest relative amount of theaflavins corresponding to 30.6%, whereas for A7.5 and W extracts they correspond to 11.8% and 7.8% of the identified compounds, respectively. Phenolic acids and coumarins were present considerably in the A7.5 and W extracts, with the amount of 15.5% and 22.6%, respectively. Alkaloids (mostly caffeine), were the highest class of identified compounds, reaching almost 50% of the total amount.

3.2.2.1 Catechins

Catechins present a maximum in the UV absorption spectra of around 270-290 nm, as many other phenolic compounds, not allowing their selective detection. Nonetheless, their

identification is easily achieved just taking into account the mass spectra by the presence of a base peak representing the protonated molecular ion $[M + H]^+$ and a characteristic fragment ion, resultant from a retro Diels-Alder reaction (RDA) of the A ring structure (Figure 15), typical to all types of catechins (Atoui *et al.*, 2005; Jiang *et al.*, 2015 Zeeb *et al.*, 2000).

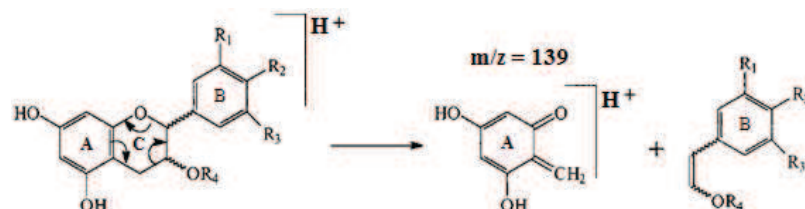


Figure 15. Retro Diels-Alder fragmentation of catechins.
(adapted from Cren-Olivé *et al.*, 2000; Zeeb *et al.*, 2000)

Accordingly, compound **8** was identified as (-)-epigallocatechin (EGC), based on its mass spectrum that shows a base peak corresponding to the $[M + H]^+$ ion at m/z 307 and the characteristic fragment ion at m/z 139 (RDA reaction) (Atoui *et al.*, 2005; Zeeb *et al.*, 2000). Along the same line, compound **12** might be assigned to (+)-catechin (C) or (-)-epicatechin (EC), as the fragmentation pathway is very similar for both: base peak at m/z 291 for $[M + H]^+$, characteristic fragment ion at m/z 139 and at m/z 273 $[M + H - H_2O]^+$; so further analyses were necessary to achieve the right identification of this compound (Yuda *et al.*, 2012; Zeeb *et al.*, 2000). Regarding compound **11**, the intense signal recorded at m/z 459 correspondent to the $[M + H]^+$ ion, the characteristic fragment $[M + H - \text{galloyl} + H - H_2O]^+$ ion of catechin gallates recorded at m/z 289 and the fragment at m/z 139 due to the RDA reaction leads to the identification of (-)-gallocatechin-3-gallate (GCG) (Atoui *et al.*, 2005). Compound **14**, with a protonated molecular ion at m/z 467 and a fragment ion at m/z 153 correspondent to a galloyl moiety was identified as an ester between epiafzelchin and gallic acid, as previously detected in black tea infusion by Atoui *et al.*, 2005. (-)-Epicatechin-3-gallate was assigned to compound **16** based on its base peak at m/z 443 $[M + H]^+$, the characteristic $[M + H - \text{galloyl} + H - H_2O]^+$ ion at m/z 273, and m/z 153 and m/z 139 correspondent to a galloyl moiety and a RDA reaction, respectively (Kiehne *et al.*, 1996). Among catechins, GCG (compound **8**) is the most representative compound present in all three extracts in dry weight, corresponding to 4.4%, 2.8% and 1.2% (w/w) total solid content of A7.5, W and E extracts, respectively.

3.2.2.2 Flavonols

Compounds **5**, **17**, **18** and **19** were classified as flavonols, due to the presence of a glycoside loss ($[Agl + H]^+$ ion) and a sodium adduct ($[M + Na]^+$ ion), characteristic of this type of flavonoids. Compound **17** was identified as quercetin 3-glycoside due to its UV maximum

absorption at 255 and 355 nm, $[M + H]^+$ ion at m/z 465, glycoside loss $[Agl + H]^+$ at m/z 303 and a sodium adduct $[M + Na]^+$ at m/z 487, being compound **19** its derivative (Atoui et al., 2005; Kiehne et al., 1996). Kaempferol 3-glycoside was attributed to compound **18** based on: m/z 449 $[M + H]^+$, m/z 471 $[M + Na]^+$, $[Agl + H]^+$ ion at m/z 287 and λ max: 262-346 nm. Compound **5** presents a $[M + H]^+$ ion at m/z 763 and it is a derivative of Kaempferol (Atoui et al., 2005).

3.2.2.3 Theaflavins

Compounds **15**, **20** and **21** belong to the theaflavins, a sub-class of phenolic compounds, resulting from the oxidation of catechins during the tea fermentation process. The mass spectrum of compound **15**, attributed to theaflavin (TF), shows a base peak recorded at m/z 565 $[M + H]^+$, followed by fragmentation ion $[M + H_2O]^+$ at m/z 547. Theaflavin-3-monogallate (TF3G) was assigned to compound **20** with a $[M + H]^+$ ion recorded at m/z 715 and a fragment m/z 699 correspondent to the loss of water. Compound **21** was identified as theaflavin-3,3'-digallate (TFDG), with a m/z 869 $[M + H]^+$ (Dou et al., 2007; Yuda et al., 2012). The theaflavin TF was the most representative of the theaflavins, representing 3.1%, 2.4% and 1.2 % (w/w) of the total solid content of A7.5, W and E extracts, respectively. The TFDG compound is also abundant in the E extracts, representing the 4th highest compound at almost 1% (w/w) of the total content of extract.

3.2.2.4 Phenolic acids and coumarins

Compounds **2** and **3** present a base peak at m/z 171 correspondent to the $[M + H]^+$ ion characteristic of gallic acid or its isomers (Kiehne et al., 1996; Stewart et al., 2005). Compound **7** presents a similar pathway pattern with compound **13**, with base peak at m/z 147, characteristic product ion at m/z 119 (loss of carbon monoxide) and an absorption maxima at 310 nm, indicating the occurrence of a coumarin and its isomer. Caffeic acid was attributed to compound **10**, with $[M + H]^+$ ion at m/z 181 and a product ion at m/z 163 (Atoui et al., 2005). The gallic acid (compound **2**) represents the 2nd most abundant compound of the W extracts, with 5.7% and corresponds to 2.0% of the extracts of A7.5, being the 4th most abundant compound.

3.2.2.5 Alkaloids and Aminoacids

Alkaloids and aminoacids were also identified among the polyphenol compounds. The alkaloid caffeine was assigned to compound **9**, presenting a base peak at m/z 195, correspondent to its

protonated molecular ion $[M + H]^+$, fragment ions at m/z 138 $[M + H - HNCO]^+$ and m/z 110 $[M + H - CO]^+$ together with a UV maximum absorption at 270 nm (Kiehne et al., 1996; Berger et al., 2009; Yuda et al., 2012). Caffeine represents the most abundant compound for all three extracts. Compound **4** was identified as theobromine as it shows a similar mass fragmentation pattern to caffeine (**9**), already reported by Berger et al., 2009, with fragment ions at m/z 138 and 110 and an intense $[M + H]^+$ ion, although, the base peak of theobromine (3,7 trimethyl xanthine) is at m/z 181, due to the absence of a methyl group compared to caffeine (1,3,7 trimethyl xanthine). Compound **1**, not detectable by UV, was identified only by mass spectra with its $[M + H]^+$ ion at m/z 175 and a fragment ion at m/z 157 $[M + H - H_2O]^+$, characteristics of the amino acid L-Theanine (Kiehne et al., 1996). Caffeine (compound **9**) is the most abundant compound present in all extracts, representing 12.4, 13.8 and 4.1% of the total solid content of the A7.5, W and E extracts, respectively.

3.2.3 Antibacterial activity

The antibacterial effect of the most suitable tea residue extract (A-7.5) samples as: fresh infusion, concentrated infusion and freeze-dried extracts, was assessed and evaluated, in order to understand the differences between different storage methodologies, regarding the maintenance of the antibacterial activity.

3.2.3.1 Infusion extract

At the beginning, a semi-quantitative evaluation of the fresh infusion extract was performed by the measurement of the inhibition zone (Figure 16) for two different amounts of extract (2.0 and 4.0 mg) deposited in the inoculated agar plate.

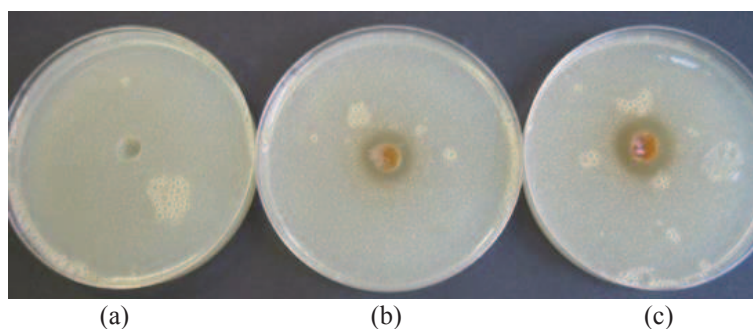


Figure 16: Test of inhibitory activity against *S. aureus* for (a) reference, (b) 2.0 mg and (c) 4.0 mg of extract.

An obvious inhibitory effect of the *S. aureus* growth is observed in Figure 16, for both samples. Moreover, the halo of inhibition is larger for the most concentrated sample, so it is more active against the bacteria, as expected.

Figure 17, instead, shows the antibacterial activity of different dilutions of the 15 times concentrated extract against *S. aureus* and *E. coli*, following the shake flask method for 3 and 8 hours contact time and Table 10 collects the values of log reduction.

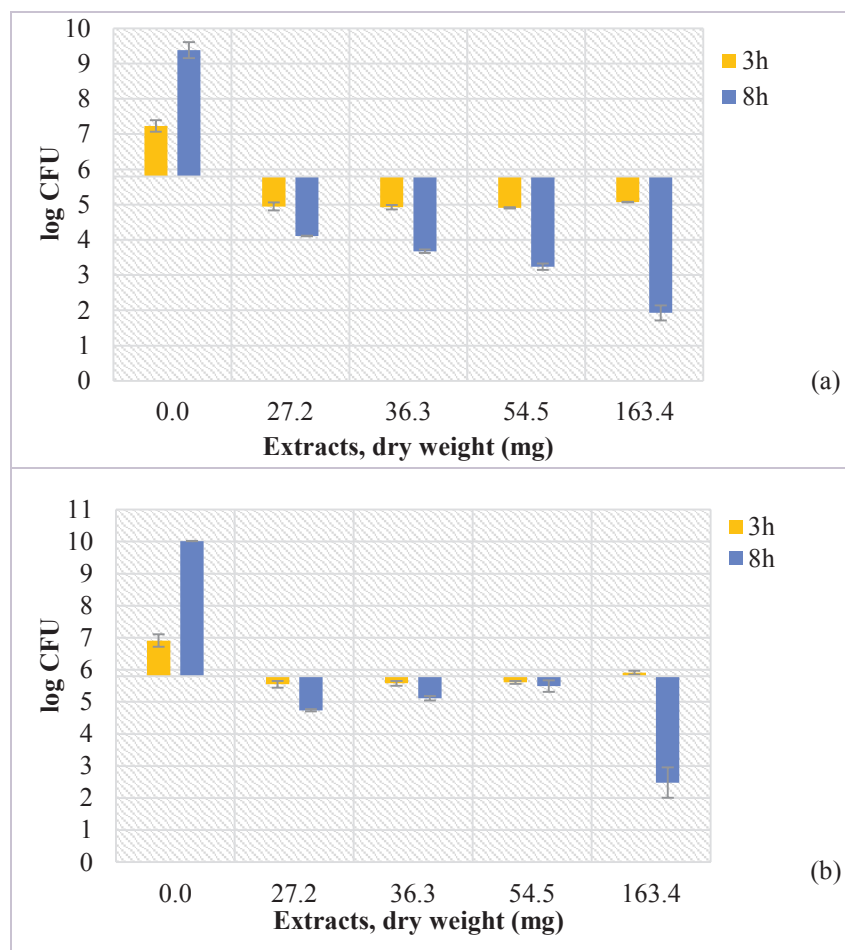


Figure 17: Antibacterial activity of the extracts against (a) *S. aureus* and (b) *E. coli*.

The activity is clearly a linear function of concentration at 8 h contact time in the case of *S. aureus* while for *E. coli* this linear relationship is not observed (Figure 17), maybe due to the lower effect of the extract on this gram-negative bacteria. In this latter case it seems that tea extract produces a bacteriostatic effect up to a step dose-limit necessary to achieve a killing of the bacterial population instead of showing a linear behaviour.

Table 10. Log reduction of the number of colonies of *S. aureus* and *E. coli* after 8h of contact time.

Extracts (dry weight, mg)	<i>S. aureus</i>	<i>E. coli</i>
	R	
27.2	5.3	4.6
36.3	5.7	4.3
54.5	6.1	3.9
163.4	7.5	6.9

Despite the precipitation observed in the 15 times concentrated samples after defrosting, as pointed out in Table 10, the antibacterial activity is clearly demonstrated.

3.2.3.2 Freeze-dried extract

Regarding the freeze-dried extracts (lyophilisation process), the test of the minimum inhibitory concentration was performed in order to define the lowest amount of these type of extracts capable to inhibit the growth of bacteria. The infusion samples tested correspond to 1.1, 2.2 and 4.4 mg of tea residue extracts and the results for *S. aureus* bacteria are shown in Figure 18.

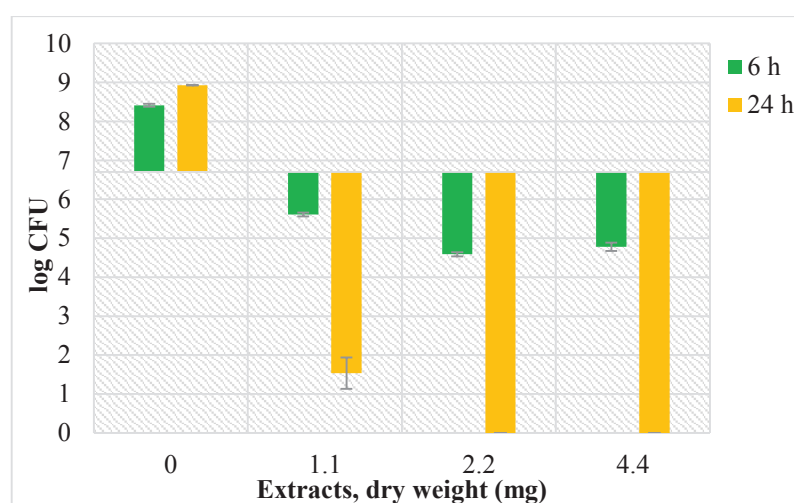


Figure 18: Antibacterial activity of tea extracts against *S. aureus*, using MIC determination.

After only 6 hours of contact time with *S. aureus*, 1.1 mg of extracts were enough to provide not only a complete inhibition of the bacterial growth, but already a bactericidal effect, corresponding to 2.8 log reduction related to the reference sample (Figure 18). With 24 h of contact time, the antibacterial activity of the extracts increases, presenting a bactericidal effect of 7.4 log reduction for the lowest amount of extract tested and a complete killing effect for both 2.2 and 4.4 mg of extracts. So, the minimum amount of extracts to inhibit the growth of *S. aureus* is even lower than 1.1 mg.

Furthermore, these results indicate that extracts dried by lyophilisation present a much higher activity than those concentrated in the rotary evaporator, so it is the better way to treat the extracts, avoiding the degradation of their active compounds and in order to keep the samples stored for long time before further experiments. The lower activity of the concentrated extracts might be related to the rotary evaporation at 50 °C, the freezing and defrost of the samples, with precipitation of part of the sample.

3.3 Development of active paper surfaces based on tea residues

Paper surfaces were rod-coated with a formulation based on black tea residue extracts as source of active compounds incorporated in an aqueous dispersion of carboxymethyl cellulose (CMC) as thickening agent, with a weight-volume ratio of (3.1:10). Initially, the antibacterial activity of the coating formulations was verified by the inhibition zone test (Table 11) measuring the halo of inhibition created by 100 μ L of formulation directly introduced in agar plates inoculated with *S. aureus*.

Table 11: Size values of inhibition zone for the CMC coating formulations.

Samples	Inhibition Zone (cm)	
	Day 1	Day3
Reference coating (only CMC)	0	0
PPCMC coating	2.2	1.9

The tea residues-based coating formulation (PPCMC) shows an inhibition effect against *S. aureus* growth as can be seen in Table 11. Considering the positive results, the PPCMC formulation was loaded on paper surfaces by rod-coating, at 125 mL/m² corresponding to a coating layer with a grammage of 15.17 g/m². Three coated paper samples, prepared by applying one, two or three layers of PPCMC, were assessed regarding the antibacterial activity against *S. aureus*, after 6 h and 24 h contact time (Figure 19), using the AATCC test method 100-2004.

Coating (g/m ²)	Extracts (g/m ²)	R (6h)	R (24h)
15.17	3.81	3.1	7.2
30.35	7.62	2.3	7.2
45.52	11.43	1.6	7.2

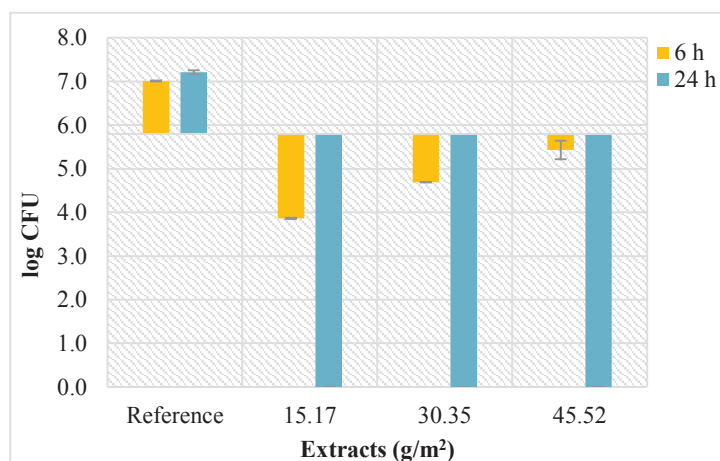


Figure 19: Antibacterial activity of PPCMC coated papers against *S. aureus*.

The coating formulation was very effective leading to a clear bactericidal effect after only 6 hours contact time (Figure 19); however, the inverse relation between the amount of extracts and the bacterial log reduction after 6 hours is still unclear and possibly due to the thicker final coating layer that may hinder the contact between bacteria and active polyphenols, delaying

their action. Nevertheless after 24 hours contact time a complete killing was observed for all three tested samples. These results show the possibility to develop antimicrobial active surfaces starting from low value tea residues. The residual amount of polyphenols is still relevant and easily extractable; besides, due to their high water solubility they can be easily handled for preparing suitable water based coating formulations. On the contrary, a potential drawback may be foreseen due to the strong brownish colour not suitable for coating white top layers. Still, the resulting active cellulosic-based packaging, by preventing the bacteria proliferation, will lead to an increase of the product shelf-life, maintaining product quality and safety, thus increasing the sustainability of the tea brewing, packaging and packed product in a complete life-cycle basis.

4. Conclusions

In this chapter, black tea brewing residues were studied to develop active paper-based packaging solutions. Thus, the best infusion conditions were found to be at 80 °C for 7.5 minutes for an infusion of 2.5 g of tea residue in 100 mL of water, considering the yield of extraction, the antioxidant activity and the total phenolic content. So, extracts obtained under these conditions (samples A-7.5) presenting the highest antioxidant activity and the highest total phenolic content were used to prepare coating formulations aimed to develop active paper samples based on tea residues. Moreover, these A7.5 extracts are constituted by 12.5% of caffeine and 4.4% of galocatechin-3-gallate, compounds known for their antioxidant/antibacterial activity. The tea-based coating formulations demonstrate a bactericidal effect against *S. aureus* of 7.4 log reduction for only 1.1 mg of extract tested in the MIC assay. The paper samples coated with a coating layer of 15.17 g/m² were very effective. The active tea-based coated papers show a complete killing effect after 24 hours contact time, although the yellow colour of the coating layer restrain their application to brown packaging products.

Chapter 3. Use of active nanoparticles to develop antibacterial paper products and their influence on packaging end of life options

1. Introduction

The introduction of nanomaterials possessing antibacterial functionality, like photo-active TiO₂ or ZnO nanoparticles (NPs), might benefit the packaging field, particularly food packaging and consumable packed devices for medical applications through the development of antibacterial paper products. In fact, paper with its porous structure is a very promising substrate for the inclusion of NPs and its functionalization can be achieved by loading even small amounts incorporated in coating formulations (Ngo *et al.*, 2011). The first examples of antibacterial paper products were developed mostly in the tissue paper based sector where in the last ten years a significant number of patents have been reported for paper wipes, hand towels and other similar products (Patel, 2009). Nanocrystalline photo-active TiO₂ particles are known to release active radical oxygen species (OH•, •O₂⁻ and HO₂•) capable to decompose organic substances and inactivate some bacteria and moulds, in the presence of water and oxygen under exposure to UV light (Goncalves *et al.*, 2009; Maness *et al.*, 1999). However, the intimate contact between TiO₂ and the cellulose may limit the applications of such materials for long periods of time because TiO₂ NPs may lead to the oxidative degradation of cellulose and successive cleavage of its polymeric chain (Goncalves *et al.*, 2009). Relatively to ZnO nanoparticles, on the other hand, their antibacterial effect is still unclear, but several investigations reported the disruption of the cell membrane activity as the major cause of bacterial killing; accordingly, the high surface area of ZnO NPs and the large number of surface defects might lead to the production of reactive oxygen species, like hydrogen peroxide harmful to bacterial cells (Huang *et al.*, 2008; Joshi *et al.*, 2012; Li *et al.*, 2011; Martins *et al.*, 2013; Xie *et al.*, 2011). Although many studies have already been carried out using these NPs, their application in coatings for the functionalization of paper based packaging remain a challenge and one of the main aspect regards their effectiveness when included in traditional coating formulations.

In this work we aimed to develop active surface systems using nanoparticles capable to kill bacteria and/or degrade contaminants in a cellulosic packaging environment intending to extend the shelf-life of the packaged product. To achieve this assignment, several studies to better understand the bactericidal action of visible light activated TiO₂ NPs against bacterial targets, when dip-coated on paper in different concentrations were performed, taking also into account

the oxidative degradation of the paper by the presence of titanium dioxide; the potential of coating formulations based on TiO₂ NPs physically grafted onto nanofibrillated cellulose (NFC), through direct mixing as well as by layer-by-layer assembly, was evaluated; the production and the bacterial assessment of a medical paper based packaging through the inclusion of ZnO NPs in a flexographic overprint varnish were considered. Additionally, preliminary studies regarding the fate and effect of the nanoparticles in the packages end-of-life was evaluated towards recyclability and biodegradability measurements.

1.1 TiO₂ history and properties

Titanium dioxide (TiO₂) has been the most widely investigated and used photocatalyst due to its strong photo-activity, high chemical and thermal stability, low cost, long durability and low toxicity (Nakata *et al.*, 2012a; Pelaez *et al.*, 2012). In the 20th century were published the first scientific studies reporting the photoactivity of TiO₂; however its use in powder form as white pigment is known from ancient times and has been widely used ever since (Kazuhito *et al.*, 2005; Matsubara *et al.*, 1995).

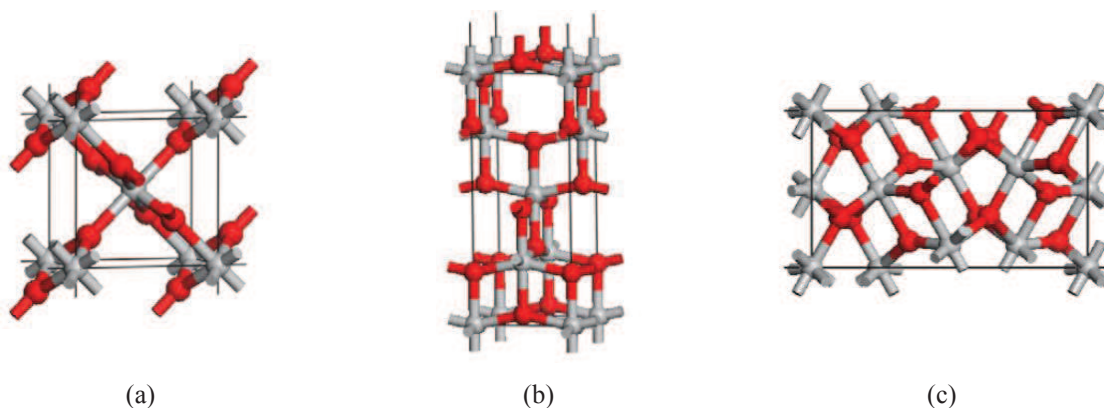
Table 12. Overview on TiO₂ structures, properties, synthesis and general applications. (Ngo *et al.*, 2011)

Structures and properties	Three major crystalline forms: anatase, rutile, brookite. Rutile is predicted to be the most stable phase, anatase is the most photoactive form. TiO ₂ surface exhibits coordination vacancies and is occupied by hydroxyl groups through water chemisorption. Raman scattering peaks of TiO ₂ nanoparticles become broader as their size decreases. Photocatalyst: wide band gap semiconductor capable of converting light energy into chemical redox energy. Reversible/switchable superhydrophilic and superhydrophobic properties.
Common methods of synthesis	Solution routes – Precipitation – Sol–gel: non-alkoxide and alkoxide – Combustion – Electrochemical Gas phase method – Chemical vapor deposition – Physical vapor deposition – Spray pyrolysis deposition
General applications	Photocatalysis Stain-proofing and self-cleaning Gas and humidity sensors Photovoltaics Photocleavage of water Photodegradation of organic pollutants

The application of TiO₂ is widely spread both in environmental and energy fields, comprising areas like air and water purification (removal of pollutants and bacteria), medicine (cancer treatment, operating room), agriculture (residual pesticides degradation), electronic equipments

(refrigerator, lights), residence (painting, tile, glass, wall paper), paper and printing industry (promote the opacity and whiteness of the paper, offset printing), energy conversion (solar cells) and water splitting (hydrogen evolution) (Nakata *et al.*, 2012).

TiO₂ can be found in nature as three different polymorphs: rutile, anatase, and brookite; where TiO₆ octahedra are formed by the co-ordination between titanium (Ti⁴⁺) atoms and six oxygen (O²⁻) atoms (Figure 20).



(a) (b) (c)
Figure 20. Crystalline forms of TiO₂: rutile (a), anatase (b) and brookite (c).
 (Ti⁴⁺ are represented in grey and O²⁻ in red, adapted from Tonomura *et al.*, 2011)

Both, rutile (Figure 20-a) and anatase (Figure 20-b) present a tetragonal spaces group but with different crystal structures: octahedra sharing edges at (0 0 1) planes for the rutile form; and the vertices sharing octahedra establishing (0 0 1) planes for anatase. Brookite (Figure 20-c) presents an orthorhombic structure, in wich both edges and vertices are shared (Pelaez *et al.*, 2012; Tonomura *et al.*, 2011). Rutile is the most stable form and together with anatase is the main polymorph of TiO₂ and the most commonly used (Pelaez *et al.*, 2012; Visai *et al.*, 2011). Moreover, anatase is the most photochemically active form, presenting a wider optical band gap of 3.2 eV, corresponding to an UV wavelength adsorption of 385 nm. Conversely, rutile presents an optical band gap of 3.0 eV, equivalent to a wavelength of 410 nm (Fu *et al.*, 2005, Visai *et al.*, 2011).

1.1.1 Principles of TiO₂ Photoreactivity

The photoreactivity of TiO₂ depends upon the absorption of photon energies greater than its band gap that leads to the formation of photo-generated charge carriers (e⁻, photoelectrons; h⁺, holes) (Nakata *et al.*, 2012a). In the case of anatase, a wavelength less than 385 nm (band gap > 3.2 eV), excites an electron from the valence band to the conduction band generating a positive hole in the valence band, as illustrated in Figure 21 (Pelaez *et al.*, 2012).

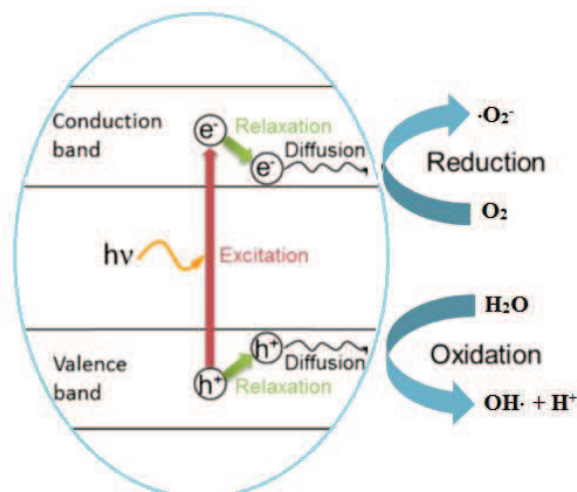


Figure 21. Scheme of the formation of holes and electrons after UV excitation.
(Adapted from Pelaez *et al.*, 2012)

This photocatalytic process is well known and mostly employed to degrade, or transform into less harmful substances, organic and inorganic compounds and even microorganisms as a redox-reaction of adsorbed substances occurs (Carp *et al.*, 2004; Ngo *et al.*, 2011; Pelaez *et al.*, 2012). So, it mainly occurs that:

- Electrons react with molecular oxygen (O_2) producing superoxide radical anions ($\cdot O_2^-$), that could also react with H^+ producing hydroperoxyl radical ($\cdot OOH$) and by electrochemical reduction generates H_2O_2 ; these reactive oxygen species may contribute to the degradation of pollutants by oxidative pathways;
- Holes react with water, producing hydroxyl radicals ($\cdot OH$), which can further oxidize and mineralize organic species producing CO_2 , H_2O and mineral salts.

Accordingly, the high redox potential of the ROS (reactive oxygen species) contributes to TiO_2 surface bacterial inactivation and their formation is related to the crystalline phase, isoelectric point, particle size and respective specific surface area, being very important the correct choice of type and source of TiO_2 , depending on the application (Yemmireddy *et al.*, 2015).

Besides, also under UV-light, the TiO_2 surface by itself could suffer a hydrophilic conversion (Figure 22). A small proportion of the h^+ photogenerated oxidize O_2^- anions, becoming trapped at lattice oxygen sites of the bulk TiO_2 . The bonds between lattice titanium and oxygen ions become weaker and may be broken by water molecules that by charge compensation release new hydroxyl groups. The increase of OH groups, with high surface energy and thermodynamically less stable, convert TiO_2 into a highly hydrophilic surface. Although, in the absence of light, atmospheric oxygen gradually substitutes the adsorbed hydroxyl groups and a

hydrophobic conversion of the surface occurs (Nakata *et al.*, 2012a; Nakata *et al.*, 2012b; Ngo *et al.*, 2011).

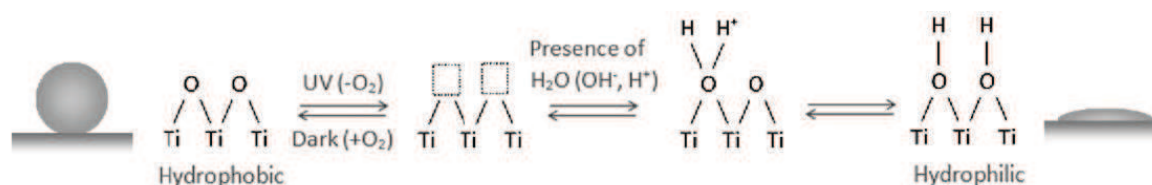


Figure 22. Photo-induced hydrophilic mechanism and hydrophobic conversion on TiO₂ surfaces. (Adapted from Ngo *et al.*, 2011)

1.1.2 Applications in paper

Cellulose paper is used in several fields, including packaging applications. The low cost and porous structure made it a very promising material and a cost-effective alternative as support for TiO₂ and other type of nanoparticles. Besides the longstanding and well-known use of TiO₂ (in bulk form) as a filler in the paper industry to improve the brightness and opacity, the photocatalytic activity of papers with TiO₂ incorporated have been the focus of increasing interest, since the first studies on photoactive TiO₂ containing paper, by Matsubara *et al.*, 1995 (Chauhan *et al.*, 2014; Zhang *et al.*, 2013). For the first time, highly photocatalytic papers were prepared, demonstrating the efficacy of cellulose as a good matrix for photo-active TiO₂ and subsequently the interesting topic lead to developments in the research field and several publications and patents have been written so far (Matsubara *et al.*, 1995; Pelton *et al.*, 2006).

For the development of highly efficient photo-active TiO₂ based papers, it is important to:

- i. prevent the possible degradation of cellulose that is due to the oxidative activity of the photo-active NPs;
- ii. assure a good correct retention and promote a homogenous distribution of the NPs over the paper substrate, avoiding their agglomeration, that will reduce/prevent the photocatalytic efficiency of the paper;
- iii. take into consideration the thickness and porosity of paper substrate;
- iv. provide a direct contact between the target molecules and the active NPs of the paper surface.

Additionally, it is necessary to avoid the possible blockage of the catalytic sites by decomposed compounds guarantying their transport/diffusion promoting the action against future targets.

There are two general procedures to incorporate nanoparticles into paper products: wet-end addition where NPs are added to the cellulose pulp before the handsheets formation, so they

adhere to individual cellulose fibres in the bulk of the product; and surface treatments, where dry paper sheet is impregnated or coated with a formulation based on nanoparticles (Ngo *et al.*, 2011; Pelton *et al.*, 2006).

1.1.2.1 Wet-end addition

The most reported and commonly used method to prepare photo-active TiO₂ based paper is the wet-end addition. This technology provides a correct distribution of TiO₂ in the entire sheet. However, in the use of anionic and colloidal stable TiO₂ nanoparticles, it is necessary to guarantee their correct retention into the cellulose fibres towards the addition of retention aids, like high-molecular-weight cationic water-soluble polymers. Likewise, the NPs are not completely loose to the water stream in the paper-forming process, although could occur aggregation of the NPs that will reduce or even inhibit their purpose to give photocatalytic properties to the paper (Pelton *et al.*, 2006).

One example of a paper containing photo-active TiO₂ NPs and prepared by the conventional wet-end addition, with also the addition of inorganic fibres and flocculants, was performed by Iguchi *et al.*, 2003. Following the same line, Zhang *et al.*, 2013, developed TiO₂ NPs based paper by loading the NPs on carbon fibres, using either Na₂SiO₃ or Al₂(SO₄)₃ as fixatives.

1.1.2.2 Surface treatments

There are several types of paper surface treatments in order to coat or impregnate nanoparticles, including: size-press, layer-by-layer assembly deposition, sol-gel method, direct assembly and in situ assembly, being the first three the most common surface treatments of paper used in association with TiO₂ NPs. Playing with the hydrophilic/hydrophobic character and porous structure of the paper it is possible to control the penetration of the NPs. Moreover concentrating them near the surface could provide a better activation of the final paper and also might prevent the degradation of the paper due to the photo-degradation of TiO₂, therefore in general terms coating techniques present more advantages than the wet-end approach (Ngo *et al.*, 2011).

To produce photocatalytic paper by size-press treatment, normally handsheets are coated with an aqueous suspension of TiO₂ NPs and several types of binders (Ngo *et al.*, 2011; Pelton *et al.*, 2006).

Regarding the sol-gel methodology, the NPs are anchored to cellulose surfaces by the introduction of negatively-charged functional groups. One example is the work carried out by Goncalves *et al.*, 2009, where TiO₂ is loaded on the surface of cellulose fibres, previously

modified by the hydrolysis of tetraethoxysilane (TEOS), octyltrimethoxysilane (OTMS) or phenyltrimethoxysilane (PTMS).

In the layer-by-layer assembly, a solid substrate adsorbs alternated charged polyelectrolytes. For instance, the LbL deposition was used to coat lignocellulose fibres with organized multilayers composed of TiO_2 nanoparticles alternated with linear PSS polyelectrolyte (poly(styrenesulfonate)) (Lu *et al.*, 2007).

1.2 ZnO nanoparticles: mechanism, structure and paper applications

ZnO nanoparticles have been shown to be effective against both Gram-negative and Gram-positive bacteria. Although the antibacterial mechanism of action of ZnO NPs is not yet well understood, some authors described the disruption of cell membrane activity by ZnO NPs as the principal cause, correlated to the direct or electrostatic interaction and cellular internalization of zinc ions and/or with the induction of ROS and H_2O_2 generated from ZnO surface by photocatalysis activation (Jones *et al.*, 2008; Joshi *et al.*, 2012; Martins *et al.*, 2013; Xie *et al.*, 2011).

The hexagonal structure of ZnO (wurtzite), composed by O^{2-} and Zn^{2+} ions tetrahedrally coordinated and arranged alternately along the c-axis, is shown in Figure 23. The piezoelectricity and pyroelectricity properties of ZnO are due to the non-centrosymmetric structure. The energy band-gap of ZnO is around 3.4 eV, what is very close to the 3.2 eV of anatase, the most photocatalytic form of TiO_2 , demonstrating that both NPs should have the same photocatalytic ability (Huang *et al.*, 2008; Tian *et al.*, 2012; Wang, 2004).

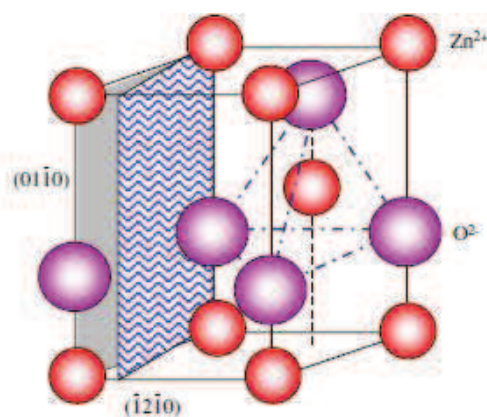


Figure 23. Tetrahedral coordination of wurtzite structure of ZnO.

Zinc oxide is a very interesting material with a very wide range of applications due to its excellent electrical, optical, catalytic and photochemical properties. Moreover, the use of ZnO

nanoparticles based coatings or thin films has been studied on functional coatings, UV inks, catalysts, sensors, portable energy, antibacterial papers, among other applications (Ghule *et al.*, 2006; Martins *et al.*, 2013; Varaprasad *et al.*, 2016; Wang, 2004).

The development of antibacterial papers based on ZnO nanoparticles, like with TiO₂, is increasing in the last years. For instance, Ghule *et al.*, 2006 reported for the first time the use of an ultrasonic approach to coat ZnO NPs on cellulosic fibres. ZnO-cellulose based nanocomposites were developed by Gonçalves *et al.*, 2009 as a result of the growth of rod-shaped particles over the cellulose surface by controlled hydrolysis of Zn(II)- amine complexes, after inducted formation of ZnO seeds by alkaline hydrolysis of aqueous Zn(II). An antimicrobial paper for facemasks, tissues, wallpapers and writing paper applications was successfully developed by Jaisai *et al.*, 2012, also through in situ growth of ZnO nanorods, although by a hydrothermal process. Martins *et al.*, 2013, instead developed for the first time new antibacterial paper by loading NFC/ZnO NPs based coating on the paper surface. These composites were prepared using polyelectrolyte linkers to electrostatic assembly ZnO NPs into NFC.

2. Materials and Methods

2.1 Nanoparticles suspensions

Commercial suspensions of nanoparticles: 6% (w/w) TiO₂ at acidic pH with an average particle size of 40 ± 10 nm (crystalline phase: anatase) and 1% ZnO in diethylene glycol (particle size 45 ± 5 nm, crystalline phase: zincite), were gently supplied by Colorobbia SPA (Italy) and used to prepare NPs-based coating formulations.

The zeta potential of the TiO₂ NPs suspension was evaluated by dynamic light scattering (DLS) analysis, using a Zetasizer Nano Series analyser (Malvern Instruments).

2.2 Paper sheets

Several types of paper were used as a substrate for the nanoparticles. Handsheets of bleached Kraft pulp (BK); handsheets of chemithermomechanical pulp (CTMP); pre-coated recycled paper (PCR) and bleached pre-coated Kraft paper (BPK). The handsheets were prepared at Innovhub SSI – paper division and the other paper samples are commercial paper board, used in food packaging and available in the market.

2.3 Functionalization of paper surfaces with active nanoparticles

Active paper samples reported in this work were prepared by applying coating formulations, based on TiO₂ nanoparticles, using dip-coating and rod-coating techniques. Instead, ZnO NPs were only used to develop an overprint varnish suitable for flexographic printing. The overprint varnish was applied onto paper samples both at laboratory and industrial pilot scale. The preparation of each type of formulation is described in details here below.

2.3.1 Aqueous suspensions of TiO₂ nanoparticles

Several aqueous dilutions from the original 6% TiO₂ nanoparticles suspension were prepared and used to directly functionalize paper substrates by dip-coating. The paper samples were soaked for 3 minutes with different concentrations of TiO₂, then withdrawn at constant speed and let them dry at room-conditions until further analysis.

2.3.2 NFC/TiO₂ coating formulations

Formulations based on the mixture of TiO₂ NPs with NFC at different ratios were prepared using two different methods, the first one consisted in the direct mixture of the two components (DM coating formulations) and the other in layer-by-layer assembly (PE coating formulations). To prepare DM formulations, TiO₂ NPs suspensions were slowly added to NFC and the mixture was kept under stirring for 30 minutes. To perform the layer-by-layer assembly (LbL) of TiO₂ NPs on NFC surface, a polyelectrolyte-assisted deposition using cationic (PDDA) and anionic (PSS) polyelectrolytes solutions (PEs) at 0.1% (w/v), prepared in 0.5M NaCl, was applied. First, the NFC suspension (20 g) was alternatively dipped and kept under stirring for 30 minutes in PDDA, PSS and again in the PDDA solution, followed by centrifugation (10 minutes, 6000 rpm) and washes to remove the excess of PEs. After this, TiO₂ NPs were slowly added on the treated NFC and the formulation was kept under stirring for 30 minutes. The NPs that were not attached to the NFC were washed off from both types of NFC/TiO₂ coating formulations. DM and PE coating formulations were then loaded on paper surfaces by rod-coating technique using a rod size 26 at 110 mm/sec. Immediately after the coating deposition all the samples were dried in an oven at 105 °C for 2 minutes.

2.3.3 ZnO overprint varnish

The ZnO NPs-based overprint varnish formulation was prepared by adding ZnO NPs at 1% (w/w) suspension in diethylene glycol to a base overprint varnish, in different basis weight ratio. The base overprint varnish was prepared with three components from BASF: 65.2% (w/w) of

a styrene-acrylic emulsion (Joncryl 90), 29.3% (w/w) of an acrylic resin in 32% (w/w) ammonia solution (Joncryl 8078) and 0.5% (w/w) of Poligen WE6, gently supplied by Multi Packaging Solutions Company. Joncryl 90 provides gloss and optical clarity, Joncryl 8078 provides pigment wetting, excellent transfer and printability, good gloss and hold out, especially for high line speed applications and Poligen WE6 acts as an emulsifier (non-ionic).

2.4 Photo-activation of the TiO₂ NPs

The photo-activation of the TiO₂ NPs deposited on the paper substrates was carried out by a 4 h exposition under a solar-like lamp system (GE ARC70/UVC/730 - 6000 lux) at room temperature and constant relative humidity.

2.5 Characterization of coated papers

2.5.1 Inductively Coupled Plasma

The amount of TiO₂ and ZnO nanoparticles retained in coated papers were determined by Inductively Coupled Plasma Mass Spectrometry (ICP-MS). The paper samples were randomised by cutting a significant amount in small pieces, then two randomised samples of approximately 100 mg each were submitted to an acidic mineralization (4 ml HNO₃ (65%) plus 2 ml H₂O₂ (35 wt. % in H₂O) and 0.25 ml HF (40%)), using 100 mL Teflon reactors, in a microwave digestion system (Anton Paar GmbH - Multiwave 3000). The resulting solution was diluted with water to 50 mL and its titanium and zinc content was measured by ICP-MS, using a Perkin Elmer Sciex Elan 9000 with a double pass Scott spray chamber, after a further dilution to bring the concentrations within the calibration ranges.

2.5.2 Scanning electron microscopy with energy dispersive X-ray spectroscopy

The scanning electron microscopy (SEM) analysis of the surface of NPs-based coated papers was performed using two different equipments. In one, dry samples were placed on a metallic aluminium stub, coated with evaporated carbon and then elemental analysis and SEM images were obtained using a field-emission gun (FEG) SEM Hitachi SU70 microscope operated at 15 kV and equipped with an energy-dispersive X-ray (EDX) spectroscopy accessory (EDX detector: Bruker AXS; Software: Quantax). In the other equipment, the samples were coated instead with gold/palladium (Metallizer: Cressington 108 auto) and the SEM images were obtained with a field-emission gun (FEG) SEM MIRA3 Tescan microscope operated at 15 kV and equipped with an EDX spectroscopy accessory (EDS XFlash 6/10 versione QUANTUM Bruker).

2.5.3 Determination of water absorptiveness – Cobb60 test

The quantity of water that can be absorbed by the surface of paper/board samples in 60 seconds was determined following the International Standard ISO535:2014, using water absorption apparatus (Figure 24) that consists in a cylindrical metal container, with an inside diameter of 5 cm, clamped to a flat base with a rubber mat, larger than the outside dimensions of the ring onto which the sample is placed.

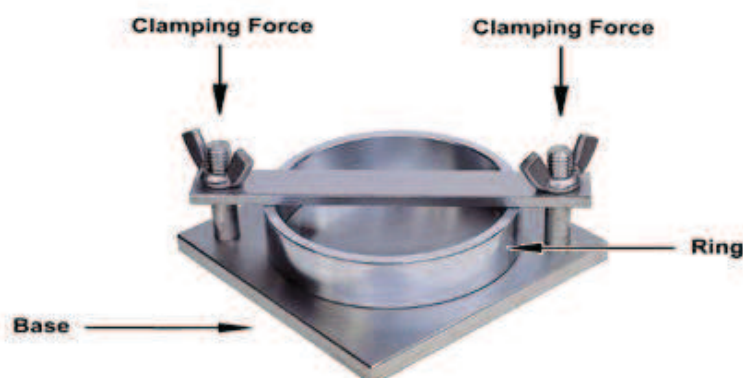


Figure 24: Water absorption apparatus.

The paper samples, after at least 24h in a conditioned room at $23\pm 1^\circ\text{C}$ and $50\%\pm$ relative humidity, were weighed and placed into the dry cylinder, then 20 mL of water ($23\pm 1^\circ\text{C}$) were poured over the test sample and after about 50 seconds (corresponding to 10 s before the 60 seconds predetermined test period) the water was poured off and the sample was taken off the apparatus. Therefore, exactly at 60 seconds of test period, the surplus water was removed from the sample by placing it between a standardized and dry blotting paper and by moving a standardized roller (2 times forwards and backwards) over the pad, paying attention to not apply any additional pressure. Finally, the sample was weighed again and the results calculated, using Equation 13, and reported as weight of water absorbed in g/m^2 .

$$\text{Weight of water (g/m}^2\text{)} = [\text{Final weight (g)} - \text{Conditioned weight(g)}] \times 400 \quad \text{Equation 13}$$

2.5.4 Degree of polymerization

The cellulose degree of polymerization (DP) of the paper samples was analysed by determination of the limiting viscosity number in a cupri-ethylenediamine (CED) solution (1.0 M in H_2O) following the method ISO 5351:2010. Therefore, samples with approximately 10 g of oven-dry mass were teared using a pair of tweezers, into small pieces. Then, 125 mg (± 0.5 mg) of each sample were weighted into a dissolving bottle, with an adequate volume. 25 ml of

distilled water, together with 5 to 10 pieces of copper wire were added to the mixture, which was shaken until complete disintegration of the test sample. 25 ml of CED solution were added and the remaining air was expelled by squeezing the bottle. After controlling that the pulp was completely dissolved, the bottle was immersed in a constant-temperature bath at 25 °C (± 0.1 °C). When the temperature has been reached, the times of efflux of the diluted solvent and the pulp solution through a capillary-tube viscometer were measured at a specified mass concentration. The intrinsic viscosity and equivalent DP were then estimated: first by calculating the viscosity ratio (η_{ratio}) through the Equation 14,

$$\eta_{ratio} = h \times t \quad \text{Equation 14}$$

where: t is the efflux time of the test solution (in seconds) and h corresponds to 0.038 s^{-1} , (obtained from the calibration procedure); and then by determining the limiting viscosity number ($[\eta]$, Equation 15), using the auxiliary table B.1 in Annex B (ISO 5351:2010),

$$\log[\eta] = \frac{\eta - \eta_0}{\eta_0 \times \rho} - k[\eta]\rho \quad \text{Equation 15}$$

Where: $\frac{\eta - \eta_0}{\eta_0 \times \rho}$ is the viscosity number (mg/g), $k = 0.13$, an empirical constant for the pulp/CED system and ρ is the mass concentration (on an oven-dry pulp basis), in grams per milliliter, of the pulp in the diluted solvent (0.5 mol/L CED solution).

2.5.5 Brightness measurements

The brightness measurements were performed with a HunterLab UltraScan® PRO – Colour Measurement Spectrophotometer according to modified ISO 2470-1:2009, where the diffuse blue reflectance factor (ISO brightness) of papers samples was measured with Illuminant C and a slightly modified instrument geometry (d/8 instead of d/0).

2.6 Antibacterial assessment

The activity of the coated paper samples against the gram-positive bacteria *S. aureus* and the gram-negative bacteria *P. aeruginosa* was assessed using the AATCC Test Method 100-2004. The antibacterial tests were conducted by spreading on the surface of the paper samples a known number of living cells (approximately 10^5 CFU - Colony Forming Units). The inoculated samples were then incubated for 24 hours under optimal bacteria growing conditions (20% nutrient broth, temperature 37 °C). Using 50 mL of neutralizing solution (L- α - Lecithin 3 g/L, sodium thiosulphate 5 g/L, L-Hystidine 1 g/L, Polysorbate80 30 g/L, KH_2PO_4 10 mL/L (pH 7.2 ± 0.2)) the surviving bacteria were extracted from the samples. Aliquots of each sample

were taken, diluted (10^0 - 10^{-5}) with physiologic solution and plated with plate count agar (PCA). After 24 h of incubation at 37 °C, the number of living cells was determined and the antibacterial efficiency (R) of the samples was finally calculated using Equation 16.

$$R \text{ (average log Reduction CFU)} = \text{Log (B/C)} \quad \text{Equation 16}$$

where: B is the average CFU of control corresponding to the living bacteria cells and C is the average CFU of examined sample, both after incubation time.

In general two antibacterial effects can be distinguished:

- i. Bacteriostatic: inhibition of bacteria growth under testing conditions favourable to bacteria proliferation, evaluated in respect to the growth of the blank sample (CFU at time 24 h);
- ii. Bactericidal: reduction (killing) of the number of bacteria initially inoculated (CFU at time 0).

2.7 Recycling test

The recyclability test was based on the Aticelca MC 501-13. A mixture of TiO₂ NPs dip-coated paper samples was disintegrated in water at 2.5% consistency in a Hobart Mixer (N20) for 10 minutes. At the end of the repulping stage, 4 L of water were added and recycled handsheets with the same grammage as before disintegration (120 g/m²) were prepared.

2.8 Biodegradability assays

The methodology used for testing the biodegradability of paper coated samples was based on the ISO 14855-1:2012 standard, which determines the aerobic biodegradability under controlled composting conditions, measuring the total amount of carbon dioxide evolved at the end of the test. The samples were ground in a coffee grinder before adding them to the inoculum compost, the different mixtures were introduced into static composting vessels and kept under optimum oxygen, temperature ($58 \text{ °C} \pm 2 \text{ °C}$) and moisture conditions for a test period of around 90 days. The carbon dioxide produced was measured each day of the experiment using a multi-channel IR detector, to determine the cumulative carbon dioxide produced both in test samples ($(\text{CO}_2)_T$, grams per vessel) and blank vessels ($(\text{CO}_2)_B$, grams per vessel). The theoretical amount of carbon dioxide (ThCO_2) that can be produced by the sample (grams per vessel) can be calculated using Equation 17.

$$\text{ThCO}_2 = M_{TOT} - C_{TOT} \frac{44}{12} \times 100 \quad \text{Equation 17}$$

Where: M_{TOT} is the total dry solids (g) in the samples introduced into the composting vessels at the beginning of the test; M_{TOT} is the total organic carbon in proportion to the total dry solids (g/g) in the samples; 44 and 12 respectively correspond to the molecular mass of carbon dioxide and the atomic mass of carbon. Finally, the degree of biodegradation of the samples (Dt, %) was evaluated using the Equation 18.

$$Dt = \frac{(CO_2)_T - (CO_2)_B}{ThCO_2} \times 100 \quad \text{Equation 18}$$

3. Results and discussion

3.1 Studies on TiO₂ photo-active NPs coated papers

Several coating systems were tested in order to optimize the inclusion of TiO₂ nanoparticles. For that, the antibacterial activity of different dip-coated papers with TiO₂ nanoparticles were previously assessed and then the inclusion of nanoparticles in nanofibrillated cellulose (NFC) matrix and their application in paper by rod-coating were evaluated. The isoelectric point (pI - the pH at which there is no net electrical charge) was determined by the measurement of the zeta potential in function of pH, that serves to identify the electrostatic behaviour of 6% TiO₂ NPs starting suspension.

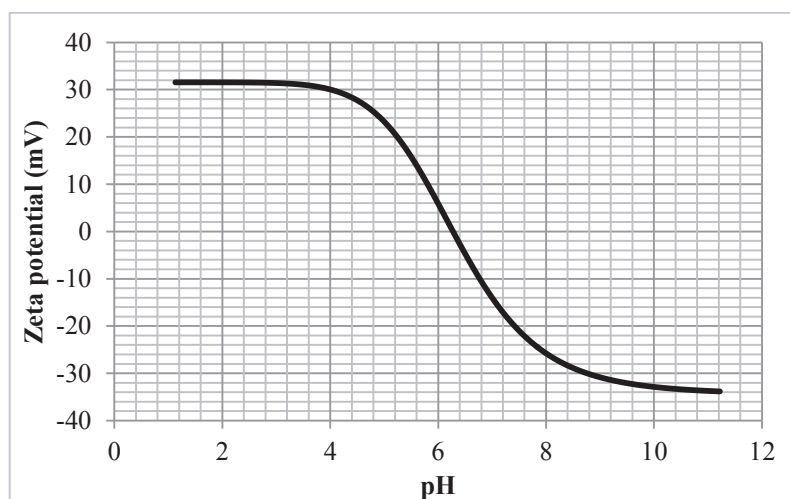


Figure 25. Zeta potential in function of pH for the TiO₂ nanoparticles suspension.

The TiO₂ NPs suspension (16.7 g diluted in 50 mL of water) with an initial pH of 1.6 presented a pI equal to 6.3, with a positive charge below this value and above a negative charge (Figure 25). In addition, it was observed an increase of the viscosity with the increase of the pH solution very likely due to the agglomeration of the NPs. In order to maintain the nano-sized particles, the suspension was used within the positive charge range in all the experiments, as recommended by Fu *et al.*, 2005.

3.1.1 Performance of photo-active TiO_2 NPs loaded on papers by dip-coating

In this study, the performance of TiO_2 NPs as active compounds for antibacterial paper surfaces was verified and compared for different types of substrates. In Table 13, the main properties of the paper samples used for the dip-coating treatments are reported. All the samples were evaluated regarding their grammage and water absorptivity, as Cob 60 test, to investigate their hydrophilic/hydrophobic character.

Table 13. Characteristics of the papers used for the dip-coating treatment.

Samples	Grammage (g/m^2)	Cobb 60 (gH_2O/m^2)	Character
BK	120	74.45	hydrophilic
CTMP	120	73.51	hydrophilic
PCR	330	98.43	hydrophilic
BPK	300	8.42	hydrophobic

3.1.1.1 Bleached Kraft paper

Bleached Kraft (BK) paper samples were dip-coated with different amounts of photo-active TiO_2 nanoparticles and their antibacterial activity was tested over *S. aureus* and *Pseudomonas aeruginosa* (Figure 26), right after photo-activation. Untreated samples under the test conditions supported a significant bacterial proliferation after 24 h contact time. The initial inoculum with approximately 10^5 cells grew up to around 10^8 cells, corresponding to a *S. aureus* growth value ($\log CFU T_{24} - \log CFU T_0$) of 2.2 log CFU and 3.2 log CFU for *Pseudomonas aeruginosa*.

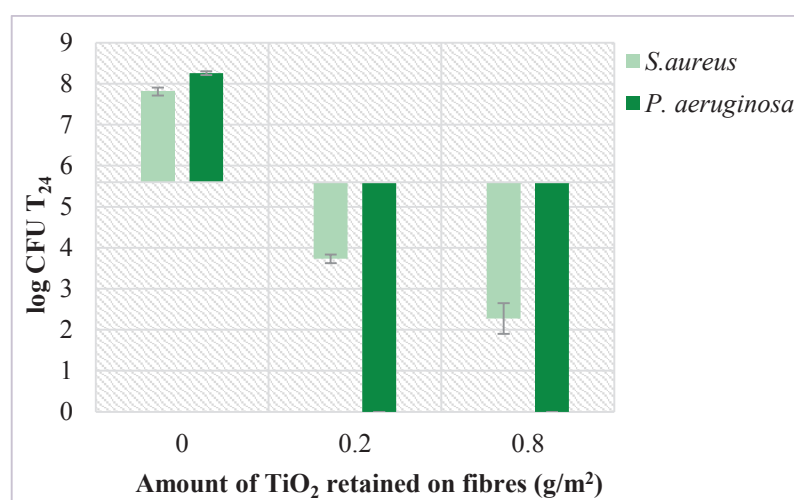


Figure 26: Antibacterial activity against *S. aureus* and *P. aeruginosa* as a function of the NPs retained on the BK coated paper.

Figure 26 clearly shows that the dip-coated paper samples displayed a significant bactericidal activity, with a decrease of 8.3 log CFU comparing to the reference sample, after 24 h contact time. Against *S. aureus* bacteria, the effect is directly proportional to the amount of TiO₂, instead against *Pseudomonas aeruginosa* both concentrations of TiO₂ caused a complete killing effect, showing that TiO₂ dip-coated papers were more active against *P. aeruginosa*.

3.1.1.1.1 Influence of the storage conditions on the antibacterial activity

Active radical oxygen species may decay over time, so the antimicrobial performance of BK dip-coated paper samples was tested also after storage under indoor light and dark conditions exposure (Figure 27).

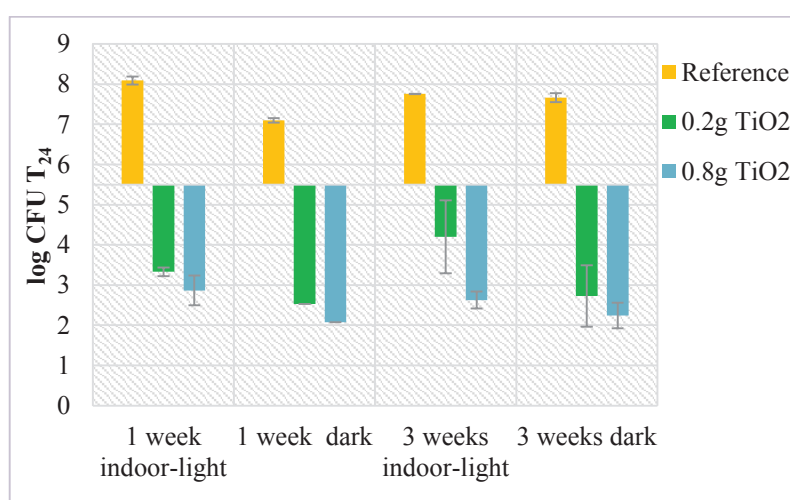


Figure 27: Antibacterial activity of BK coated paper against *S. aureus* at different storage conditions.

The antibacterial activity of photo-active BK paper against *S. aureus*, as illustrated in Figure 27, is maintained with only a slight decrease over a period of three weeks under indoor-light and dark conditions exposure.

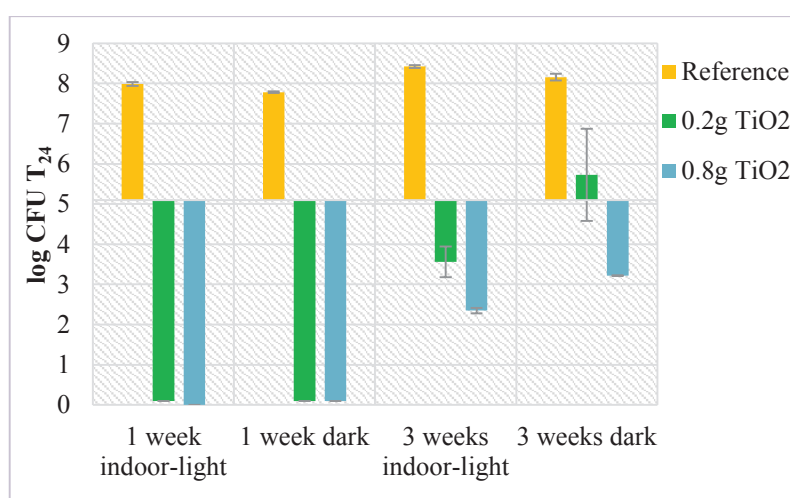


Figure 28: Antibacterial activity of BK coated paper against *P. aeruginosa* at different storage conditions.

Besides, the activated paper samples presented even a stronger bactericidal effect against *P. aeruginosa*, with a complete killing effect observed after a week of storage (Figure 28).

3.1.1.1.2 Effect of TiO₂ nanoparticles on the fibre degradation over time

The antibacterial effect of TiO₂ is due to the active radical oxygen species generated in the presence of H₂O and O₂ and under UV irradiation (Goncalves *et al.*, 2009). These active radicals may produce cellulose oxidation and in the end depolymerise the cellulose chain as reported by Pelton *et al.*, 2006 and also demonstrated by Marques *et al.*, 2006. Cellulose depolymerisation may directly affect several paper properties whereas cellulose oxidation mainly affects brightness of the paper samples producing a yellowish colour detrimental for paper surfaces that need to be printed. In this work the influence of the TiO₂ NPs application on properties of cellulose fibres was investigated by measuring cellulose depolymerisation and by brightness measurements. The degradation behaviour as a reduction of the relative degree of cellulose polymerization over time, presented in Figure 29, was obtained by viscosity measurements of the coated papers fibre dissolved in cupriethylenediamine (CED).

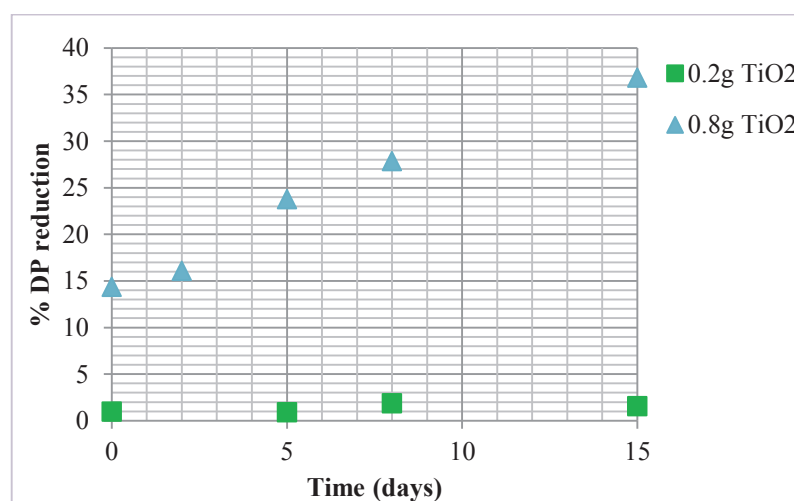


Figure 29: Cellulose degree of polymerization reduction behaviour over time.

After two weeks the dip-coated papers (BK paper) containing 0.8 g of TiO₂ caused a significant reduction in the degree of polymerization, reaching a value of 37% after 15 days of TiO₂ functionalization. On the contrary, for the lowest amount of TiO₂ (0.2 g) basically no degradation of the fibres was detected (Figure 29). The possible yellowing of the paper can be verified through brightness measurements as they are correlated (Biermann, 1996). The measurements were performed at 457 nm, over time and the results can be verified in Figure 30.

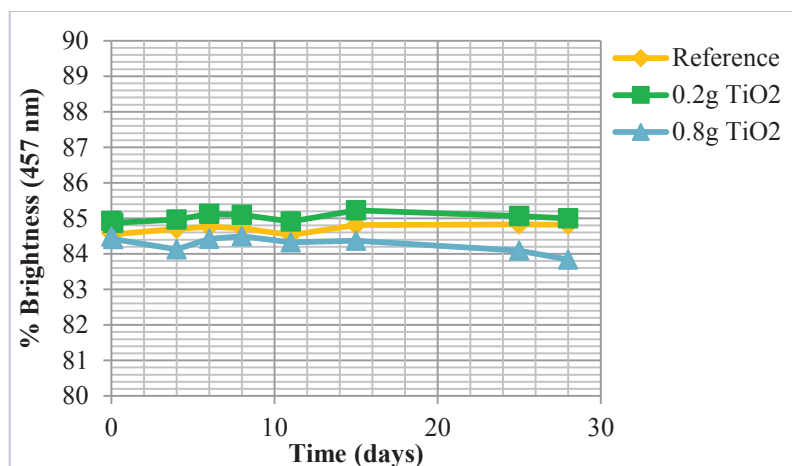


Figure 30: Brightness behaviour of BK paper as a function of time.

As illustrated in Figure 30 after almost 30 days of studies, the BK papers coated with 0.2 g and 0.8 g of TiO₂ NPs per square meter and the reference sample present a similar behaviour. The small reduction observed at the highest nanoparticle concentration is not critical for this property, being within the standard deviation of the results. Accordingly, it was shown that at low TiO₂ concentration the fibres were not degraded. Further visualization of the samples, after months of storage, reveals only a slight yellowing of the paper with most concentrated NPs.

3.1.1.2 Chemithermomechanical paper

In order to compare the influence of the pulp on the antibacterial activity of the TiO₂ NPs retained on the paper surface, handsheets of a chemithermomechanical pulp (CTMP) with a grammage of 120 g/m² were prepared as a paper substrate for dip-coating assays. The assessment of the antibacterial activity of the paper dip-coated with different concentrations of TiO₂, toward *S. aureus* and *P. aeruginosa* over three weeks, is presented in Figure 31(a) and (b), respectively.

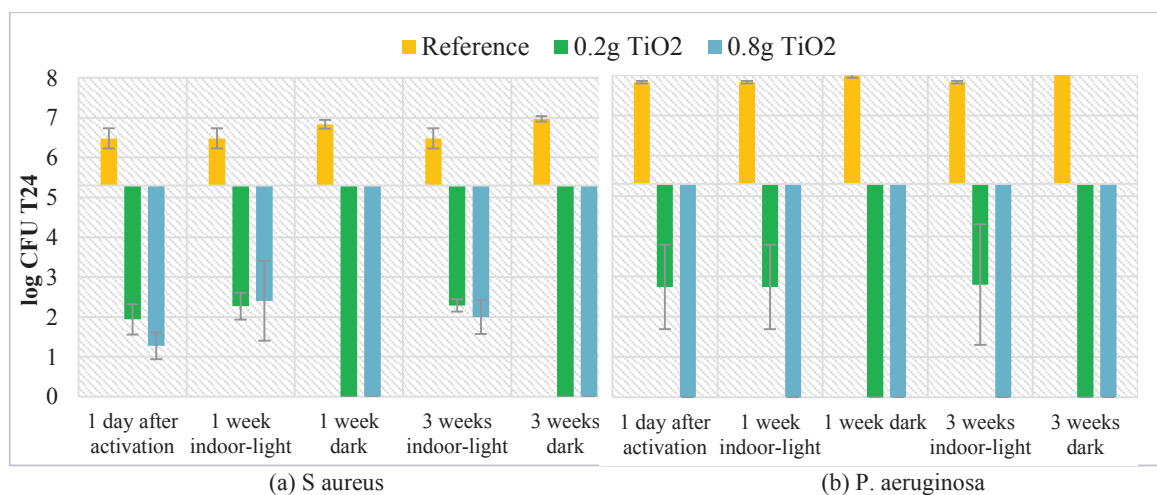


Figure 31: Antibacterial activity toward (a) *S. aureus* and (b) *P. aeruginosa* of the CTMP coated paper.

Comparing both microorganisms and treated samples a bactericidal effect was observed even after a 3 weeks period of storage (indoor-light conditions) after TiO₂ light activation. Data reported in the figures show that immediately after activation the effect of antibacterial paper with highest concentration of TiO₂ against *P. aeruginosa* was stronger than against *S. aureus*, with an antibacterial efficiency equal to 7.8 log against 5.2 log, respectively. After three weeks the behaviour did not change considerably for both bacteria. Besides, it can be observed that towards *P. aeruginosa* the highest concentration of TiO₂ nanoparticles retained on the fibres continues displaying a complete killing effect. According to the reported results we can state that both concentrations of photo-active TiO₂ nanoparticles, deposited by dip-coating on handsheets made of CTMP, present a strong and very stable antibacterial activity over three weeks time.

Also the effect of TiO₂ nanoparticles on the optical properties of this type of paper (CTMP) was evaluated by means of brightness evaluation over time (Figure 32).

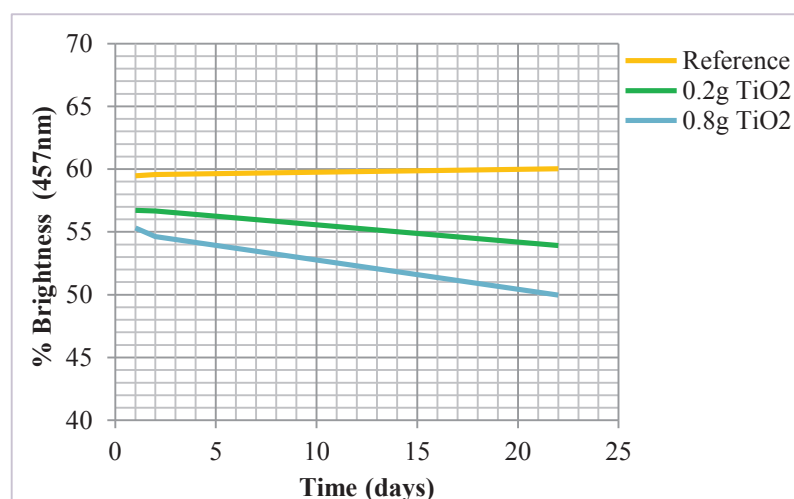


Figure 32: Brightness behaviour of CTMP coated paper as a function of time.

The results reported in Figure 32, although tested for a shorter period with respect to BK, show a slightly higher decay of the brightness value over time, especially for the paper with the highest amount of NPs. Moreover, after several months of visualization, the yellowing of the paper increased considerably for both papers, becoming even brown, contrarily to what occurred for BK samples. The paper loaded with 0.8 g of TiO₂ per square meter presented a darker brown coloration, as expected. As can be noted, CTMP initial brightness is lower than BK by more than 20 points due to the greater amount of lignin present in the fibres. The higher brightness reduction over time is very likely due to the different chemical composition of CTMP

and its greater lignin content. Lignin moieties present in the cell wall are likely being oxidised faster than cellulose, producing the darker colour.

3.1.1.3 Pre-coated recycled paper

A pre-coated recycled paper (PCR) was also used to prepare TiO₂ NPs–based paper surfaces. Even though the samples were prepared in the same conditions, two different PCR samples with 1.0 and 1.7 g/m² of TiO₂ retained on the surface were achieved, as measured by ICP-MS. The higher amount of NPs on the PCR samples, compared to BK and CTMP samples (0.2 and 0.8 g/m²), might be associated to the higher grammage of PCR samples (330 g/m² against 120 g/m²), that allowed a higher retention of the NPs on their surface. These samples were evaluated regarding their possible antibacterial activity against *S. aureus* bacteria (Figure 33).

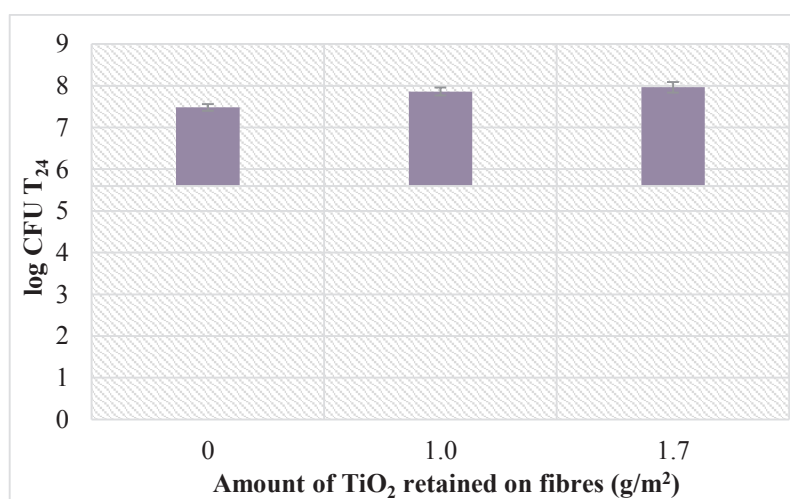


Figure 33. Antibacterial activity of TiO₂ PCR coated paper against *S. aureus*.

Despite the large quantity of NPs, both PCR samples did not show any antibacterial effect against *S. aureus* as can be noted in Figure 33, contrarily to what expected, taking into account the very positive results exhibited on BK (Figure 26) and CTMP (Figure 31 (a)) samples against the same bacteria. All the three type of samples, BK, CTMP and PCR, presented a similar Cobb60 value, so a relatively comparable hydrophilicity, ruling out this aspect for being responsible of the unsatisfactory results. On the other hand, the thicker grammage of the PCR paper board combined with the huge amount of inorganics (around 18.5%, mainly calcium carbonate), detected by SEM-EDX analysis (Figure 34), possibly cause a deeper impregnation of TiO₂ into the samples, that remains covered by the other minerals. The NPs of the PCR samples may be inaccessible to the contact with bacteria or most likely even unable to be light activated, resulting in the absence of any antibacterial effect.

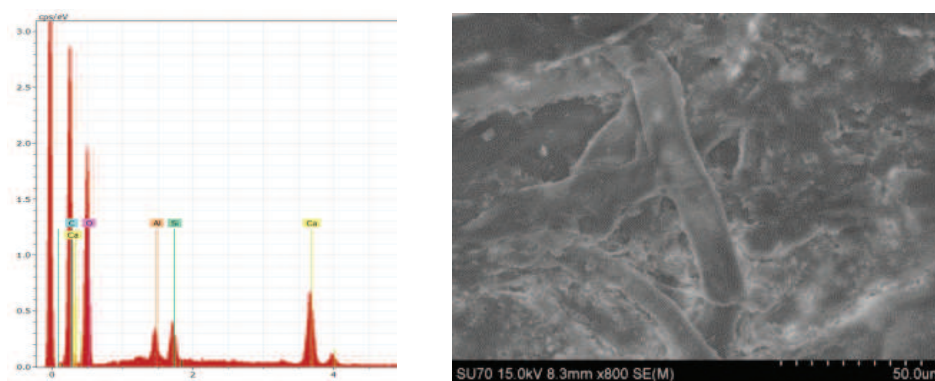


Figure 34. SEM-EDX analysis of the PCR paper surface.

3.1.1.4 Bleached pre-coated Kraft paper

Bleached pre-coated Kraft (BPK) paper board samples, a hydrophobic paper board intended for food contact, were also dip-coated with TiO₂ nanoparticles and tested against *S. aureus*. The results of antibacterial tests are summarized in Table 14, as average log reduction.

Table 14. Antibacterial results for BPK coated samples.

Sample	log ₁₀	R
BPK1 (0.15 g TiO ₂ /m ² paper)	5.6	0
BPK2 (0.20 g TiO ₂ /m ² paper)	5.6	0

For these samples, the absence of antibacterial effect observed in Table 14, could be a consequence of the low Cobb 60 value (8.42 g H₂O/m², as indicated in Table 13). The higher hydrophobicity of the BPK samples most likely was the cause of the low retention of the NPs, as only 0.15 g and 0.20 g of TiO₂ were effectively attached, and the non-homogenous distribution on the paper surface. Nevertheless, it shall be pointed out that at 0.2 g/m² concentration the BPK sample was shown to produce a clear antibacterial effect, thus further investigations would be necessary to fully understand the reason of these outcomes.

Eventually, to overcome the lower retention on more hydrophobic surfaces, a different route was pursued and investigated, by the preparation of formulations based on NFC and photo-active TiO₂ nanoparticles, applied on paper surfaces by rod-coating, as described further.

3.1.2 Development of active papers based on NFC/TiO₂ coating formulations

The preparation of coating formulations based on mixtures of nanofibrillated cellulose and nanoparticles of TiO₂ aimed to overcome the problematic related to the low retention efficiency of NPs by the paper/board substrate, which might be associated with the hydrophobic character of the surfaces and composition/quality of the pulp fibres (e.g. inorganic components resulting

from recycled fibres). As explained by Schütz et al., 2012, the electrostatic interactions between the positive charge groups of the NPs and the dissociated carboxylic group of the NFC (with a higher superficial area than cellulose - paper itself), permit a better accessibility of a higher range of inorganic content. Besides, optical and mechanical properties of the resulting material could be enhanced by the correct balance between the dispersion of NPs and NFC in aqueous media and their electrostatic interactions.

3.1.2.1 TiO₂ deposition onto NFC: Direct-mixture versus Layer-by-Layer Assembly

A rod-coating technique was used to apply two different types of formulations based on NFC and photo-active TiO₂ NPs prepared by: i) direct-mixture (DM formulations), where the nanoparticles were directly combined exploiting the negative charge of the NFC; and ii) by layer-by-layer assembly, i.e. polyelectrolyte-assisted deposition (PE formulations), where NFC was previously treated with polyelectrolytes in order to increase its negative charge.

The amount of nanoparticles retained on NFC was function of their initial concentration in the mixture, the efficiency of the process was calculated as percentage of NPs retained on NFC with respect to their initial concentration in the treatment. The results are described in Table 15 and illustrated in Figure 35.

Table 15. Retention efficiency of the NFC/TiO₂ NPs based coating formulations.

Formulation	Amount of TiO ₂ in NFC (w/w)		Efficiency (%)
	Initial	Final	
DM	5.6	3.14	55.82
	14.4	5.79	40.14
	33.3	7.96	23.88
	50.0	13.74	27.48
	66.7	15.81	23.72
PE	5.0	3.42	68.39
	14.3	6.21	43.28
	33.3	11.49	34.53
	50.0	18.70	37.39
	66.7	21.58	32.35
PE(2)	10.0	6.00	60.00
	25.0	15.00	60.00
	35.3	24.98	70.69
	50.0	29.00	58.00
	67.7	31.82	46.96
PE(3)	8.0	6.00	75.00
	18.0	14.00	77.78
	36.3	31.77	87.44
	55.0	35.00	63.64
	68.2	35.91	52.62

At the lower TiO₂ NPs concentration in the mixture the retention on NFC was approximately 50% both for DM and PE formulations, as can be seen in the Table 15. However, when the NPs concentration was increased the efficiency of the NPs retention was always about 10% higher for the PE formulations independently from their initial concentration. Additionally, it is observed that increasing the negative charge of the NFC by adding more layers of PSS (negative charged polyelectrolyte), for a total of 2 layers for PE(2) formulations and 3 layers for PE(3) formulations, the NPs retention was enhanced in comparison to direct mixture formulations, thus allowing a higher total amount of TiO₂ NPs in the coating formulation from 8 up to 30-35% (Figure 35).

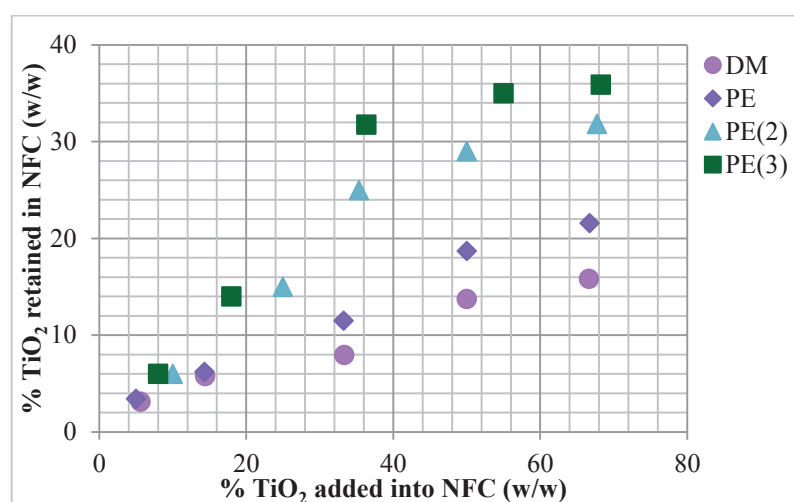


Figure 35: Relation between the amounts of TiO₂ NPs initially added and finally retained on the NFC.

Furthermore, under the best conditions, so for the PE(3) formulation with around 35% TiO₂ NPs concentration, due to the greater electrostatic interaction, the retention of TiO₂ was almost 90% (Table 15) of the nanoparticles added to the mixture.

3.1.2.2 Antibacterial assessment

The enhanced NFC/TiO₂ formulations were coated on the surface of the hydrophobic bleached pre-coated Kraft (BPK) paper board in different concentrations, resulting in two samples with 0.8 g and 4.1 g of TiO₂ per square meter of surface, respectively. Both samples were assessed regarding to the antibacterial activity against *S. aureus* bacteria (Table 16).

Table 16. Antibacterial activity of rod-coated NFC/TiO₂ based BPK paper board against *S. aureus*.

Sample	log ₁₀	R
BPK - 0.8 g TiO ₂ /m ² paper	5.6	1.8
BPK - 4.1 g TiO ₂ /m ² paper	5.6	2.7

As shown in Table 16, the BPK coated paper samples with NFC-TiO₂ formulations presented a bacteriostatic effect against *S. aureus* with 1.8 log reduction for only 0.8 g of TiO₂ nanoparticles deposited on the paper surface with an increase of the antibacterial effect for the higher concentration samples.

These results show that layer-by-layer assembly represents a suitable technique to increase TiO₂ nanoparticles retention onto NFC. These formulations can be used to coat hydrophobic paper samples where the efficiency of direct NPs impregnation is very low.

3.2 Advances on ZnO NPs cellulose-based packaging to reduce medical cross contamination

Antimicrobial resistance is commonly found in long-term-care facilities due to healthcare-associated infections (HAIs) and use of antimicrobials in acute care. In European countries, 6 out of 100 patients (country range 2.3%-10.8%) acquire at least one HAI in hospitals, as reported in the surveillance report 2011-2012 of the European Centre for Disease Prevention and Control (ECDC) (Suetens *et al.*, 2013). The development of active cellulose-based packaging to reduce microbial cross-contamination seems to be a good solution to minimize the problematic of HAIs in hospitals and a good opportunity for the cellulose-based packaging industry, as very few packages with these characteristics are commercially available.

In this part of the work, the aim was to develop an innovative cellulose-based packaging solution for medical applications based on an overprint varnish containing active inorganic NPs. This application and the relative process scale up was part of the “proof of concept” of the NewGenPak project. Upon selection of the most suitable concepts Multipackaging Solutions Company (partner of the NEWGENPAK project) invited three early stage researchers (ESRs) to participate and run a pilot trial at their manufacturing facility in Belfast - Northern Ireland.

3.2.1 Development of an inorganic-based overprint varnish for flexography printing

To develop an overprint varnish formulation for the industrial flexographic printing trial, nanoparticles of titanium dioxide and zinc oxide were initially studied with respect to their compatibility with the base overprint varnish recommended by the Multipackaging Solutions (MPS) Company. TiO₂ NPs were found to be incompatible with the varnish components and the main reason was due to the pH, equal to 9. TiO₂ NPs at pH higher than 4 are not stable and start to aggregate, as demonstrated in section 3.1, and should be used at lower pH (Fu *et al.*, 2005). ZnO NPs, on the other hand, were compatible with the varnish components. Therefore

they were selected to be included in the base overprint varnish; besides, ZnO NPs are simpler than TiO₂ to use at industrial scale due to the fact that they do not necessarily require photo activation.

For medical packaging applications, as the idea is to prevent the cross contamination due to the handling of the packaging, the varnish should be used in the external part, contrarily to what happens in food packaging when the active compounds should be in direct contact with the food product, so in the internal surface. Therefore, for the industrial trial several parameters had to be taken into account, particularly optical properties of the external surface and the machine runnability (viscosity, solid content).

Three different formulations of ZnO NPs-based overprint varnish were prepared: 20-80; 15-85 and 10-90 ratios in weight, taking into consideration the limitation of 30-40% of solid content required for the final overprint varnish. To ensure the transferability of the overprint varnish to the board, the rheology behaviour of the formulations was studied and compared with 4 commercial varnishes (C1, C2, C3 and C4) (Figure 36). The commercial coating formulations C1 and C4 correspond to the lower and upper level of acceptable rheology behaviour, respectively.

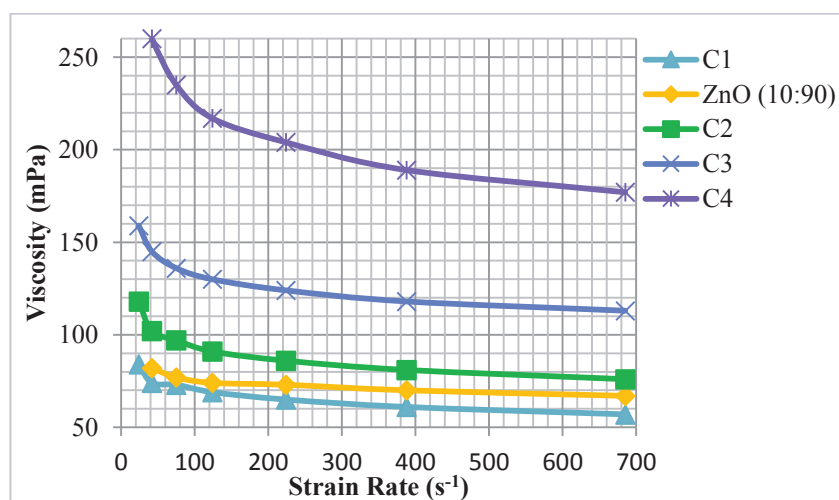


Figure 36: Rheology measurements of ZnO overprint varnish and commercial reference varnishes.

The ZnO NPs-based overprint varnish formulations with ratios of 20:80 and 15:85 basis weight presented a non-proper rheology behaviour (below C1). The other formulation has an acceptable rheology behaviour, between C1 and C2, as can be seen in Figure 36. Although the ZnO NPs-based varnish with a ratio of 10:90 was in the relatively low viscosity acceptable range, it was chosen to be scaled up and used for the industrial trial.

3.2.2 Packaging design and industrial-trial demonstration

For the packaging demonstrator, a high quality board, constituted by a layer of chemithermomechanical pulp (CTMP) between two layers of chemical pulp, with one side fully coated (triple coating) and a light coating in the reverse side (Figure 37), was purchased from StoraEnso, Sweden, to be used in the pilot trial.

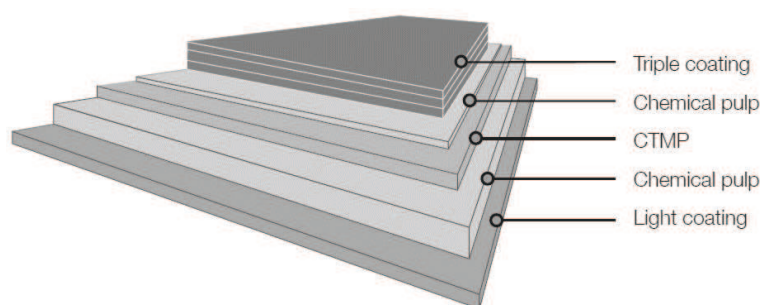


Figure 37: Cross-section of the cardboard used for the packaging demonstrator.

The specifications of the cardboard are summarized in Table 17.

Table 17. Specifications of the cardboard used for the packaging demonstrator.

Property, Unit	Tolerance	Specifications	Standards
Grammage, g/m ²	+3%/-5%	280	ISO 536
Thickness, μm	±5%	440	ISO 534
Bending stiffness DIN 5° MD, mNm	-15%	43.0	ISO 2493
Bending stiffness DIN 5° CD, mNm	-15%	18.3	
Bending moment Taber 15° MD, mNm	-15%	21.5	
Bending moment Taber 15° CD, mNm	-15%	9.8	
Bending resistance L&W 15° MD, mN	-15%	445	
Bending resistance L&W 15° CD, mN	-15%	202	
Moisture, %	±1	8.3	
ISO Brightness C/2°, %, Top	min. 87	90	ISO 2470
ISO Brightness C/2°, %, Reverse	min. 85	88	
CIE Whiteness D65/10°, Top		120	ISO 11475
CIE Whiteness D65/10°, Reverse		114	
Surface Smoothness, PPS 10, μm	max. 1.7	1.0	ISO 8791-4
Gloss 75°, %		45	ISO 8254-1
Scott Bond, J/m ²	min. 100	145	TAPPI 569
Cobb 60, g/m ² , Top	max. 60	30	ISO 535
Cobb 60, g/m ² , Reverse	max. 60	30	

An innovative box packaging design was chosen by MPS and a specific layout was designed by Sheffield Hallam University (project coordinator of the NEWGENPAK project), including

the logo of all the NGP partners and other information providing details of the project, as can be seen in Figure 39.



Figure 38: Layout design of SAFEBOX.

The box planned for syringe packages, classically used in hospitals and handled by a high number of people, was accordingly entitled “SAFEBOX”.

The NEWGENPAK researchers participate in the industrial trial, run out at the MPS Company’s facility in Belfast, Northern Ireland, which lasted approximately one week, including proper cutting design, production and converting operations (Figure 39).



Figure 39: Design and different steps in the development of SAFEBOX.

3.2.2.1 Performance of the ZnO NPs–based packaging demonstrator – SAFEBOX

At industrial scale, the transferability of the developed ZnO NPs–based overprint varnish resulted in good machine runnability and maintenance of the packaging material properties. The SAFEBOX demonstrators presented a final overprinting grammage of 2 g per square meter, as recommended for flexography printing, corresponding to 5.6 mg/m² of active ZnO NPs. Also

printed board with base overprint varnish without ZnO NPs was submitted to flexography printing as a reference for further testing.

The optical properties of the: i) SAFEBOX, ii) printed board with only base overprint varnish (as reference sample) and iii) printed board without overprint varnish samples were verified regarding brightness behaviour over time (Figure 40).

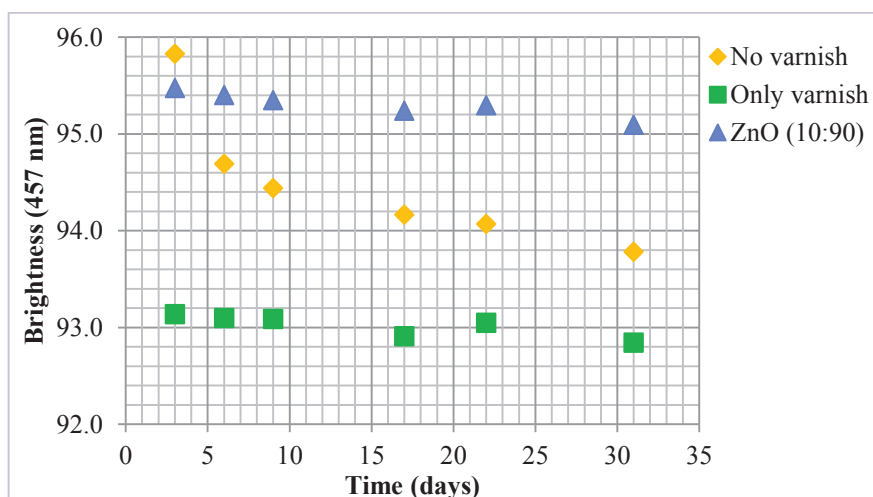


Figure 40: Brightness behaviour of the SAFEBOX and reference boards.

A regular and similar brightness behaviour for SAFEBOX (ZnO (10:90)) and reference samples (only varnish) can be seen in Figure 40. Besides, the brightness of the SAFEBOX is slightly higher, what can be considered an advantage in a consumer perspective. For the printed board without any overprint varnish (no varnish), the optical properties, as expected, suffer a decay regarding the brightness values, losing the colours of the layout over time due to the absence of an overprint varnish to protect them.

The antibacterial activity of the ZnO NPs-based packaging demonstrator was tested against *S. aureus*, following the AATCC Test Method 100-2004 adapted to hydrophobic surfaces (Table 18).

Table 18. Antibacterial results for ZnO NPs based samples.

Amount of ZnO loaded on paper (mg/m ²)	log _{r0}	R
5.6	6.8	0.7

The SAFEBOX surface presented a limited bacteriostatic effect of only 0.7 log reduction compared to the reference sample, as it is shown in Table 18. Moreover, observing Figure 41, relative to the surface morphology of the ZnO NPs packaging demonstrator analysed by SEM-EDX analysis, not only was confirmed the low amount of NPs present on the paper surface but also could be verified a non-homogeneous distribution. Consequently and unfortunately, the

SAFEBOX was not satisfactory regarding the expected application, to contribute in the antimicrobial cross contamination reduction in health-care facilities.

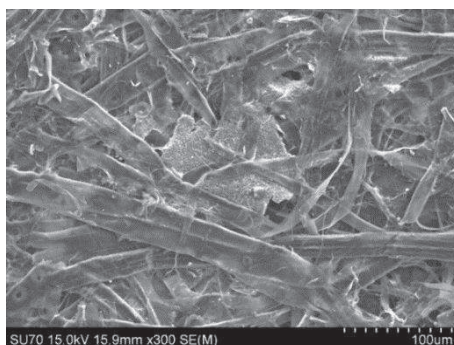


Figure 41: SEM image of SAFEBOX surface.

However, the low amount of ZnO NPs present in the SAFEBOX surface was due to industrial requirements and technical constraints. So, in order to verify the true potentiality of those type of varnishes/packaging, at laboratory scale three more samples were prepared and applied with a different technique - rod-coating deposition. The coating formulations had the same basic components but were richer in ZnO NPs, besides also the resulting grammage of the coating layer was increased to around 90 g/m², being the final amount of ZnO NPs loaded on the board: 283.3 mg, 504.0 mg and 1512.0 mg. Those rod-coating ZnO-based samples were then assessed regarding their antibacterial activity (Figure 42).

Sample	R
5.6 mg	0.7
238.3 mg	1.6
504.0 mg	2.9
1512 mg	3.8

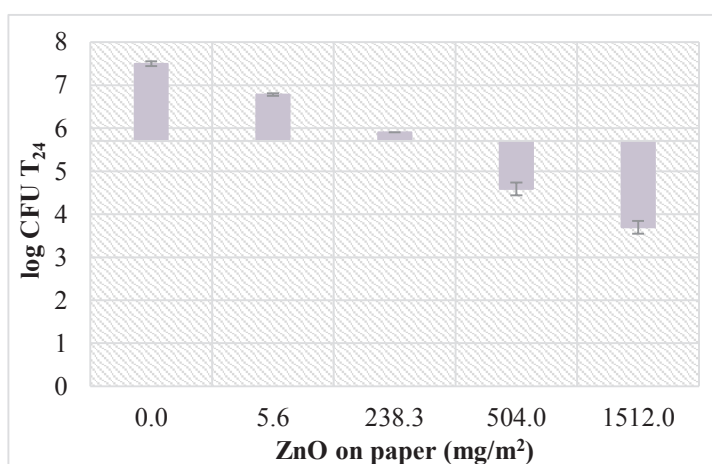


Figure 42: Antibacterial activity against *S. aureus* as function of ZnO NPs load in the coating formulation.

As illustrated in Figure 42, coated paper samples with 238.3 milligrams of ZnO on the surface present a bacteriostatic effect with 1.6 log reduction of the CFU after 24 h contact time. Furthermore, bactericidal effects were observed for 504 mg and 1512 mg of NPs with 2.9 and 3.8 CFU log reduction, respectively. Since the hydrophobicity of the surface was similar, this

parameter is very likely less relevant on the antibacterial activity in comparison to the total amount of NPs in the coating formulation.

The good results obtained at lab scale by rod-coating, where the ratio among the varnish components was changed and thicker coating layers were applied, are currently not yet achievable in a flexographic industrial printing technology. In this latter case, only a very thin coating layer can be deposited onto the paper surface to ensure the required speed of the printing machine, therefore more work is needed to find out the possibility to increase the concentration of active NPs in such a thin layer either by increasing their concentration in the stock suspension (originally is only 1%) or completely modifying the overprint formulation thus allowing a greater share of NPs suspension.

3.3 Sustainability – Packaging End of life

3.3.1 Recycling process - The fate of the nanoparticles

The possible release of the nanoparticles to the water stream after the disposal of the NPs-cellulose-based packaging could represent an environmental and public-health issue. In order to understand the fate of the nanoparticles, TiO₂ nanoparticles dip-coated Kraft paper samples were submitted to a recycling process, as a preliminary case study.

In the Figure 43 is shown the disintegration process of the papers, that was based on the standards Tappi T 205-om 88 and Aticelca MC 208-72 and the handsheets preparation using the recycled pulp.



Figure 43: Preparation of recycled paper samples.

Due to the difficulty to measure the NPs concentration in a highly diluted process water, their mass balance was determined by assessing their total amount in the handsheets before and after the recycling process. The recycled pulp-based handsheets were therefore analysed regarding their content in TiO₂ (ICP measurements) and compared with the initial samples (Table 19).

Table 19. TiO₂ concentration of the paper samples.

Sample	TiO ₂ , g/m ²
Initial sample	1.47
Recycled sample	1.31

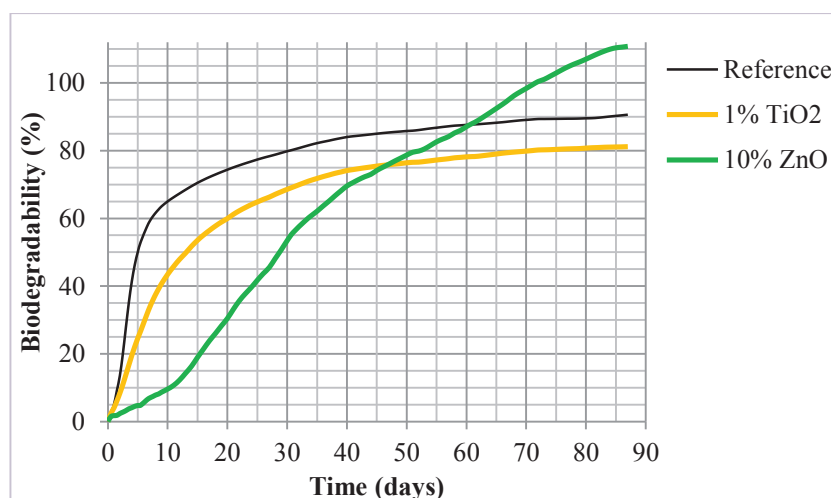
Considering the difference on the amount of NPs, comparing initial and recycled samples, a loss to the water stream of about 10.8% was estimated. Accordingly around 89% of the NPs are still attached to the cellulose fibres by electrostatic interactions, after one cycle of recycling. These results are just a rough estimation and more analysis should be done to obtain a clear conclusion.

3.3.2 Effect of the nanoparticles on the biodegradability

The biodegradability of different samples coated with active nanoparticles was studied, taking into consideration the parameters set by the European standard EN 13432:2000 and the methodology used to determine the degree of biodegradation was based on the ISO 14855-1:2012 standard. The effect of nanoparticles (NPs) inclusion on biodegradability was verified for two different case studies: i) 1% TiO₂ and 10% ZnO dip-coated paper samples; and ii) SAFEBOX - packaging demonstrator.

3.3.2.1 Dip-coated paper samples

Active coated papers were prepared by dip-coating Kraft paper samples into different nanoparticles formulations: 1% (w/w) TiO₂ and 10% (w/w) ZnO. The effect of the NPs on the biodegradability of the samples is reported and compared with untreated reference paper (Figure 44).

**Figure 44.** Degree of biodegradation over time for Kraft paper coated with nanoparticles.

The TiO₂ coated paper presents a very similar kinetic behaviour to the reference sample, the lag phase is very limited but the degradation rate is lower taking slightly more time to reach the plateau (around 70 days). At the end of the test, the mean degree of biodegradation, after 90 days of assessment, corresponds to 80% against the 90% of the reference sample. The final biodegradation of 89% almost reached the pass level foreseen in the EN 13432 standard, which states that at least 90% in total or 90% of the maximum degradation of the reference substance after a plateau should be reached for both test material and reference substance.

For the ZnO coated samples the biodegradation behaviour is quite different. Initially, a clear delay in starting the degradation phase can be observed (Figure 44), this lag phase last around 10 days, afterwards the degradation rate increases more rapidly than the other samples reaching a final degree of biodegradation greater than 100%. These “erroneous” results for biodegradation are normally related to the excessive production of CO₂ in compost due to the addition of the test material (priming effect) and for this case it might be function of the type of NPs and/or its higher NPs concentration, in relation to the amount of NPs in the TiO₂-based samples (Kikuzaki *et al.*, 2002). However, since the reported results were obtained by one single test at the moment we cannot state surely that the addition of the ZnO formulation on the paper samples is definitely the cause of this priming effect. Independently from the type of NPs used, the results presented in Figure 44 further show that the presence of active NPs might influence the lag phase and the rate of biodegradation of a paper coated sample, therefore when developing a new packaging product with the intention of claiming the compostability as end-of-life option, the biodegradability of the material must be taken in due account. Nevertheless, it is also clear that the presence of active ingredients does not necessarily prevent the biodegradation of the material in a rich microbial environment as it is the compost.

Although the good results for the final biodegradation, where the 1% TiO₂ coated paper almost reached the 90% set pass level whereas 10% ZnO overcame it, taking into consideration the EN 14032 standard, further investigations should be performed to better understand whether the type of NPs or their concentrations is the critical parameter to reach the pass level.

3.3.2.2 Packaging demonstrator - SAFEBOX

A biodegradability assessment of the SAFEBOX (ZnO NPs-based packaging demonstrator) was performed (Figure 45). In this case the reference board by itself was not specifically designed for being biodegradable, therefore the aim of this case study was just compare the

effect of the nanoparticles and overprint varnish on the biodegradability behaviour of the packaging product.

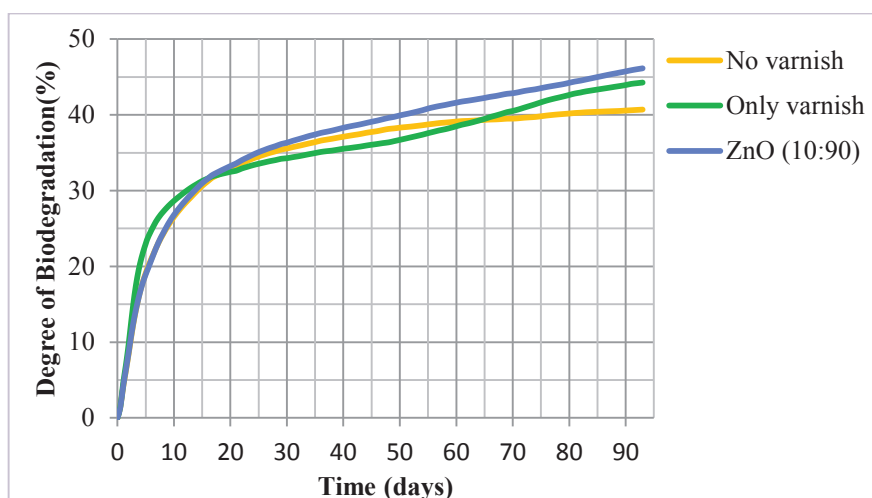


Figure 45. Degree of biodegradation over time for SAFEBOX and reference samples.

In Figure 45, it can be observed the relation between SAFEBOX (ZnO (10:90)), printed board with base overprint varnish (only varnish) and printed board without overprint varnish samples (no varnish). The behaviour of these three samples are very similar with only a very slight increase of the final biodegradation degree when the product is coated with ZnO nanoparticles. Nonetheless, the differences among samples are very little and it can be therefore concluded that the inclusion of NPs, at the concentration used, in the base varnish does not reduce the final biodegradation of the board sample. The low absolute biodegradation value of the board tested is most likely due to other parameters such as for example the high hydrophobicity of the coating that might not allow a sufficient water uptake for the action of the microbial population present in the reactor.

4. Conclusions

The active components used in this part of the work were photo-active TiO_2 and ZnO inorganic nanoparticles, taking into account that coating formulation, deposition techniques and properties of the paper surface are critical parameters to obtain an efficient antibacterial paper.

Direct application of photo-active TiO_2 nanoparticles on the paper surface by dip-coating displayed good results in terms of antimicrobial activity. Moreover, the results show that 0.2% of photo-active TiO_2 nanoparticles, deposited by dip-coating on handsheets made from chemical pulp (Kraft), have strong antibacterial activity without affecting average cellulose DP and handsheets brightness. According to the data the antibacterial activity is reasonably stable

for at least three weeks, showing only a small reduction when the samples are stored at room conditions in the presence of indoor light. However, the retention of the nanoparticles was found highly dependent on the hydrophilic character of the surface and the overall efficiency of nanoparticles retention was low. The inclusion of TiO₂ NPs in NFC matrix may widen the application allowing easier coating of more hydrophobic paper. In this case, the antibacterial activity was reduced; nevertheless, it remained sufficient to maintain bacterial proliferation under control. The best options were to use a direct nanoparticle suspension dip-coating for hydrophilic paper and a coating based on the inclusion of nanoparticles in the nanofibrillated cellulose (NFC) matrix in the case of hydrophobic paper.

The trial was successfully carried out with the active formulation based on ZnO nanoparticles. The newly developed active overprint varnish did not cause any particular adverse effect neither on process runnability during the production, nor on mechanical and optical properties of final package, showing a smooth handling of the process. Nevertheless, in order to cope with all necessary mechanical parameters, the amount of active ZnO nanoparticles in the final formulation was too low to show a significant antibacterial effect even when a second printing layer was laid on the surface. The flexography application of active inorganic nanoparticles onto cellulose based packaging seems a reasonable way of delivering active surfaces, however, the concentration of nanoparticles stock solution and a better understanding of the influence of the hydrophobicity of the surface are critical issues for further investigation.

Regarding the fate of the NPs on packaging end-of-life options, laboratory tests showed a reasonable good retention of TiO₂ nanoparticles in the fibres submitted to one cycle of recyclability and an only marginal effect of active ingredients on biodegradability performance.

Chapter 4. Concluding Remarks

Antibacterial cellulose-based materials for active food packaging solutions were successfully developed in this thesis. In a first approach, polyphenols extracted from black tea brewing residues were studied as active compounds and used to prepare a CMC-based coating formulation. The antibacterial activity of the resulting paper coated with just 3.8 g/m² of this formulation was very high showing a complete killing of *S. aureus*. Photo-active TiO₂ inorganic nanoparticles were used in a second approach, with the following remarks:

- i. TiO₂ NPs possess a broad spectrum of activity against gram positive and gram negative bacteria;
- ii. TiO₂ can be directly impregnated by dip-coating or spray dried onto hydrophilic paper surfaces which exhibit a strong antibacterial activity (6-7 log reduction) against gram positive and gram negative bacteria as well as an acceptable stability over a period of 3-4 weeks with limited fibre degradation;
- iii. The antibacterial activity of these TiO₂ impregnated paper surfaces lasts at least 3-4 weeks showing limited reduction, particularly for *S. Aureus*;
- iv. TiO₂ can be electrostatically bonded onto nanofibrillated cellulose (NFC) fibres to develop suitable coating formulations for hydrophobic surfaces. Layer by-layer deposition was found to substantially increase the number of TiO₂ NPs combined with NFC;
- v. The antibacterial activity of the paper treated with TiO₂-NFC was significantly lower (2-3 log reduction) in comparison to direct impregnation of TiO₂ NPs into a hydrophilic paper surface (6-7 log reduction).

Moreover, an industrial trial with the objective to produce an antibacterial packaging for preventing cross-contamination in hospitals was performed using an overprint ZnO NPs based varnish formulation. Unfortunately, technical production constraints and restrictions did not permit to load more than 5.6 mg/m² of active compound, resulting in a packaging surface with low bacteriostatic effect (less than one log reduction). Nevertheless, promising results can be achieved with the possibility to increase the amount of NPs loaded on the packaging surface as it was demonstrated at lab scale, where papers with about 1.5 g/m² of ZnO NPs on the surface showed a bactericidal effect, up to 4 log reduction, against *S. aureus*. Additionally, preliminary tests regarding the end-of-life options such as recyclability and biodegradability have shown a negligible environmental impact related to the incorporation of NPs on the packaging materials.

Among the possible lines of pursuit of this work, it would be interesting to tackle the following topics:

- i. Investigate the potentialities of other tea brewing residue compounds, such as polysaccharides and proteins for other type of applications;
- ii. Better understand the influence of the hydrophobicity of the packaging material surface on the coating process;
- iii. Perform shelf-life assessments using target products packed in the active solutions produced to confirm their antibacterial activity in-vivo;
- iv. Develop the studies on the end-of-life options and realize health-risk surveys associated to the use of nanoparticles to understand the sustainability and feasibility of this kind of package materials.

Chapter 5. Bibliography

- Akrami, F., A. Rodríguez-Lafuente, K. Bentayeb, D. Pezo, S. R. Ghalebi, and C. Nerín. Antioxidant and antimicrobial active paper based on Zataria (*Zataria multiflora*) and two cumin cultivars (*Cuminum cyminum*). *LWT - Food Science and Technology* 60 (2, Part 1):929-933. 2015.
- Almajano, M. P., R. Carbó, J. A. L. Jiménez, and M. H. Gordon. Antioxidant and antimicrobial activities of tea infusions. *Food Chemistry* 108 (1):55-63. 2008.
- Anand, J., B. Upadhyaya, P. Rawat, and N. Rai. Biochemical characterization and pharmacognostic evaluation of purified catechins in green tea (*Camellia sinensis*) cultivars of India. *3 Biotech* 5 (3):285-294. 2015.
- Anesini, C., G. E. Ferraro, and R. Filip. Total polyphenol content and antioxidant capacity of commercially available tea (*Camellia sinensis*) in Argentina. *J Agric Food Chem* 56 (19):9225-9229. 2008.
- Appendini, P., and J. H. Hotchkiss. Review of antimicrobial food packaging. *Innovative Food Science & Emerging Technologies* 3 (2):113-126. 2002.
- Atoui, A. K., A. Mansouri, G. Boskou, and P. Kefalas. Tea and herbal infusions: Their antioxidant activity and phenolic profile. *Food Chemistry* 89 (1):27-36. 2005.
- Bajpai, P. Paper and Paperboard Industry. In *Pulp and Paper Industry: Chemicals*: Elsevier, 13-24. 2015.
- Bansal, S., S. Choudhary, M. Sharma, S. S. Kumar, S. Lohan, V. Bhardwaj, N. Syan, and S. Jyoti. Tea: A native source of antimicrobial agents. *Food Research International* 53 (2):568-584. 2013.
- Barrett, D. G., T. S. Sileika, and P. B. Messersmith. Molecular diversity in phenolic and polyphenolic precursors of tannin-inspired nanocoatings. *Chemical Communications* 50 (55):7265-7268. 2014.
- Berger, S., and D. Sicker. *Classics in Spectroscopy*: Wiley. 2009.
- Biermann, C. J. *Handbook of Pulping and Papermaking*: Elsevier Science. 1996.
- Brody, A. L., E. P. Strupinsky, and L. R. Kline. *Active Packaging for Food Applications*: CRC Press. 2001.
- Burt, S. Essential oils: their antibacterial properties and potential applications in foods—a review. *International Journal of Food Microbiology* 94 (3):223-253. 2004.
- Cabrera, C., R. Giménez, and M. C. López. Determination of Tea Components with Antioxidant Activity. *Journal of Agricultural and Food Chemistry* 51 (15):4427-4435. 2003.
- Carloni, P., L. Tiano, L. Padella, T. Bacchetti, C. Customu, A. Kay, and E. Damiani. Antioxidant activity of white, green and black tea obtained from the same tea cultivar. *Food Research International* 53 (2):900-908. 2013.
- Carp, O., C. L. Huisman, and A. Reller. Photoinduced reactivity of titanium dioxide. *Progress in Solid State Chemistry* 32 (1-2):33-177. 2004.

- Chan, E. W. C., E. Y. Soh, P. P. Tie, and Y. P. Law. Antioxidant and antibacterial properties of green, black, and herbal teas of *Camellia sinensis*. *Pharmacognosy Research* 3 (4):266-272. 2011.
- Chauhan, I., and P. Mohanty. In situ decoration of TiO₂ nanoparticles on the surface of cellulose fibers and study of their photocatalytic and antibacterial activities. *Cellulose*:1-13. 2014.
- Cheynier, V. Phenolic compounds: from plants to foods. *Phytochemistry Reviews* 11 (2-3):153-177. 2012.
- Chow, H. H. S., and I. A. Hakim. Pharmacokinetic and chemoprevention studies on tea in humans. *Pharmacological Research* 64 (2):105-112. 2011.
- Cren-Olivé, C., S. Déprez, S. Lebrun, B. Coddeville, and C. Rolando. Characterization of methylation site of monomethylflavan-3-ols by liquid chromatography/electrospray ionization tandem mass spectrometry. *Rapid Communications in Mass Spectrometry* 14 (23):2312-2319. 2000.
- Cushnie, T. P. T., and A. J. Lamb. Recent advances in understanding the antibacterial properties of flavonoids. *International Journal of Antimicrobial Agents* 38 (2):99-107. 2011.
- Daglia, M. Polyphenols as antimicrobial agents. *Current Opinion in Biotechnology* 23 (2):174-181. 2012.
- Dainelli, D., N. Gontard, D. Spyropoulos, E. Zondervan-van den Beuken, and P. Tobback. Active and intelligent food packaging: legal aspects and safety concerns. *Trends in Food Science & Technology* 19, Supplement 1 (0):S103-S112. 2008.
- Dou, J., V. S. Lee, J. T. Tzen, and M. R. Lee. Identification and comparison of phenolic compounds in the preparation of oolong tea manufactured by semifermentation and drying processes. *J Agric Food Chem* 55 (18):7462-7468. 2007.
- ECR. Packaging in the Sustainability Agenda: A Guide for Corporate Decision Makers. *ECR Europe and European Organization for Packaging and the Environment (EUROPEN)*. 2009.
- Engelhardt, U. H. 3.23 - Chemistry of Tea. In *Comprehensive Natural Products II*, edited by H.-W. Liu and L. Mander. Oxford: Elsevier, 999-1032. 2010.
- EU. Directive 94/62/EC of 20 December 1994 on packaging and packaging waste of the European Parliament and Council of the European Union. 1994.
- EU. Regulation (EC) n° 1935/2004 of the European Parliament and of the Council of 27 October 2004 on materials and articles intended to come into contact with food and repealing Directives 80/590/EEC and 89/109/EEC. 2004.
- EU. Commission Regulation (EC) n° 450/2009 of 29 May 2009 on active and intelligent materials and articles intended to come into contact with food. 2009.
- EY. Unwrapping the packaging industry - Seven factors for success. 2013.
- FAO. Appropriate food packaging solutions for developing countries. *Food and Agriculture Organization of the United Nations*. 2014.
- Farhoosh, R., G. A. Golmovahhed, and M. H. H. Khodaparast. Antioxidant activity of various extracts of old tea leaves and black tea wastes (*Camellia sinensis* L.). *Food Chemistry* 100 (1):231-236. 2007.

- Fernandes, S. C. M., P. Sadocco, A. Alonso-Varona, T. Palomares, A. Eceiza, A. J. D. Silvestre, I. Mondragon, and C. S. R. Freire. Bioinspired Antimicrobial and Biocompatible Bacterial Cellulose Membranes Obtained by Surface Functionalization with Aminoalkyl Groups. *ACS Appl Mater Interfaces* 5 (8):3290-3297. 2013.
- Friedman, M., P. R. Henika, C. E. Levin, R. E. Mandrell, and N. Kozukue. Antimicrobial Activities of Tea Catechins and Theaflavins and Tea Extracts against *Bacillus cereus*. *Journal of Food Protection* 69 (2):354-361. 2006.
- Fu, G., P. S. Vary, and C.-T. Lin. Anatase TiO₂ Nanocomposites for Antimicrobial Coatings. *The Journal of Physical Chemistry B* 109 (18):8889-8898. 2005.
- Ghule, K., A. V. Ghule, B.-J. Chen, and Y.-C. Ling. Preparation and characterization of ZnO nanoparticles coated paper and its antibacterial activity study. *Green Chemistry* 8 (12):1034-1041. 2006.
- Gonçalves, G., P. A. A. P. Marques, C. P. Neto, T. Trindade, M. Peres, and T. Monteiro. Growth, Structural, and Optical Characterization of ZnO-Coated Cellulosic Fibers. *Crystal Growth & Design* 9 (1):386-390. 2009.
- Goncalves, G., P. A. A. P. Marques, R. J. B. Pinto, T. Trindade, and C. P. Neto. Surface modification of cellulosic fibres for multi-purpose TiO₂ based nanocomposites. *Composites Science and Technology* 69 (7-8):1051-1056. 2009.
- Harbowy, M. E., D. A. Balentine, A. P. Davies, and Y. Cai. Tea Chemistry. *Critical Reviews in Plant Sciences* 16 (5):415-480. 1997.
- Haslam, E. Thoughts on thearubigins. *Phytochemistry* 64 (1):61-73. 2003.
- Huang, J., K. Huang, S. Liu, Q. Luo, and M. Xu. Adsorption properties of tea polyphenols onto three polymeric adsorbents with amide group. *Journal of Colloid and Interface Science* 315 (2):407-414. 2007.
- Huang, Z., X. Zheng, D. Yan, G. Yin, X. Liao, Y. Kang, Y. Yao, D. Huang, and B. Hao. Toxicological Effect of ZnO Nanoparticles Based on Bacteria. *Langmuir* 24 (8):4140-4144. 2008.
- Ignat, I., D. G. Radu, I. Volf, A. I. Pag, and V. I. Popa. Antioxidant and antibacterial activities of some natural polyphenols. *CELLULOSE CHEM. TECHNOL.* 47 (5-6):387-399. 2013.
- ISO535:2014. Paper and board - Determination of water absorptiveness - Cobb method.
- Jaisai, M., S. Baruah, and J. Dutta. Paper modified with ZnO nanorods – antimicrobial studies. *Beilstein Journal of Nanotechnology* 3:684-691. 2012.
- Jeszka-Skowron, M., M. Krawczyk, and A. Zgoła-Grześkowiak. Determination of antioxidant activity, rutin, quercetin, phenolic acids and trace elements in tea infusions: Influence of citric acid addition on extraction of metals. *Journal of Food Composition and Analysis* 40 (0):70-77. 2015.
- Jones, N., B. Ray, K. T. Ranjit, and A. C. Manna. Antibacterial activity of ZnO nanoparticle suspensions on a broad spectrum of microorganisms. *FEMS Microbiol Lett* 279 (1):71-76. 2008.
- Joshi, P., S. Chakraborti, P. Chakrabarti, S. P. Singh, Z. A. Ansari, M. Husain, and V. Shanker. ZnO Nanoparticles as an Antibacterial Agent Against E. coli. *Science of Advanced Materials* 4 (1):173-178. 2012.

Kazuhiro, H., I. Hiroshi, and F. Akira. TiO₂ Photocatalysis: A Historical Overview and Future Prospects. *Japanese Journal of Applied Physics* 44 (12R):8269. 2005.

Kerry, J., and P. Butler. Smart Packaging Technologies for Fast Moving Consumer Goods. In *Smart Packaging Technologies for Fast Moving Consumer Goods*, edited by P. B. Joseph Kerry: John Wiley & Sons, Ltd. 2008.

Kiehne, A., and U. H. Engelhardt. Thermospray-LC-MS analysis of various groups of polyphenols in tea. *Zeitschrift für Lebensmittel-Untersuchung und Forschung* 202 (1):48-54. 1996.

Kikuzaki, H., M. Hisamoto, K. Hirose, K. Akiyama, and H. Taniguchi. Antioxidant Properties of Ferulic Acid and Its Related Compounds. *Journal of Agricultural and Food Chemistry* 50 (7):2161-2168. 2002.

Li, M., L. Zhu, and D. Lin. Toxicity of ZnO Nanoparticles to Escherichia coli: Mechanism and the Influence of Medium Components. *Environmental Science & Technology* 45 (5):1977-1983. 2011.

Li, S., C.-Y. Lo, M.-H. Pan, C.-S. Lai, and C.-T. Ho. Black tea: chemical analysis and stability. *Food & Function* 4 (1):10-18. 2013.

Lim, L. T. 4.52 - Active and Intelligent Packaging Materials. In *Comprehensive Biotechnology (Second Edition)*, edited by M. Moo-Young. Burlington: Academic Press, 629-644. 2011.

Lu, Z., S. Eadula, Z. Zheng, K. Xu, G. Grozdits, and Y. Lvov. Layer-by-layer nanoparticle coatings on lignocellulose wood microfibrils. *Colloids and Surfaces A: Physicochemical and Engineering Aspects* 292 (1):56-62. 2007.

Maness, P.-C., S. Smolinski, D. M. Blake, Z. Huang, E. J. Wolfrum, and W. A. Jacoby. Bactericidal Activity of Photocatalytic TiO₂ Reaction: toward an Understanding of Its Killing Mechanism. *Applied and Environmental Microbiology* 65 (9):4094-4098. 1999.

Marques, P. A. A. P., T. Trindade, and C. P. Neto. Titanium dioxide/cellulose nanocomposites prepared by a controlled hydrolysis method. *Composites Science and Technology* 66 (7-8):1038-1044. 2006.

Martins, N. C. T., C. S. R. Freire, C. P. Neto, A. J. D. Silvestre, J. Causio, G. Baldi, P. Sadocco, and T. Trindade. Antibacterial paper based on composite coatings of nanofibrillated cellulose and ZnO. *Colloids and Surfaces A: Physicochemical and Engineering Aspects* 417 (0):111-119. 2013.

Matsubara, H., M. Takada, S. Koyama, K. Hashimoto, and A. Fujishima. Photoactive TiO₂ Containing Paper: Preparation and Its Photocatalytic Activity under Weak UV Light Illumination. *Chemistry Letters* 24 (9):767-768. 1995.

Nakata, K., and A. Fujishima. TiO₂ photocatalysis: Design and applications. *Journal of Photochemistry and Photobiology C: Photochemistry Reviews* 13 (3):169-189. 2012a.

Nakata, K., T. Ochiai, T. Murakami, and A. Fujishima. Photoenergy conversion with TiO₂ photocatalysis: New materials and recent applications. *Electrochimica Acta* 84 (0):103-111. 2012b.

Namal Senanayake, S. P. J. Green tea extract: Chemistry, antioxidant properties and food applications – A review. *Journal of Functional Foods* 5 (4):1529-1541. 2013.

- Ngo, Y. H., D. Li, G. P. Simon, and G. Garnier. Paper surfaces functionalized by nanoparticles. *Adv Colloid Interface Sci* 163 (1):23-38. 2011.
- Patel, M. Industry Insight: Developments in Antibacterial Paper. 2009.
- Payra, D., M. Naito, Y. Fujii, and Y. Nagao. Hydrophobized plant polyphenols: self-assembly and promising antibacterial, adhesive, and anticorrosion coatings. *Chemical Communications* 52 (2):312-315. 2016.
- Pękal, A., P. Drózdź, M. Biesaga, and K. Pyrzynska. Evaluation of the antioxidant properties of fruit and flavoured black teas. *European Journal of Nutrition* 50 (8):681-688. 2011.
- Pękal, A., P. Drózdź, M. Biesaga, and K. Pyrzynska. Screening of the antioxidant properties and polyphenol composition of aromatised green tea infusions. *J Sci Food Agric* 92 (11):2244-2249. 2012.
- Pelaez, M., N. T. Nolan, S. C. Pillai, M. K. Seery, P. Falaras, A. G. Kontos, P. S. M. Dunlop, J. W. J. Hamilton, J. A. Byrne, K. O'Shea, M. H. Entezari, and D. D. Dionysiou. A review on the visible light active titanium dioxide photocatalysts for environmental applications. *Applied Catalysis B: Environmental* 125 (0):331-349. 2012.
- Pelton, R., X. Geng, and M. Brook. Photocatalytic paper from colloidal TiO₂--fact or fantasy. *Adv Colloid Interface Sci* 127 (1):43-53. 2006.
- Peng, Y., Y. Wu, and Y. Li. Development of tea extracts and chitosan composite films for active packaging materials. *International Journal of Biological Macromolecules* 59:282-289. 2013.
- Pereira de Abreu, D. A., J. M. Cruz, and P. Paseiro Losada. Active and Intelligent Packaging for the Food Industry. *Food Reviews International* 28 (2):146-187. 2012.
- Pereira, P., M.-J. Cebola, M. C. Oliveira, and M. G. Bernardo-Gil. Supercritical Fluid Extraction vs Conventional Extraction of Myrtle Leaves and Berries: Comparison of Antioxidant Activity and Identification of Bioactive Compounds. *The Journal of Supercritical Fluids*. 2015.
- Perva-Uzunalić, A., M. Škerget, Ž. Knez, B. Weinreich, F. Otto, and S. Grüner. Extraction of active ingredients from green tea (*Camellia sinensis*): Extraction efficiency of major catechins and caffeine. *Food Chemistry* 96 (4):597-605. 2006.
- Piergiovanni, L., and S. Limbo. *Food packaging: Materiali, tecnologie e qualità degli alimenti*: Springer Milan. 2010.
- Radji, M., R. A. Agustama, B. Elya, and C. R. Tjampakasari. Antimicrobial activity of green tea extract against isolates of methicillin-resistant *Staphylococcus aureus* and multi-drug resistant *Pseudomonas aeruginosa*. *Asian Pacific Journal of Tropical Biomedicine* 3 (8):663-667. 2013.
- Robertson, G. L. *Food Packaging: Principles and Practice, Third Edition*: Taylor & Francis. 2012.
- Roger, M. R., P. Roger, and A. T. Mandla. Cell Wall Chemistry. In *Handbook of Wood Chemistry and Wood Composites, Second Edition*: CRC Press, 33-72. 2012.
- Saini, S., M. N. Belgacem, K. Missoum, and J. Bras. Natural active molecule chemical grafting on the surface of microfibrillated cellulose for fabrication of contact active antimicrobial surfaces. *Industrial Crops and Products* 78:82-90. 2015a.

- Saini, S., N. Belgacem, J. Mendes, G. Elegir, and J. Bras. Contact Antimicrobial Surface Obtained by Chemical Grafting of Microfibrillated Cellulose in Aqueous Solution Limiting Antibiotic Release. *ACS Appl Mater Interfaces* 7 (32):18076-18085. 2015b.
- Sang, S., J. D. Lambert, C.-T. Ho, and C. S. Yang. The chemistry and biotransformation of tea constituents. *Pharmacological Research* 64 (2):87-99. 2011.
- Sang, S., J. D. Lambert, S. Tian, J. Hong, Z. Hou, J.-H. Ryu, R. E. Stark, R. T. Rosen, M.-T. Huang, C. S. Yang, and C.-T. Ho. Enzymatic synthesis of tea theaflavin derivatives and their anti-inflammatory and cytotoxic activities. *Bioorganic & Medicinal Chemistry* 12 (2):459-467. 2004.
- Schieber, A., F. C. Stintzing, and R. Carle. By-products of plant food processing as a source of functional compounds — recent developments. *Trends in Food Science & Technology* 12 (11):401-413. 2001.
- Schütz, C., J. Sort, Z. Bacsik, V. Oliynyk, E. Pellicer, A. Fall, L. Wågberg, L. Berglund, L. Bergström, and G. Salazar-Alvarez. Hard and Transparent Films Formed by Nanocellulose–TiO₂ Nanoparticle Hybrids. *PLoS ONE* 7 (10):e45828. 2012.
- Sileika, T. S., D. G. Barrett, R. Zhang, K. H. A. Lau, and P. B. Messersmith. Colorless Multifunctional Coatings Inspired by Polyphenols Found in Tea, Chocolate, and Wine. *Angewandte Chemie International Edition* 52 (41):10766-10770. 2013.
- Silva, E. M., D. R. Pompeu, Y. Larondelle, and H. Rogez. Optimisation of the adsorption of polyphenols from *Inga edulis* leaves on macroporous resins using an experimental design methodology. *Separation and Purification Technology* 53 (3):274-280. 2007.
- Siripatrawan, U., and B. R. Harte. Physical properties and antioxidant activity of an active film from chitosan incorporated with green tea extract. *Food Hydrocolloids* 24 (8):770-775. 2010.
- Stewart, A. J., W. Mullen, and A. Crozier. On-line high-performance liquid chromatography analysis of the antioxidant activity of phenolic compounds in green and black tea. *Molecular Nutrition & Food Research* 49 (1):52-60. 2005.
- Stodt, U. W., J. Stark, and U. H. Engelhardt. Comparison of three strategies for the isolation of black tea thearubigins with a focus on countercurrent chromatography. *Journal of Food Composition and Analysis* 43:160-168. 2015.
- Stratil, P., B. Klejdus, and V. Kubáň. Determination of Total Content of Phenolic Compounds and Their Antioxidant Activity in Vegetables Evaluation of Spectrophotometric Methods. *Journal of Agricultural and Food Chemistry* 54 (3):607-616. 2006.
- Statistics, M. R. C. Global Smart Packaging Market Outlook (2014-2022). 2015.
- Suetens, C., S. Hopkins, J. Kolman, and L. D. Högberg. Point prevalence survey of healthcare-associated infections and antimicrobial use in European acute care hospitals 2011–2012, edited by E. C. f. D. P. a. C. (ECDC). Stockholm. 2013.
- Suppakul, P., J. Miltz, K. Sonneveld, and S. W. Bigger. Active Packaging Technologies with an Emphasis on Antimicrobial Packaging and its Applications. *J Food Sci* 68 (2):408-420. 2003.
- Tan, J. B. L., and Y. Y. Lim. Critical analysis of current methods for assessing the in vitro antioxidant and antibacterial activity of plant extracts. *Food Chemistry* 172 (0):814-822. 2015.

- Tian, C., Q. Zhang, A. Wu, M. Jiang, Z. Liang, B. Jiang, and H. Fu. Cost-effective large-scale synthesis of ZnO photocatalyst with excellent performance for dye photodegradation. *Chemical Communications* 48 (23):2858-2860. 2012.
- Tonomura, O., T. Sekiguchi, N. Inada, T. Hamada, H. Miki, and K. Torii. Band Engineering of Ru/Rutile-TiO₂/Ru Capacitors by Doping Cobalt to Suppress Leakage Current. *Journal of The Electrochemical Society* 159 (1):G1-G5. 2011.
- van der Pijl, P. C., M. Foltz, N. D. Glube, S. Peters, and G. S. M. J. E. Duchateau. Pharmacokinetics of black tea-derived phenolic acids in plasma. *Journal of Functional Foods* 17:667-675. 2015.
- Varaprasad, K., G. M. Raghavendra, T. Jayaramudu, and J. Seo. Nano zinc oxide–sodium alginate antibacterial cellulose fibres. *Carbohydrate Polymers* 135:349-355. 2016.
- Vermeiren, L., F. Devlieghere, M. van Beest, N. de Kruijf, and J. Debevere. Developments in the active packaging of foods. *Trends in Food Science & Technology* 10 (3):77-86. 1999.
- Visai, L., L. De Nardo, C. Punta, L. Melone, A. Cigada, M. Imbriani, and C. R. Arciola. Titanium oxide antibacterial surfaces in biomedical devices. *Int J Artif Organs* 34 (9):929-946. 2011.
- Vuoti, S., E. Laatikainen, H. Heikkinen, L.-S. Johansson, E. Saharinen, and E. Retulainen. Chemical modification of cellulosic fibers for better convertibility in packaging applications. *Carbohydrate Polymers* 96 (2):549-559. 2013.
- Wang, Y., and C. T. Ho. Polyphenolic chemistry of tea and coffee: a century of progress. *J Agric Food Chem* 57 (18):8109-8114. 2009.
- Wang, Z. L. Nanostructures of zinc oxide. *Materials Today* 7 (6):26-33. 2004.
- Xie, Y., Y. He, P. L. Irwin, T. Jin, and X. Shi. Antibacterial activity and mechanism of action of zinc oxide nanoparticles against *Campylobacter jejuni*. *Appl Environ Microbiol* 77 (7):2325-2331. 2011.
- Yang, D., J. Liang, Y. Wang, F. Sun, H. Tao, Q. Xu, L. Zhang, Z. Zhang, C.-T. Ho, and X. Wan. Tea Waste: an Effective and Economic Substrate for Oyster Mushroom Cultivation. *J Sci Food Agric*:n/a-n/a. 2015.
- Yemmireddy, V. K., and Y.-C. Hung. Selection of photocatalytic bactericidal titanium dioxide (TiO₂) nanoparticles for food safety applications. *LWT - Food Science and Technology* 61 (1):1-6. 2015.
- Yi, S., W. Wang, F. Bai, J. Zhu, J. Li, X. Li, Y. Xu, T. Sun, and Y. He. Antimicrobial effect and membrane-active mechanism of tea polyphenols against *Serratia marcescens*. *World Journal of Microbiology and Biotechnology* 30 (2):451-460. 2014.
- Yi, T., L. Zhu, W.-L. Peng, X.-C. He, H.-L. Chen, J. Li, T. Yu, Z.-T. Liang, Z.-Z. Zhao, and H.-B. Chen. Comparison of ten major constituents in seven types of processed tea using HPLC-DAD-MS followed by principal component and hierarchical cluster analysis. *LWT - Food Science and Technology* 62 (1, Part 1):194-201. 2015.
- Yuda, N., M. Tanaka, M. Suzuki, Y. Asano, H. Ochi, and K. Iwatsuki. Polyphenols extracted from black tea (*Camellia sinensis*) residue by hot-compressed water and their inhibitory effect on pancreatic lipase in vitro. *J Food Sci* 77 (12):H254-261. 2012.

Zandi, P., and M. H. Gordon. Antioxidant activity of extracts from old tea leaves. *Food Chemistry* 64 (3):285-288. 1999.

Zeeb, D. J., B. C. Nelson, K. Albert, and J. J. Dalluge. Separation and Identification of Twelve Catechins in Tea Using Liquid Chromatography/Atmospheric Pressure Chemical Ionization-Mass Spectrometry. *Analytical Chemistry* 72 (20):5020-5026. 2000.

Zhang, J., W. Liu, P. Wang, and K. Qian. Photocatalytic behavior of cellulose-based paper with TiO₂ loaded on carbon fibers. *Journal of Environmental Chemical Engineering* 1 (3):175-182. 2013.

Zhao, R., Y. Yan, M. Li, and H. Yan. Selective adsorption of tea polyphenols from aqueous solution of the mixture with caffeine on macroporous crosslinked poly(N-vinyl-2-pyrrolidinone). *Reactive and Functional Polymers* 68 (3):768-774. 2008.

Appendix

Scientific Dissemination

(within the NewGenPak project)

Articles in refereed international journals

Saini, S., N. Belgacem, J. Mendes, G. Elegir, and J. Bras. Contact Antimicrobial Surface Obtained by Chemical Grafting of Microfibrillated Cellulose in Aqueous Solution Limiting Antibiotic Release. *ACS Appl Mater Interfaces* 7 (32):18076-18085. 2015.

Zhang, H., D. Bussini, M. Hortal, G. Elegir, J. Mendes, and M. J. Beneyto. PLA coated paper containing active inorganic nanoparticles: material characterization and fate of nanoparticles in the paper recycling process. *Waste Management*, submitted. 2015.

Oral Communications

Joana A. S. Mendes, Sara Daina, Daniele Bussini, Giovanni Baldi, Alessandro Adobati, Sara Limbo, Graziano Elegir, “Development of Antibacterial Paper Surfaces based on photo-active TiO₂ nanoparticles for food packaging applications”, SLIM for young 2015 – Special 7th edition of Shelf Life International Meeting, October 21-23, 2015, Monza, Italy.

Joana A. S. Mendes, “Paper packaging based on photoactive inorganic nanoparticles: activity and influence on end of life options”, COST Action FP1405 meeting: Existing technologies and current developments in active and intelligent packaging, September 15-16, 2015, Aveiro, Portugal.

Joana A. S. Mendes, “Photoactive nanoparticles in paper-based packaging: a study on their antibacterial effect and impact on end of life options”, NewGenPak International Seminar, June 8, 2015, Valencia, Spain.

Joana A. S. Mendes, Ricardo J. B. Pinto, Carmen Freire, Giovanni Baldi, Graziano Elegir. “Antibacterial coating formulations based on NFC and photo-active TiO₂ nanoparticles”, ICNF2015 – 2nd International Conference on Natural Fibers, April 27-29, 2015, Azores, Portugal.

Joana Mendes, “Development of antibacterial papers by incorporation of active nanoparticles”, 46th Aticelca Congress, May 28, 2015, Sestri Levante, Italy.

Joana A. S. Mendes, Graziano Elegir, Patrizia Sadocco, Giovanni Bald. “Antibacterial activity of TiO₂ coated paper for food packing applications”, 109th Annual General Meeting 2014, Conference and Expo, June 24-26, 2014, Frankfurt, Germany.

Seema Saini, Mohamed Naceur Belgacem, Joana Mendes, Graziano Elegir, Julien Bras. “Grafting of Benzyl Penicillin on Microfibrillated cellulose: Water based method”, TAPPI-Nano, June 23-26, 2014, Vancouver, Canada.

Joana A. S. Mendes. “Antibacterial photo-active TiO₂ dip-coated paper”, EFPRO – CEPI seminar: New ideas for the paper industry – Young researchers' presentations, European Paper Week, November 26-28, 2013, Brussels, Belgium.

Joana A. S. Mendes, Graziano Elegir. “Newgenpak project: Una scuola internazionale per lo sviluppo dell’imballaggio cellulosico innovativo e sostenibile”. Convegno: Imballaggi in carta e cartone: nuove soluzioni sostenibili, January 30, 2013, Milan, Italy.

Poster Presentations

Joana A. S. Mendes, Sara Daina, Ricardo J. B. Pinto, Carmen Freire, Giovanni Baldi, Graziano Elegir. “Development of Antibacterial Paper Surfaces based on NFC and Photo-Active TiO₂ Nanoparticles”. IFIB 2015 – 4th Italian Forum on Industrial Biotechnology and Bioeconomy, September 24-25, 2015, Pavia, Italy.

Joana A. S. Mendes, Graziano Elegir, Giovanni Baldi. “Contact active materials for developing innovative antimicrobial paper based packaging”. Joint Conference PTS/COST FP 1003 On Innovative Packaging, May 20-21, 2014, Munich, Germany.

Joana A. S. Mendes, Graziano Elegir, Patrizia Sadocco, Giovanni Baldi. “Photoactive titanium dioxide for paper based packaging applications”. NanotechItaly2013 International Conference, November 27-29, 2013, Venice, Italy.

Joana A. S. Mendes, Sara Daina, Patrizia Sadocco, Graziano Elegir. “Antibacterial activity of TiO₂ on dip-coated papers for food contact packaging applications.” IFIB 2013 - 3rd Italian Forum on Industrial Biotechnology and Bioeconomy, October 22-23, 2013, Naples, Italy.

Invitations

Speaker in the Seminar: The Two Team Project - Revealing the Details, Glance into the future – A Young Researchers View, European Paper Week, November 26-28, 2013, Brussels, Belgium.

Interviews

IPW magazine, The magazine for the international pulp and paper industry, January/February 2014.

Smart Cities in Europe, HVB Communicatie, November 2013

(<http://www.smartcitiesineurope.com/2013/12/young-researchers-link-passive-houses-and-tomatoes-to-the-paper-industry/>).

Industria della Carta, April 2013 (<http://www.industriadellacarta.it/numeri/201302-aprile/>).

Marie Curie Ambassador activities

Presentations to Industry and Academia: “How to apply for a MCA grant!”, University of Aveiro, June 25, 2013, Aveiro, Portugal and University of Insubria, May 30, 2013, Como, Italy.

Member of the organization committee of the Open Day for young students at Sheffield Hallam University, UK, September 2013.